ABSTRACT

Title of Dissertation: REGULATORY FUNCTIONS OF THE ACTIN CYTOSKELETON IN B CELL RECEPTOR SIGNALING

Chaohong Liu, Doctor of Philosophy, 2013

Dissertation Directed by: Wenxia Song, Associate Professor, Cell Biology and Molecular Genetics

The binding of antigen (Ag) to the B cell receptor (BCR) induces the activation of intracellular signaling and the reorganization of the actin cytoskeleton. However, the function of actin reorganization and the mechanisms by which BCR signaling and actin reorganization is coupled have not been well studied. This thesis has investigated how BCR signaling regulates actin reorganization and how actin remodeling in turn influences BCR signalig. My studies show that the key stimulatory signaling molecule of the BCR, Bruton's tyrosine kinase (Btk), is critical for actin polymerization at the activation surface and BCR clustering and B cell spreading, events that are essential for signaling initiation and amplification. The key inhibitory signaling molecule, SH2-containing phosphatidylinositol-5 phosphatase (SHIP-1), is important for removal of F-actin from the activation surface, and actin-mediated B cell contraction and the formation of BCR central clusters. SHIP-1 suppresses actin polymerization by inhibiting Btk-dependent activation of Wiskott-Aldrich syndrome protein (WASP). These results suggest that BCR signaling can regulate B cell morphology and surface BCR clustering via modulationg actin dynamics. To understand the roles of actin reorganization in BCR signaling, I investigated the effects of gene knockout of the two actin regulators, WASP and its homolog, neuronal (N)-WASP. My results show that both WASP and N-WASP are required for optimal BCR clustering, B cell spreading, and BCR signaling, but they play distinct roles. WASP promotes actin polymerization, B cell spreading, BCR clustering, and signaling amplification, and N-WASP inhibits actin polymerization at the activation surface and promotes B cell contraction, BCR central cluster formation, and signaling attenuation. Importantly, B cell-specific N-WASP knockout causes increases in the levels of autoantibody. In addition, WASP and N-WASP negatively regulate each other, compete for Arp2/3, and are inversely regulated by Btk and SHIP-1. Taken together, these results demonstrate that the balance of stimulatory and inhibitory BCR signaling controls actin dynamics and organization through regulating the activities of WASP and N-WASP. Actin remodeling in turn amplifies BCR signaling activation or down regulation by modulating B cell morphlogy and the organization of surface BCRs.This research reveals a bidrectional feedback loop between BCR signaling and the actin cytoskeleton.

REGULATORY FUNCTIONS OF THE ACTIN CYTOSKELETON IN B CELL RECEPTOR SIGNALING

By

Chaohong Liu

Dissertation submitted to the Faculty of the Graduate School of the
University of Maryland, College Park, in partial fulfillment
of the requirements for the degree of
Doctor of Philosophy
2013

Advirory Committee:

Professor Wenxia Song, Chair/Advisor
Professor Arpita Upadhyaya
Professor Kenneth Frauwirth
Professor Xiaoping Zhu
Professor Zhengguo Xiao

© Copyright by
Chaohong Liu
2013

ACKNOWLEDGMENTS

At the end of leaving University of Maryland, I have started to write this first and most important page in my thesis.

I want to give my maximal acknowledgment to my current Ph.D advisor, Dr. Wenxia Song. Her nice personality in the Cell Biology class for graduate students and great reputation in the department attracted me to study immunology research in her lab in 2008. During these five years, not only I have learned how to do research in a scientific way, but also how to overcome the difficulties and face the challenges with a calm and peaceful heart in the science career. She is always helpful whenever my research meets challenges and never loses her patience to guide me on the right track to science. She can always give support and comfort when my experiments didn't work. Although these five years are busy, I have worked in a very flexible environment. Lot's of her philosophy and value have encouraged me to go forward in the science field.

I am glad that I have a great committee that always gives me help and suggestions. I really appreciate Dr. Zhu and Dr. Xiao to write the recommendation letters during their busy schedule and to send the letters out on time, and this is really helpful for getting the on-site interview chance for the potential postdoc labs. Whenever we meet together, Dr. Zhu and Dr. Xiao always communicate with me about my research progress and give valuable and constructive suggestions. Dr. Frauwirth is on the same floor and can be always reachable, I am so impressive with the broad and deep knowledge he has. Whenever I meet the dead end in the science, he can always point out another way to shed the forward direction. Not only on the general direction on science, but also he can offer a lot of experience and tips for the detail of the experiments. Dr.Upadhyaya is an expert on the microscope and biophysics field, and she is generous to share all what she knows and taught me a lot of things that we are weak on it. As the director of gradute program, Dr. Jeffrey DeStefano and Michelle Brooks gave their help on the graduate students' life as much as they can, especially the international students who usually meet different challenges. So we can focus on our research instead of considering the trivial stuffs in life.

I also need to acknowledge my master advisor, Dr. Xinwen Chen. He has paid attention to every progress I have made. Although I already graduated from Wuhan Institute of Virology for around 7 years, he always gives me suggestions and offers as much as help as he can not only in science but also in life. Another previous advisor I need to appreciate is Dr. Vernon Reinhold, who directly recruited me from China and initiated my research life here. He always emails me and asks my situation and guides me how to fit this society.

I am very fortunate to have a good lab environment to work with. Katie can always make the lab in a good order and is the first labmate who showed me the basic technique for the immunology. Heather is a great co-worker who shared a lot of TIRF experience with me on the research. Mark can really give some fun to the lab when we are tired of doing experiments in the lab. Mechelle and Dr.Zhao have refreshed our lab. Melanie, Grace and Gladys tried their best to help my work in their busy schedule of the class. I also want to thank the previous lab members. Shruti and Greg can always give their opinions on the project I am doing with their previous experience. Karen always uses her accumulated experimental experience to guide us, Katharina can fulfill our immunology knowledge with her own project and Vonetta can always give us guide on the graduate student life. Melvin always gives me the essence of American culture. Nowadays science is an interdicipline work, King, Brian and Christy from Dr. Upadhyaya's lab helped me a lot on the microscope.

At the end, I really appreciate the support from all the members in my family, especially on the spirit level at any time. They make me work hard forever and never feel alone in this world.

TABLE OF CONTENTS

ACKNOWLEDGEMENTS..ii

TABLE OF CONTENTS...v

LIST OF FIGURES...viii

LIST OFABBREVIATIONS…………………………………………………………………xi

CHAPTER 1: GENERAL INTRODUCTION………………………………………………1
1.1 B lymphocytes...2
1.2 B lymphocyte development and maturation...4
1.3 B cell effector responses and memory..10
1.4 The BCR and its signaling pathways..12
1.5 Early event of BCR signaling..15
1.6 Btk and SHIP-1 in B cell signaling... 21
1.7 BCR-mediated antigen uptake and processing pathways.............................. 25
1.8 Actin reorganization during BCR activation..27
1.9 Roles of the actin cytoskeleton in BCR signaling……………………………...29
1.10 The role of WASP and N-WASP in B-cells..31
1.11 Hypothesis..34
1.12 Significance...35

CHAPTER 2: A BALANCE OF BRUTON'S TYROSINE KINASE AND SHIP ACTIVATION REGULATES B CELL RECEPTOR CLUSTER FORMATION BY CONTROLLING ACTIN REMODELING...36
2.1 Abstract...36
2.2 Introduction..37
2.3 Materials and Methods..40
2.3.1 Mice and Cells...40
2.3.2 Preparation of monobiotinylated Fab' Ab……………………………………….40
2.3.3 Preparation of Ag-tethered planar lipid bilayers…………………………….…..41
2.3.4 Total internal reflection fluorescence microscopy……………………………....41
2.3.5 Analysis of the mobility and fluorescence intensity of BCR clusters……………43
2.3.6 Analysis of Actin Nucleation Sites.. 43
2.3.7 Statistical analysis..44
2.4 Results.. 45
2.4.1 Btk and SHIP-1 regulate B cell spreading and BCR aggregation.....................45
2.4.2 The centripetal movement of BCR microclusters is inhibited in SHIP-1$^{-/-}$ *B cells* 52
2.4.3 The growth of BCR microclusters is inhibited, but the signaling capability of BCR microclusters is enhanced in SHIP-1$^{-/-}$ *B cells*……………………………………55
2.4.4 Btk and SHIP-1 play opposing roles in actin reorganization.............................60
2.4.5 SHIP-1 regulates WASP activation, B cell spreading, and BCR cluster formation

in a Btk-dependent manner...67
2.4.6 B cell spreading, BCR cluster formation, and tyrosine phosphorylation are reduced in $WASP^{-/-}$ B cells……………………………………………………..67
2.5 Discussion..68

CHAPTER 3. ACTIN REORGANIZATION IS REQUIRED FOR THE FORMATION OF POLARIZED BCR SIGNALOSOMES IN RESPONSE TO BOTH SOLUBLE AND MEMBRANE ASSOCIATED ANTIGEN………………………………………………76

3.1 Abstract...76
3.2 Introduction...77
3.3 Materials and Methods..82
3.3.1 Mice and Cells...82
3.3.2 Model antigens……………………………………………………………..82
3.3.3 Confocal fluorescence microscopy and image analysis………………………83
3.3.4 Total internal reflection microcopy and image analysis……………………….84
3.3.5 Analysis of actin nucleation sites…………………………………………....85
3.3.6 Treatment of latrunculin B and Jasplakinolide..86
3.3.7 Flow cytometry analysis... 86
3.3.8 Statistical Analysis..86
3.4 Results.. 87
3.4.1 Both soluble and membrane-associated antigens induce the recruitment of F-actin to BCR aggregates...87
3.4.2 Both soluble and membrane-associated antigens induce actin polymerization at BCR aggregates 88
3.4.3 Both soluble and membrane-associated antigens induce the mobilization of actin regulators, cofilin and gelsolin…………………………………………………94
3.4.4 Disruption of the actin cytoskeleton alters BCR activation in response to both Soluble and membrane-associated antigens as well as antigen-independent BCR signaling……………………………………………………………………102
3.5 Discussion…………………………………………………………………… 110

CHAPTER 4: UNIQUE ROLES OF NEURONAL WISKOTT-ALDRICH SYNDROME PROTEIN IN THE NEGATIVE REGULATION OF B CELL RECEPTOR SIGNALING AND AUTOIMMUNITY...117

4.1 Abstract...117
4.2 Introduction..118
4.3 Materials and Methods..122
4.3.1 Mice and cells..122
4.3.2 Preparation of Antigen-tethered Planar Lipid Bilayers....................................123
4.3.3 Total Internal Reflection Microscopy 124
4.3.4 Calcium Flux...125
4.3.5 BCR Internalization..125
4.3.6 Flow CytometryAnalysis……………………………………………………....126
4.3.7Inhibitors………………………………………………………………………...126

*4.3.8 Serological Analysis…………………………………………………………..*126
*4.3.9 Statistical Analysis……………………………………………………………..*127
4.4 Results.. 127
*4.4.1 Both WASP and N-WASP are activated in response to antigenic stimulation but With different timing..*127
*4.4.2 Both WASP and N-WASP are critical for antigen-induced BCR aggregation and B cell morphological changes but the two play distinct roles............................*131
*4.4.3 BCR signaling is enhanced and prolonged in N-WASP KO B cells................*136
*4.4.4 The level of autoantibody is elevated in mice with B cell specific N-WASP gene deletion...*141
*4.4.5 WASP promotes and N-WASP inhibits F-actin accumulation in the B cell Contact zone……………………………………………………………………*144
*4.4.6 N-WASP plays a dominant role in BCR internalization…………………………*146
*4.4.7 Mutual regulation between WASP and N-WASP……………………………...*152
*4.4.8 The activation of WASP and N-WASP is inversely regulated by BCR signaling………………………………………………………………………*155
4.5 Discussion...158

CHAPTER 5. GENERAL CONCLUSIONS AND FUTURE EXPERIMENTS………..167

REFERENCES..174

LIST OF FIGURES

Figure1.1.Stages of B-cell development…………………………………………………..7

Figure1.2.BCR signaling pathway………………………………………………………...16

Figure1.3.Protein structure of WASP and N-WASP…………………………………….32

Figure2.1.Both Btk and SHIP-1 regulate B-cell spreading and BCR cluster formation and accumulation in response to membrane associated antigen……………………46

Figure2.2.The effect of Btk deficiency on BCR cluster formation and B-cell spreading is not due to B-cell developmental defect in xid mice…………………………………50

Figure2.3.SHIP-1 deficiency inhibits the centripetal movement of BCR microclusters……………………………………………………………………………..53

Figure2.4. SHIP-1 deficiency increases the signaling capability but inhibits the growth of BCR microclusters…………………………………………………………………….58

Figure2.5.Btk and SHIP-1 have opposing roles in antigen-induced actin reorganization……………………………………………………………………………62

Figure2.6.SHIP-1 regulates WASP activation, B-cell spreading, and BCR cluster formation and accumulation in a Btk dependent manner……………………………65

Figure2.7.WASP deficiency inhibits BCR cluster formation, B-cell spreading, and tyrosine phosphorylation………………………………………………………………… 69

Figure3.1.The recruitment of F-actin to BCR aggregates in B-cells stimulated by membrane associated or soluble antigen……………………………………………… 89

Figure3.2.Both membrane-associated and soluble antigens trigger actin polymerization at BCR aggregates……………………………………………………92

Figure3.3.Both membrane-associated and soluble antigens induce the recruitment of cofilin in a signaling-dependent manner………………………………………………97

Figure3.4.The recruitment of gelsolin to BCR clusters in B-cells stimulated by soluble or membrane-associated Ag……………………………………………………………100

Figure3.5.Inhibition of actin reorganization blocks BCR aggregation and cell spreading in membrane-associated antigen-stimulated B-cells……………………103

Figure3.6.Disruption of the actin cytoskeleton alters signal activation in response to both membrane-associated and soluble antigens and antigen-independent signal activation……………………………………………………………………………..106

Figure4.1.N-WASP is activated following WASP activation upon antigen stimulation…………………………………………………………………………………129

Figure4.2.Antigen induced BCR aggregation and B cell spreading depend on both WASP and N-WASP………………………………………………………………………134

Figure4.3.Differential effects of WASP and/or N-WASP KO on BCR signaling…….139

Figure4.4.The serum levels of anti-nuclear and anti-dsDNA antibody are elevated in cNKO mice…………………………………………………………………………………142

Figure4.5.WASP promotes and N-WASP inhibits the F-actin accumulation in the B cell contact zone……………………………………………………………………… 148

Figure4.6.N-WASP plays a dominant role in BCR internalization……………………150

Figure4.7.WASP and N-WASP negatively regulates each other……………………153

Figure4.8.WASP and N-WASP are inversely regulated by Btk and SHIP-1………156

Figure4.9.A working model for the coordination of N-WASP with WASP in the regulation of BCR signaling……………………………………………………………164

LIST OF ABBREVIATIONS

AF	Alexa Fluro
AU	Arbitrary unit
BCR	B-cell receptor
Btk	Bruton’s tyrosine kinase
cDKO	Double knockout
cNKO	B cell specific N-WASP knockout;
FI	Fluorescence intensity
FIR	Fluorescence intensity ratio
IRM	Interference reflection microscopy
KO	Knockout
mAg	Membrane associated antigen
MFI	Mean fluorescence intensity
N-WASP	Neuronal Wiskott-Aldrich syndrome proteins
pAkt	Phosphorylated Akt
PBMC	Peripheral blood mononuclear cells
pBtk	Phosphorylated Bruton’s tyrosine kinase
p-Cofilin	Phosphorylated cofilin
PI3K	PI3 kinase
PI(3,4,5)P_3	Phosphatidylinositol-3,4,5-triphosphate
PLCγ2	Phospholipase Cγ2
pN-WASP	Phosphorylated N-WASP

pSHIP	Phosphorylated SHIP
pWASP	Phosphorylated Wiscott Aldrich symptom protein;
pY	Phosphotyrosine;
sAg	Soluble antigen;
SHIP-1	SH2-containing inositol-5 phosphatase-1;
TFI	Total fluorescence intensity;
TIRFm	Total internalization reflection microscopy;
TLR	Toll-like receptor;
Tf	Transferrin;
WKO	WASP knockout;
WASP	Wiskott-Aldrich syndrome proteins;

Chapter 1: General introduction

The immune system is a biological organization that is constituted by cells and molecules and functions to protect host against infections. A collective and coordinated reaction of the immune system to a foreign substance is called an immune response. Immune responses can be elicited not only by microbes, but also by molecules such as proteins and polysaccharides. The immune system can detect foreign substances from viruses to parasites and distinguish foreign substances from host self.

The immune system consists of two major branches: innate and adaptive immunity. The innate immunity is also called natural or native immunity. The innate immune system is characterized by rapid immune response to microbes and reacting in a similar way to repeated infections. The innate immune system exists before infection, is relatively non-specific, and does not confer long-lasting immune response against a pathogen. However, it is conserved among most organisms for protecting against foreign substances. The principle components of innate immune system include physical or chemical barriers, phagocytic cells or nature killer cells, blood proteins and cytokines. The innate response is elicited by structures that are conserved among the broad groups of microbes. These structures are recognized by pattern recognition receptors on immune cells.

In contrast to innate immune system, adaptive immune system can remember and response more vigorously to repeated exposures to the same microbe and distinguish different but closely related microbe and molecules. Adaptive immunity is highly specific, thereby called specific immunity. Foreign substances that can trigger specific immune responses are called antigens. For specific immune responses, an antigen is recognized and remembered through a group of signature structures and surfaces, called epitopes. There are two types of adaptive immune responses: humoral immunity and cell-mediated immunity. Humoral immunity is mediated by immunoglobulin proteins or antibodies generated by B cells and B cell effectors. Cell-mediated immunity is mediated by T lymphocytes. Humoral immunity generally targets extracellular microbes and their toxins, while cell-mediated immunity targets intracellular microbes, killing host cells with intracellular pathogens.

1.1 B lymphocytes

B lymphocytes, the cells that mediate antibody responses, refer to bursa-derived or bone marrow-derived lymphocytes. B cells recognize antigen by membrane immunoglobulin-based B cell antigen receptor (BCR) expressed on the cell surface. The binding of antigen to the BCR induce signal cascades in the cytoplasm. The antigen-BCR is taken up by B cells through endocytosis and processed into peptides through proteolysis. The processed peptides are presented by MHC class II molecules on the B cell surface to activate helper T cells. Activated T cells release cytokines to activate B cells [1]. Activated B cells undergo clonal expansion and differentiation into plasma cells, leading to the production of specific antibodies that circulate in blood and lymph organs. The binding of antibody to pathogens and toxins prevents them from interacting with host targets, consequently achieving neutralization. Bound antibodies activate complement cascades and phagocytosis by phagocytes, which lead to the destruction of pathogens [2].

The antibody induction process is different between the first and the following encountering of B cells with the same antigen, which has been classified into primary and secondary antibody response. When encountering an antigen for the first time naive B cells initate a primary antibody response, which is characterized as a slow (taking two weeks), short-lived (lasting for one to two weeks) and low affinity IgM dominant response. A secondary antibody response is induced by memory B cells that are generated during the primary response. Differing from the primary antibody response, the secondary antibody reponse is fast, robustic, and long lasting, consisting of great amounts of and high affinity antibodies. The activation of B cells initiates from the binding of the BCR. The BCR is a complex of membrane immunoglobulin (mIg) and Igα/Igβ heterodimer. Cross-linking mIg by antigens leads to the phosphorylation of Igα and Igβ, which initiates BCR signaling cascades. The signaling cascades activates multiple transcriptional factors, such as Myc, NFAT, NF-κB and AP-1, which induce the expressions of critical genes that are required for the activation and proliferation of B cells. Antigen binding also induces BCR internalization of antigen into the endosomal system. In endosomes, antigen is proteolytically fragmented into peptides, which are displayed by MHC class II molecules on the B cell surface to attract CD4+ helper T cells. Activated B cells are antigen presenting cells (APCs) and express the costimulatory molecules B7-1 and

B7-2 that are essential for T cell activation. Through antigen presentation, B cells acquire T cell help and regulate other immune branches by modifying T cell activities [3,4].

B cells encounter antigens in well organized follicles localized in the secondary lymph tissues. Antigens are drained from lymphatic and blood circulation and transported by dentritic cells and macrophages into the secondary lymphoid tissues. Folllowing antigenic activation, B cells migrate to T cell zones, where B cells engage cognate CD4+ helper T cells through antigen-MHC class II complexes and B7 costimulators. Activated T cells increase the expression level of CD40 ligand (CD40L), which binds its receptor, CD40, on the B cells and secrete IL-2, IL-4 and IL-5. These together promote B cell proliferation and differentiation [3,4].

1.2 B lymphocyte development and maturation

B cells are derived from hematopoietic stem cells in the bone marrow together with all blood cells. The maturation process of B cell from common lymphoid progenitors occurs in the bone marrow, different from T cells that will migrate from bone marrow to thymus to fulfill the maturation [2,5].The precursors of B cells undergo several distinct stages to develop into mature B cells (Fig 1.1), including pro-B cells, pre-B cells, immature B cells, transitional B cells and mature naive B cells [5,6,7]. Cytokines and membrane-bound proteins expressed by stromal cells in the bone marrow are very important for the maturation of B cells in these stages [5,6]. IL-7 is essential for B cell development, since mice with IL-7 or IL-7 receptor deficiency have almost no mature B cells [8]. Besides IL-7, the adhesive interactions between developing B cells and the adhesion molecules such as VCAM-1 and VLA-4 on the marrow stromal cells are critical for the proliferation of immature B cells [9].

Each developmental stage is marked by the expression of distinct genes. In addition to expressing Igα/β heterodimer, the signaling component of the BCR, the key event of B cell development is Ig gene recombination, which generates a diverse repertoire of Ig and Ig-based BCR. Functional mIg genes are created by a process called somatic recombination, in which a limited set of germline DNA sequences that are initially separated from one another are brought together by enzymatic deletion and religation [10]. V(D)J recombination generates hilghly varied antigen binding abilities of Ig. The immunoglobulin gene is made up of three separate loci that encode Ig κ light chain, Ig λ light chain and Ig heavy chains. The heavy chain locus rearranges first on one of the two chromosomes, and the productive rearrangement of one heavy chain allele inhibits the rearrangement of the other allele, which is called allelic exclusion. The successful gene rearrangement of heavy chain locus generates Ig μ chains, which form a complex with invarible surrogate light chains to become pre-BCR. The expression of pre-BCR marks the generation of pre-B cells and is critical for the development of B cells from pre-B cells forward. Signals from pre-BCR stimulate the rearrangement of Ig light chain. The κ locus rearranges first, and the productive recombination of the κ locus inhibits the rearrangement of the λ locus, which is called light chain isotype exclusion.

Each germline Ig locus is made up of three different types of gene segments, the

V, C and joining (J) segments and each Ig heavy chain locus has additional diversity (D) segments. V(D)J recombination is mediated by two enzymes, RAG1 and RAG2, which are expressed exclusively in lymphocytes [10]. Pro-B cells express B cell specific genes, such as CD19 and CD10, but not Ig. Pre-B cell is the earliest cell type that expresses μ heavy chain that is associated with invariant surrogate light chains, λ5-V-pre-B, as pre-BCR that is required for the maturation of B cells. The successful rearrangement of κ or λ light chain enables the expression of mIgM-based B cells, which leads to B cell development into immature B cell stage. The expresson of mIgM allows immature B cells to bind antigen. Immature B cells undergo apoptosis upon recoganiztion of self-antigens in the bone marrow. This negative selection process is essential for generating the B cells populations that only recognize foreign pathogenic antigens. There are two known negative selection mechanisms. The binding of immature B cells to high affinity multivalent antigens induces programmed cell death, leading to clonal deletion [11,12,13]. However, these immature B cells can be rescued by Ig editing and become into non-auto reactive B cells. The binding of immature B cells to low valent, low affinity soluable antigens leads to B cell anergy. Anergic B cells, which lose IgM expression but gain IgD expression, do not respond to antigenic stimulation after migrating to perphery. After migrating to the secondary lymphoid tissues, immature B cells further matured into transitional B cells. Mature native B cells coexpress IgM- and IgD-based BCRs at the cell surface [2,14,15].

Fig1.1. Stages of B-cell development. B-cell development occurs in both the bone marrow and peripheral lymphoid tissues such as the spleen. In the bone marrow, development progresses through the pro-B-cell, pre-B-cell and immature-B-cell stages. During this differentiation, rearrangements at the immunoglobulin locus result in the generation and surface expression of the pre-B-cell receptor (pre-BCR, which is comprised of an Igμ heavy chain and surrogate light chains (VpreB or $V_{\lambda}5$)) and finally a mature BCR (comprised of rearranged heavy- and light-chain genes) that is capable of binding antigen. At this immature stage of development, B cells undergo a selection process to prevent any further development of self-reactive cells. Both receptor editing and clonal deletion have a role at this stage. Cells successfully completing this checkpoint leave the bone marrow as transitional B cells, eventually maturing into mature follicular B cells (or marginal-zone B cells). Following an immune response, antigen-specific B cells develop into either plasma (antibody-secreting) cells or memory B cells. Transitional 3 (T3) B cells, once thought to be part of the linear development from immature to mature B cells, are now thought to represent primarily self-reactive anergic B cells (also known as An1 B cells) [16].

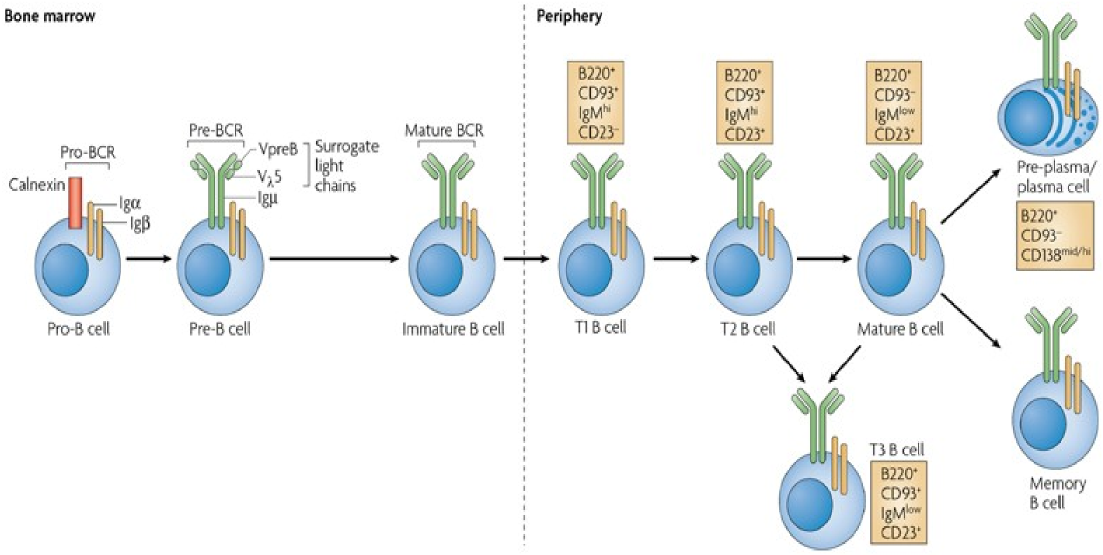
Bone marrow
Periphery
Pro-BCR
Calnexin
Igα
Igβ
Pro-B cell
Pre-BCR
VpreB
$V_\lambda 5$
Igμ
Surrogate light chains
Pre-B cell
Mature BCR
Immature B cell
$B220^+$ $CD93^+$ IgM^{hi} $CD23^-$
T1 B cell
$B220^+$ $CD93^+$ IgM^{hi} $CD23^+$
T2 B cell
$B220^+$ $CD93^-$ IgM^{low} $CD23^+$
Mature B cell
Pre-plasma/ plasma cell
$B220^+$ $CD93^-$ $CD138^{mid/hi}$
Memory B cell
T3 B cell
$B220^+$ $CD93^+$ IgM^{low} $CD23^+$

In the peripheral lymphoid organs, naive mature B cells enccounter antigens and acquire T cell help, which lead to cell proliferation and heavy chain class switching from μ and δ into γ, α or ε depending on the cytokine environment. Activated B cells differentiate into plasma cells that secrete antibodies or membrane Ig-expressing memory B cells that persist for long time. Besides naive mature B cells matured in the bone marrow which are also called B2 B cells, there is another B cell population, called B1 cells. B1 cells are originated from the fetal liver and primarily found in the peritoneum [17,18]. There are two subsets of B1 B cells: B1a B cells that express CD5 and B1b B cells that are negative with CD5. B1 B cells express high levels of mIgM on the cell surface, and their IgM-based BCR have relatively low affinity and polyspecificity to common surface patterns of pathogens but limited repertoires [17,18]. B1 B cells develop before the maturation of B2 B cells and function to maintain IgM antibody and mount rapid IgM antibody responses to pathogens. Because it occurs before B2 B cell-mediated antibody response and in a T cell independent manner, B1 B cell-mediated antibody responses are considered as a part of innate immunity [17,18].

The subsets of mature B cells in the peripheral lymphoid organs include follicular B cells and marginal zone B cells. Follicular B cells reside in B cell zones of the primary follicles, around the follicular dendritic cells in the white pulp of the spleen and cortical areas of peripheral lymph nodes [19]. Majority of B cells in the peripheral lymphoid organs are follicular B cells that can be distinguished from marginal zone B cells using surface markers ($CD19^{+}$ $CD23^{high}$ $CD21^{low}$). Marginal zone B cells are non-circulating B cells that are segregated anatomically to the marginal zone of the folicules and can be identified with the surface marker as CD19^{+} CD23^{low} CD21^{high} cells [19]. Similar to B1 B cells, marginal zone B cells can response to the blood-borne antigens rapidly as the first line of defense in a T cell-independent manner, and has a lower activation threshold than that of follicular B cells[20,21].

1.3 B cell effector responses and memory

The generation of secondary antibody response and memory B cells requires helper T cells. Because T cells are limilted in their antigen recognition to proteins and some polysaccharide, T cell dependent antigens are primarily protein antigens. T cell dependent antibody responses are highly specific, high affinity and isotype switched [22]. Antigens, which T cells are unable to recognize but are able to activate B cells to proliferate and differentiate into plasma cells without T helper cells, are considered as T cell independent antigens. These antigens usually contain multiple identical epitopes such as polysacchrides and glycolipds and can cross-link B cell receptors efficiently [23,24]. T cell independent antibody responses are relatively low affinity and mainly consist of IgM [23,24]. Signals from pathogen pattern recongnition receptors are critical for inducing an effective antibody response from T cell independent antigen.

From the recognition of antigen to the generation of antibodies, B cells mount antibody response via a series of sequential events, including recognition, activation, proliferation and differentiation phases. At the recognition stage, antigens binding to the BCR induces biochemical signal cascades in B cells [25]. In addition to antigenic signals, the activation of B cells can be enhanced by complement proteins, which bind to the type 2 complement receptor CD21 complexed with the costimulatory molecule CD19 on B cells [26,27], and by molecules with pathogenic patterns, which binds Toll like receptors (TLRs). Activated B cells enlarge their size, expand their biosynthetic organelles, and increase gene transcription and translation, including antiapoptotic genes, MHC class II molecules, costimulatory moelcues (B7-2 and B7-1) for T cell activation, and cytokine receptors. The early phase occurs at the boarder of T cell-rich zones and primary follicles, which results in the B cell proliferation and germinal center formation. The late phase occurred in the germinal centers where B cells undergo isotype switching, affinity maturation and differentiation into memory B cells and plasma cells[28,29,30,31,32,33]. During affinity maturation process, B cells with high affinity to antigen are selected to differentiate into memory B cells and plasma cells secreting high affinity antibody[28,29,30,31,32,33]. Memory B cells are responsible for mounting the secondary antibody responses. These B cells express mIg with high affinity, and also have abilities to persist and to rapidly proliferate and differentiate into plasma cells upon antigenic stimulation[34,35,36], Unlike their precusors, plasma cells lose the expression of the BCR, MHC class II, and most of B cell markers, thereby no long being able to undergo isotype switching or present antigens [34,35,36]. It recently has been shown that a low level of mIg influences the lifespan and location of plasma cells together with other signals, such as T cell cytokines during plasma cell differentiation[34,35,36]. However, how memory B cells and long-lived plasma cells persist and how memory B cells mount fast and robust antibody responses remain elusive.

1.4 The BCR and its signaling pathways

All BCRs have the same basic structure but have a variable region for binding to different antigens. The core structure of each BCR is mIg, composed of two identical heavy chains and two identical light chains. Each heavy chain covalently links to a light chain by a disulfide bond, and two heavy chains are also connected by at least one disulfide bond. Both heavy and light chains have a variable region at the N-terminus and constant regions at the C-terminus [37,38,39,40,41]. The heavy chain V region is composed of one Immunoglobulin (Ig) domain and C region is composed of three or four Ig domains. The light chain V region has one Ig domain and C region has one Ig domain. The V regions of a heavy chain and a light chain together form antigen binding sites. There are hypervariable regions in the variable domain, which are called complementarity-determining regions (CDR) because the hypervariable regions are complementary to the three-dimensional structure of bound antigen [42,43]. CDR3 is the most variable region [44]. BCRs have five classes based on the structure of the C regions of the heavy chain. The same isotype BCRs have the same amino acid sequence for the C regions of the heavy chain. Different from secreted Ig, membrane Ig (mIg) has a transmembrane domain in each of the two heavy chains, which anchor Ig at the membrane. In addition, mIgs do not form polymers, unlike pentamers of secreted IgM and dimers of secretory IgA. Membrane IgM and mIgD molecules only have three amino acids extended to the cytoplasm, but mIgG and mIgE have up to 30 amino acid residues. Membrane Igs are non-covalently associated with Igα/Igβ heterodimer by charges, which contain an immunoreceptor tyrosine-basied activation motif (ITAM) in each cytoplasmic tail. Igα/Igβ heterodimer is responsible for signal transduction and essential for the expression of mIgM and mIgD at the cell surface [45,46,47]. When BCRs are cross-linked by antigens, the tyrosines in the ITAMs of Igα and Igβ are phosphorylated by Src family tyrosine kinases, such as Lyn, Blk and Fyn. The tyrosin kinase Syk then binds to the phsphorylated ITAM domain of Igα/Igβ via its SH-2 domain, which activates autophosphorylation and its kinase activity. Once activated, Syk activates multiple downstream signaling molecules. One of these is the phosphatidylinositol phospholipase γ2 (PLCγ2), which hydrolyze phosphatidylinositol bisphsphate (PIP$_2$) into inositol trisphosphate (IP$_3$) and diacylglycerol (DAG). IP$_3$ activates the intracellular Ca2$^+$ release from ER, which leads to the rapid influx of Ca^{2+} from the extracellular environment. Ca^{2+} influx induces the translocation of PKC to the plasma membrane where PKC is activated by DAG [48,49,50,51]. The activated PKC in turn phsphorylates and activates multiple signaling molecules. After BCRs are cross-linked by antigens, Ras protein is also activated through an adaptor protein complex, Grb2 and SOS, which leads to the activation of mitogen-activated protein (MAP) kinases [48,49,50,51]. The activated downstream signaling molecules ultimately activate transcription factors that induce the expression of genes whose products are required for activation of B cells (Fig 1.2) [48,49,50,51].

There are several BCR coreceptors that are known to be involved in B cell activation. CD19 is a B cell specific co-stimulaotry molecule that is expressed from the early stage of B cell development until B cells differentiate into plasma cells. CD19 acts as a signaling component of a co-receptor complex containing CD21 and CD81. CD21, a complement receptor, becomes cross-linked with the BCR through complement opsonized antigen. This cross-linking brings the co-receptor complex near the BCR, where CD19 is phosphorylated by Src-family kinases. The phosphorylated cytoplasmic tail of CD19 recruits PI3 kinase and Bruton's tyrosine kinase [52], which decreases the threshold and increase the magnitude of BCR signaling. The binding of antigen to the BCR also induces the recruitment of CD19 to the BCR, which enhances BCR signaling [53]. However, the mechanism underlying such CD19 recruitment remains elusive.

FcγRIIB is the inhibitory coreceptor of the BCR. This receptor is a single chain glycoprotein consisting of an Fc-binding extracellular domain and a cytoplasmic domain containing a distinctive immunoreceptor tyrosine-based inhibitor motif (ITIM). FcγRIIB binds the Fc region of IgG with low affinity. IgG-antigen immune complexes that co-ligate BCR with FcγRIIB induce phosphorylation of tyrosines in the ITIM, which is required for its inhibitory activity [54]. The phosphorylated ITIM provides a binding site for the SH2 domain of the inhibitory signaling molecule SHIP and enables the activation of SHIP by Lyn. SHIP abrogates BCR signaling mediated via ITAM by hydrolyzing phosphatidylinositol-3,4,5- biphosphate [PI(3,4,5)P_3] into PI(3,4)P_2. In the absence of PI(3,4,5)P_3, PI(3,4,5)P_3 binding proteins (e.g. Btk, Akt and PLCγ2) are released from the membrane and this blocks calcium flux by preventing influx of extracellular calcium through the capacitance-coupled channel [55,56]. Consequently, FcγRIIB phosphorylation leads to an arrest of BCR triggered proliferation and down regulation of antibody production, cytokine release, proliferation, and cell survival [57,58,59,60].

1.5 Early event of BCR signaling

The initiation of BCR activation has long been shown to require receptor cross-linking by antigen [61,62], which oligomerizes or organizes surface BCRs into two dimensional clusters of different sizes depending on the valence and physical configuration of the antigen. Clustered receptors are preferentially associated with cholesterol- and glycolipid-rich lipid rafts, where ITAMs are phosphorylated by lipid raft-resident Src kinases, such as Lyn [63,64,65]. Phosphorylated ITAMs recruit downstream kinases and adaptor proteins. The key upstream signaling molecule Syk kinase binds to fully phosphorylated ITAMs, which activates its tyrosine kinase activity. Active Syk in turn phosphorylates and activates signaling molecules that are recruited to the BCR and lipid rafts, including phospholipase Cγ2 (PLCγ2), phosphoinosital-3 kinase (PI3K), Bruton's tyrosine kinase (Btk), and adaptor proteins, BLNK and Grb2, as well as costimulatory coreceptor CD19 [66,67]. These lead to the formation of signalosomes and the induction of biochemical cascades in the cytoplasm from the signalosomes.

Although traditional biochemical techniques have characterized chemical components of BCR signaling pathways and provide us a foundation to understand

Fig 1.2. B cell receptor signaling. The B cell antigen receptor (BCR) is composed of membrane immunoglobulin (mIg) molecules and associated Igα/Igβ (CD79a/CD79b) heterodimers (α/β). The mIg subunits bind antigen, resulting in receptor aggregation, while the α/β subunits transduce signals to the cell interior. BCR aggregation rapidly activates the Src family kinases Lyn, Blk, and Fyn as well as the Syk and Btk tyrosine kinases. This initiates the formation of a "signalosome", composed of the BCR, the aforementioned tyrosine kinases, adaptor proteins such as CD19 and BLNK, and signaling enzymes such as PLCγ2, PI3K, and Vav. Signals emanating from the signalosome activate multiple signaling cascades that involve kinases, GTPases, and transcription factors. This results in changes in cell metabolism, gene expression, and cytoskeletal organization. The complexity of BCR signaling permits many distinct outcomes, including survival, tolerance (anergy) or apoptosis, proliferation, and differentiation into antibody-producing cells or memory B cells. The outcome of the response is determined by the maturation state of the cell, the nature of the antigen, the magnitude and duration of BCR signaling, and signals from other receptors such as CD40, the IL-21 receptor, and BAFF-R. Many other transmembrane proteins, some of which are receptors, modulate specific elements of BCR signaling. A few of these, including CD45, CD19, CD22, PIR-B, and FcγRIIB1 (CD32), are indicated here in yellow. The magnitude and duration of BCR signaling are limited by negative feedback loops including those involving the Lyn/CD22/SHP-1 pathway, the Cbp/Csk pathway, SHIP, Cbl, Dok-1, Dok-3, FcγRIIB1, PIR-B, and internalization of the BCR. In vivo, B cells are often activated by antigen-presenting cells that capture antigens and

display them on their cell surface. Activation of B cells by such membrane-associated antigens requires BCR-induced cytoskeletal reorganization. Illustration reproduced courtesy of Cell Signaling Technology, Inc. (www.cellsignal.com)

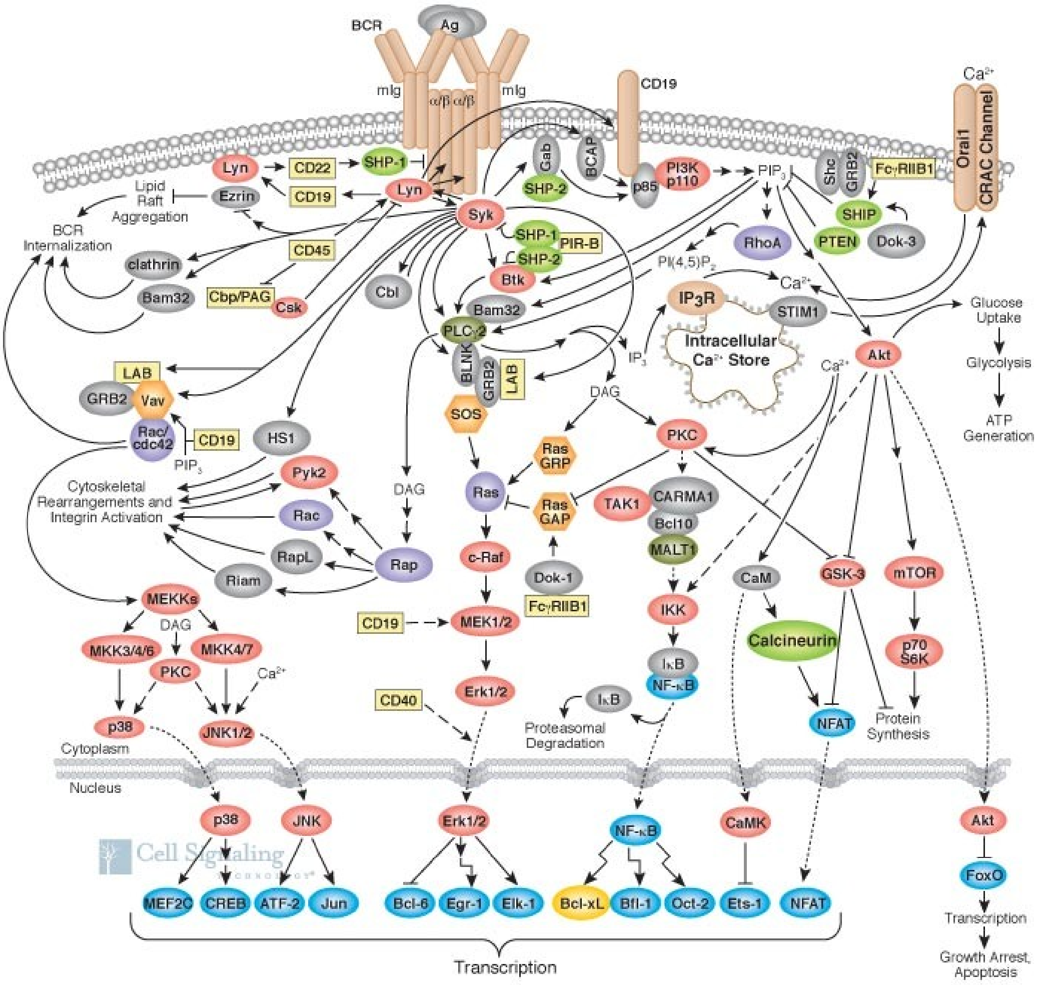
BCR
Ag
mIg
α/β α/β
mIg
CD19
Ca²⁺
Orai1
CRAC Channel
Lyn
CD22
SHP-1
Lyn
CD19
Lipid
Raft
Aggregation
Ezrin
BCR
Internalization
Gab
SHP-2
BCAP
p85
PI3K
p110
PIP₃
Shc
GRB2
FcγRIIB1
SHIP
PTEN
Dok-3
Syk
SHP-1
PIR-B
SHP-2
Btk
RhoA
PI(4,5)P₂
clathrin
Bam32
CD45
Cbp/PAG
Csk
Cbl
Bam32
PLCγ2
IP₃R
Ca²⁺
STIM1
Intracellular
Ca²⁺ Store
IP₃
Glucose
Uptake
Glycolysis
ATP
Generation
Akt
Ca²⁺
BLNK
GRB2
LAB
LAB
GRB2
Vav
Rac/
cdc42
CD19
PIP₃
HS1
SOS
DAG
PKC
Ras
GRP
Ras
Ras
GAP
TAK1
CARMA1
Bcl10
MALT1
Cytoskeletal
Rearrangements and
Integrin Activation
Pyk2
Rac
RapL
Riam
Rap
DAG
c-Raf
Dok-1
FcγRIIB1
CD19
MEK1/2
Erk1/2
CD40
CaM
GSK-3
mTOR
Calcineurin
p70
S6K
IKK
IκB
NF-κB
IκB
Proteasomal
Degradation
NFAT
Protein
Synthesis
MEKKs
DAG
MKK3/4/6
MKK4/7
PKC
Ca²⁺
p38
JNK1/2
Cytoplasm
Nucleus
p38
JNK
Erk1/2
NF-κB
CaMK
Akt
FoxO
Transcription
Growth Arrest,
Apoptosis
MEF2C
CREB
ATF-2
Jun
Bcl-6
Egr-1
Elk-1
Bcl-xL
Bfl-1
Oct-2
Ets-1
NFAT
Transcription
Cell Signaling
TECHNOLOGY

signaling events in B cell activation, it cannot provide information on the precise molecular mechanisms underlying the spatiotemporal dynamics of early B cell activation. The predominant form of antigen *in vivo* has been suggested to be attached to membrane surfaces, such that B cell membranes interact with other membranes to form BCR clusters and an immunological synapse [68]. Recent advances in high resolution live cell imaging, including total internal reflection fluorescence microscopy (TIRFm), enable us to reveal molecular details of receptor activation at the cell surface in real time. Upon interacting with antigen, particularly membrane-associated antigen, BCRs at the B cell surface briefly increase their lateral mobility (seconds) [69,70]. This is followed by immobilization of surface BCRs upon antigen engagement and concurrent formation of BCR microclusters [71]. While the microclusters interact with lipid rafts and lipid raft-associated Lyn, tyrosine phosphorylation activities in the microclusters rise and Syk is recruited to BCR microclusters [61,72,73]. Many signaling molecules are subsequently recruited to BCR microclusters, such as CD19, PLCγ2 and Btk [53,74], indicating that these microclusters function as signalosomes. BCR microclusters grow during the next few minutes by recruiting more receptors into clusters while moving towards one pole of the cells. In B cells interacting with membrane-associated antigen, BCR microclusters move towards the center of the B cell membrane region that contacts with the antigen presenting membrane (B cell contact zone). While moving centripetally, BCR microclusters merge into each other, forming a central cluster, a molecular complex similar to the immunological synapse formed between T cells and antigen presenting cells [68,75]. B cell membranes go through a spreading and contraction process after interaction with membrane bound antigens. This process is dependent on the ligand affinity and requires signaling and the actin cytoskeleton. The magnitude of the signal determines the extent of spreading and the extent of BCR aggregation, which influences the degree of B cell activation. The spreading area is dependent on the antigen density and antigen affinity [76]. Most of these results were obtained through B cells activated by membrane-associated and immobilized antigen. Dynamic clustering of surface BCRs is also a target for inhibitory signaling molecules. Colligation of the BCR with FcγRIIB by immune complexes inhibits the interaction of the BCR with lipid rafts and the formation of BCR microclusters and central clusters [63,77]. These further support that molecular dynamics and reorganization of BCRs at the B cell surface is a key event and regulatory target for BCR and B cell activation.

While antigen-induced receptor clustering has been clearly demonstrated to be required for BCR signaling activation [68,75], recent studies has shown that surface BCRs exist as clusters in nano-scales in the absence of antigen binding, which was demonstrated by single molecular imaging using direct stochastic optical reconstruction microscopy (dSTORM) [78] and molecular interaction using Forster resonance energy transfer [79]. These BCR clusters apparently are smaller than those induced by antigen, considering the number of BCRs in each cluster, since they are not detectable under confocal fluorescence microscope. In addition to their sizes, BCR conformation and BCR-BCR interactions within these nano-clusters likely are different from those within antigen-induced clusters. The lateral dynamics of these BCR nano-clusters have been implicated for regulating tonic signaling in resting B cells [78], and BCRs in nano-clusters have been postulated to be in an inhibitory conformation [80]. The physical constraint that antigen exerts onto BCRs has been shown to cause conformational changes of BCR [71,81], which can force BCRs in nano-cluster to change their ways to interact with each other and to reorganize into different types of clusters.

1.6 Btk and SHIP-1 in B cell signaling

Bruton's tyrosin kinase (Btk) is a key stimulatory kinase downstream both the BCR and CD19 [82]. The gene of *btk* is located in the X chromasome and encodes a cytoplasmic kinase. The mutations of Btk in human have been found to cause X-linked agammaglobulinemia (XLA) and in mice cause X-linked immunodeficient disease (Xid) [83]. XLA patients neither have B cells nor antibodies. Btk belongs to Tec family kinases that includes Tec expressed in both B and T cells and Itk expressed in T but not B cells. In addition to a kinase domain, Btk contains multiple protein-protein interaction domains, including a Src homology (SH) 1 domain (SH1), a SH2 domain, a SH3 domain, and a pleckstrin homology (PH) domain at the N-terminus [84,85,86,87]. Besides B cells, Btk is also expressed in myeloid and erythroid cells. Btk is expressed in most stages of B cell development but not in the plasma cells [88,89,90]. Btk has been shown to have critical roles in BCR signaling during B cell development and the activation of mature B cell stage as well as B cell signaling in response to CD40L, IL-5 and IL-10 [91,92,93,94,95,96]. XLA patients are found to have deletions, insertions and/or point mutations in Btk gene, which abolish Btk function and block B cell development in the early stages. Xid mice were found to have a point mutation in the PH domain, which prevents Btk from binding to PtdIn(3.4.5)P_3, consequently inhibiting Btk activation. However, this point mutation only leads to an inhibition but not a complete blockage of the B cell development [97,98]. The numbers of mature B2 cells in the spleen and B1a B cells in the peritoneum are significantly reduced in Xid mice, where most B cells are in the pre-B cell stage [83]. Consequently, the mice have decreased levels of IgM and IgG3 in the serum, reflecting a reduction of T cell independent antibody (type II) responses. B cells from Xid mice show defective proliferation in response to anti-immunoglobulin and anti-CD40 antibodies. Btk has multiple upstream activators, including Src family kinase such as Lyn, the product of PI3K, PIP3 [99]. In the absence of Lyn, Btk can still be activated, probably due to redundant functions of other Src family kinase proteins such as Fyn and Blk [99]. Direct association of PKCβ with Btk has been reported in mast cells. In B cells, Btk exhibits hyperphosphorylation upon BCR cross-linking in PKCβ deficient mice [100,101], suggesting PKCβ as a downstream terminator of Btk signaling [99]. The PH domain of Btk binds PI(3,4,5)P_3 with a high affinity [102,103], which brings Btk to the plasma membrane where it is phosphorylated by Src kinases. Overexpression of PI3K, which increases PI(3,4,5)P_3 production, leads to Btk hyperphosphorylation and synergistically promotes the $Ca2^+$ influx with PI3K [56]. The downstream effectors of Btk in B cells include PLCγ2 and phosphotidylinosital-5 kinase (PI5K). The activation of PI5K increases the production of PtdIn(4,5)P_2, and activated PLCγ2 hydrolyzes PI(4,5)P_2 into IP3 and DAG, which induces $Ca2^+$ flux into the cytoplasm [104]. The activation of Btk promotes the activation of the MAP kinase p38 and pJUNK [105], which leads to the transcription and translation of regulators for cell cycle and apoptosis [99], such as cdk2, cdk4, cyclins D2 and Bcl-x l[106].

SHIP-1 is a major inhibitory molecule in the signal transduction pathway of the BCR. It is a phosphatidyinosital-5 phosphatase with 145 kDa molecular weight and contains multiple protein-protein interaction domains, including an N-terminal SH2 domain, a proline rich domain (PRD) and two NPXY amino acid sequence at the C-terminus [107]. The SH2 domain of SHIP binds to phosphorylated tyrosine (pY) of ITIM [108]. The PRD preferentially binds to the SH3 domain of Grb2 and PLCγ [109]. The NPXY motifs bind to the phophoretyrosine base domain in Shc upon their own phosphorylation [110]. SHIP hydrolyzes PtdIn(3,4,5)P_3 into PtdIn(3,4)P_2 [110]. In B cells, SHIP is activated following BCR signaling activation by Lyn-mediated phosphorylation and by binding to partially phosphorylated ITAMs of the BCR. When BCR is colligated with FcRIIB, SHIP is recruited faster in a higher level than that of BCR cross-link only [111,112]. Recently SHIP is found to be activated in anergic B cells [113]. SHIP-mediated hydrolysis of PI(3,4,5)P_3 eliminates the docking sites for several PH domain containing proteins such as Btk, PLCγ and Akt. The tyrosine phsphorylation of NPXY is considered to be a sign of the activation of SHIP [114]. SHIP-1 knockout mice constructed by Humphries' group show aberrant B cell development with a reduced number of immature B cells in the bone marrow[115], while B cells from these mice show enhanced proliferation and survival, as well as increased activation levels of MAP kinases and Akt in vitro[115]. In SHIP-1 knockout mice, total IgG levels in the serum and T cell independent type II immune response to

TNP-ficoll are increased [116]. Since many immune cells express SHIP-1, such as macrophages, NK cells, dendratic cells and mast cells, SHIP-1-deficiency in those cells could contribute to the B cell phenotype [116]. Bollad's group constructed B cell specific SHIP-1 knockout mice used Cre-lox system. CD19 driven Cre recombinase is regulated by the CD19 promoter and deletes the *ship1* gene at the pro-B cell stage, providing an optimal system to study B cell intrinsic function of SHIP-1 [116]. In B cell specific SHIP-1 knockout mice, there are no obvious defects in the development of B cells in the bone marrow [116]. The common phenotype of total and B cell specific SHIP-1 knockout mice is the reduction in the number of recirculating B cells in the bone marrow and the spontaneous formation of the germinal center and antibody producing cells [116]. Peripherial B cells in B cell-specific knockout mice undergo spontaneous isotype switching but fail to increase BCR affinity through affinity maturation [116]. B cell specifc SHIP-1 knockout mice respond poorly against T cell dependent and independent antigens as well as the viral challenges. CD4 T cell specific SHIP-1 knockout mice, where SHIP deletion occurs at the double positive stage of T cell development, have no defects in T cell development in the thymus or peripherary, in contrast with the reduced number of peripheral T cells in the germline SHIP-1 deletion mice[116,117]. However, the number of regulatory T cells is increased in both germline SHIP deletion mice and T cell specific SHIP deletion mice. In addition, there is no difference on the phosphorylation levels of PLCγ, ZAP70, Akt, Erk and Ca^{2+} flux, as well as the in vivo proliferation in response to antigen stimulation [116]. In CD4 T cell specific SHIP-1 knockout mice, T cells polarize toward Th1 responses and diminish Th2 responses by regulating sensitivity to cytokines[116,117].

1.7 BCR-mediated antigen uptake and processing

In addition to the induction of BCR signaling activation, antigen binding also triggers rapid BCR internalization [118,119,120,121]. BCR internalization leads to antigen uptake into the endosomal system, where protein antigens are fragmented and assembled with MHC class II molecules. Antigenic peptides are then presented with MHC class II at the B cell surface for T cell recognition [122,123]. The interaction of B cells with T helper cells through antigen presentation induces the formation of immunological synapses at the interface between B and T cells. Signaling transduced through the synapse activates T cells, and activated T cells in turn provide B cells with additional stimulatory signals. The signals provided by T helper cells are essential for the generation of T cell dependent humoral memory responses [124,125,126,127,128,129]. The BCR can endocytose constitutively at a low rate. The binding of antigen, which induces signaling, dramatically increases BCR endocytosis. BCR internalization has been shown to be clathrin-mediated [119,130,131] and dynamin dependent [132,133]. Our lab has previously demonstrated that antigen-induced BCR internalization, but not the constitutive internalization of the receptor in the absence of antigens, requires actin remodeling [134]. Inhibition of actin remodeling results in the accumulation of antigen bound BCRs in long invaginated clathrin coated pits. Our lab has identified actin binding protein 1 (Abp1, HIP-55 or SH3P7) as a linker between the actin cytoskeleton and the endocytosis machinery, based on its ability of simultaneously binding to F-actin and the PRD domain of dynamin 2 and the inhibitory effect of its gene knockout on BCR internalization [135]. The current model of my lab is that Abp1 brings the actin cytoskeleton to the dynamin restricted neck of clathrin coated pits, where actin generates a final push for the detachment of clathrin-coated vesicles from the plasma membrane. Since the constitutive internalization of the BCR is not dependent on the actin cytoskeleton, actin becomes one of the elements that help to speed up antigen uptake. The BCR can also be internalized in clathrin-independent pathway, since clathrin deficiency reduces 70% but not 100% of BCR internalization [130]. Interestingly, the 30% clathrin-independent BCR internalization was found to depend on the actin cytoskeleton. How actin contributes to this BCR internalization pathway is not clear.

In addition to facilitate the membrane fission of clathrin-coated pits, the actin cytoskeleton may also be involved in concentrating BCR-antigen complexes into clathrin-coated pits and generating membrane curvature for the formation of clathrin coated pit during BCR internalization. While the role of the actin cytoskeleton in generating BCR containing clathrin-coated pits has not been examined, the coordination of actin with Bar domain-containing proteins in membrane deformation has been extensively studied [136,137,138,139,140]. It is logical to speculate that BCR clustering facilitates BCR internalization. Blockage of BCR clustering by the actin stabilizer jasplakinolide not only inhibits BCR signaling, but also receptor internalization [134]. However, whether BCR internalization is directly regulated by the kinetics and magnitude of BCR clustering and requires the formation of the BCR central cluster remain to be determined.

Besides the initiation of antigen processing and presentation, BCR internalization can regulate receptor signaling function [141]. Chaturvedi et al. [133] show that the BCR forms different signaling complexes at different cellular locations. Phosphorylated Lyn, Syk and Erk are recruited to both the cell surface and endosomes, while the MAP kinases p38 and Jnk are recruited to endosomes but not the plasma membrane in response to antigenic stimulation. Inhibition of BCR internalization by the dynamin inhibitor dynasore or actin depolymerization increases the phosphorylation of MAP kinases, MEK1 and Erk but decreases the phosphorylation of AKT, consequently deregulating the activation of downstream transcription factors. While the dynamin inhibitor and actin depolymerization may alter BCR signaling independent of receptor internalization, these data collectively support the notion that actin-dependent BCR internalization can regulate BCR signaling by modulating the cellular location of the receptor.

1.8 Actin reorganization during BCR activation

Early studies have long noticed that B cell activation by antigen or mitogen induces actin remodeling [142,143]. The cortical actin network is the primary actin structure in B cells due to limited cytoplasmic spaces of lymphocytes at the resting stage. The cortical actin network generally provides structural support for the plasma membrane, and its dynamic reorganization generates cell morphologic changes. The cortical actin is a network of actin bundles and branches organized by a group of actin cross-linking proteins, which generate filopodia and lamellipodia, respectively [144]. The actin network is tethered to the plasma membrane through ezrin/radixin/ moesin (ERM) family proteins that are capable of binding both F-actin and transmembrane proteins [145,146]. The actin cytoskeleton is highly dynamic, constantly undergoing polymerization, depolymerization, association and disassociation with actin binding proteins. In addition to cell morphology, recent biophysical and cell biological studies reveal critical functions for the cortical actin in controlling molecular dynamics and organization at the cell surface [147,148]. Through interacting with membrane anchor proteins, actin dynamics physically influence lateral movement of membrane proteins that extend their cytoplasmic tails into the cortical actin network and create temporal mobility barrier, which leads to transient compartmentalization of different groups of membrane proteins. In B cells, mobility barrier generated by the cortical actin has been demonstrated by the following findings. Surface BCRs in actin- and ezrin-poor regions have a higher lateral mobility than those BCRs in actin- and ezrin-rich regions, and deletion of the cytoplasmic tails of the BCR releases it from lateral mobility barrier [70,149]. Therefore, the involvement of the actin cytoskeleton in the organization of surface BCRs into signalosome is evident.

The binding of antigen to the BCR first induces a very transient disassembly of the cortical actin network, which is concurrent with the brief increase in BCR lateral mobility discussed earlier [69,70]. The actin disassembly is dependent on cofilin-mediated actin severing and the disassociation of ezrin from the plasma membrane [69,70,150]. In B cells, ezrin has been shown to link the actin cytoskeleton to the plasma membrane by binding to a lipid raft-anchored protein, Csk-binding protein [150]. The disassociation of ezrin from Csk-binding protein is the result of ezrin phosphorylation induced by BCR signaling. The disassociation and severing of the actin network free BCRs and other membrane proteins from mobility barrier, allowing them to reorganize. Following this brief disassembly, actin undergoes a rapid and dramatic reassembly. The reassembly does not restore actin back to the pre-activation structure, rather into dynamic, polarized, and BCR-centric organizations.

1.9 Roles of the actin cytoskeleton in BCR signaling

The actin cytoskeleton has been demonstrated to have critical roles in BCR signaling. Actin regulates BCR signaling by modulating receptor organization at the B cell surface and B cell morphology. BCR induced signaling is a fast event where Ca^{2+} flux is triggered within a second, thereby requiring a rapid clustering of surface BCRs. BCR aggregation at the plasma membrane is dependent on the level of their lateral freedom for receptor-receptor interaction in the two dimensional fluid membrane. BCRs at the surface region with a relatively low level of F-actin have found to have higher lateral mobility than those at the surface region with a relatively high level of F-actin and tethered to the actin cytoskeleton by ezrin [149], which indicates the cortical actin network can control BCR lateral mobility and create boundaries for the lateral movement of BCRs and BCR signaling complexes. While the binding of multivalent ligands can provide the initial force to overcome this lateral confinement, reducing actin-generated confinement has been shown to be critical to BCR aggregation and signaling activation. Depolymerization of the actin cytoskeleton by treatment of latrunculin increases the lateral mobility of BCRs [149]. These results support the model that the cortical actin network in inactive and resting B cells inhibits BCR aggregation by limiting receptor lateral mobility and the dynamics of cortical actin organization can regulate both the basal and activation levels of signaling. The transient dephosphorylation of ezrin and actin depolymerization induced by BCR-antigen interaction is concurrent with a transient increase in the lateral movement of surface BCRs [69,70,149]. Manipulations of ezrin and meosin by siRNA knockdown, dominant negative and constitutively active mutants significantly affect the magnitude of BCR aggregation [70]. These data indicate that the decoupling and disassembly of the cortical actin, which provide more lateral freedom for surface BCRs, is a critical step for the initiation of BCR aggregation and signaling activation.

An early observation of antigenic activation influencing the physical relationship of both BCR and signaling molecules with the cytoskeleton [151,152,153,154] suggests another mechanism for actin to facilitate signaling: the actin cytoskeleton with actin adaptor proteins potentially serve as scaffoldings to bring signaling molecules physically close to the BCR. The reassembly of the actin cytoskeleton and the re-association of active ezrin with a lipid raft-associated protein after the initial detachment and disassembly [69,70,149,155,156] combines the lateral confinement of both the actin cytoskeleton and the lipid domain can further compartmentalize membrane proteins for receptor aggregation and receptor signaling complex formation. These hypotheses require further examination.

1.10 The role of WASP and N-WASP in B-cells

Antigen induced actin remodeling is dependent on BCR signaling. Signaling molecules regulate actin dynamics or organization by controlling the activities of a group of actin regulators. WASP is an actin nucleation promoting factor that is expressed exclusively in hematopoetic cells [157,158,159,160]. WASP belongs to a family of proteins including N-WASP and WAVE. WASP and N-WASP share similar proteins domains such as WASP-homology 1 domain, GTPase binding domain and VCA domain [157,158,159,160]. However, N-WASP has an extra IQ doman that can bind to calmodulin and verprolin domain (Fig 1.3.). In the unactivated condition, the GTPase binding domain interacts with the VCA domain, forming a closed auto-inhibited conformation [157,158,159,160]. The binding of Cdc42 and $PI(4,5)P_2$ to WASP leads to open comformation, which enables the binding of the VCA domain to Arp2/3 complex, which initiates the actin polymerization [157,158,159,160,161]. The open conformation allows the phosphorylation of its conserved tyrosine and serines, which further stabilizes the open and active conformation of WASP [162,163].

WASP is well known for its function in actin reassembly following BCR activation. The importance of this actin nucleation promoting factors in B cells is demonstrated by complicated immune disorders, including immune deficiency, autoimmune diseases, and lymphatic cancers, caused by WASP deficiency [164,165,166] and B cell autoimmunity resulted from B cell-specific WASP gene deletion [167,168].

Figure 1.3. Domain structure of WASP and N-WASP with sites of interaction between COOH- and NH_2-termini, and binding by other factors. The NH_2 terminus of WASP and N-WASP contain an EVH1/WH1 domain that binds the proline-rich protein, WIP. The NH_2 terminus of N-WASP also binds PIP_2, F-actin, and, through its IQ domain, calmodulin. The GTPase-binding domain (GBD) includes a Cdc42/Rac interactive binding (CRIB) motif and surrounding sequences. The GBD preferentially binds Cdc42 over Rac, and GTP-Cdc42 over GDP-Cdc42. In N-WASP, the basic sequence (B) binds PIP_2 . The PRD binds profilin, as well as several SH3-containing proteins, including: adaptors Nck and Grb2, tyrosine kinases, PLCγ1, and syndapin I. The VCA/WA (WASP homology II and acidic region) domain is the minimal fragment able to activate nucleation by the Arp2/3 complex. The V motif binds monomeric actin (G-actin), whereas the CA motif binds the Arp2/3 complex [169].

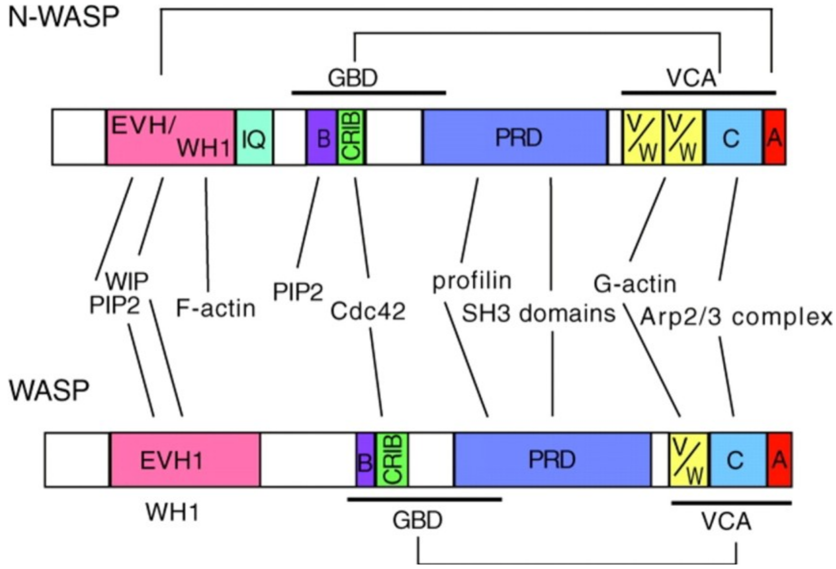
N-WASP
GBD
VCA
EVH/
WH1
IQ
B
CRIB
PRD
V/W
V/W
C
A
WIP
PIP2
F-actin
PIP2
Cdc42
profilin
SH3 domains
G-actin
Arp2/3 complex
WASP
EVH1
B
CRIB
PRD
V/W
C
A
WH1
GBD
VCA

Our lab has demonstrated that Btk is a main upstream signaling molecule responsible for WASP activation. Btk activates WASP by inducing the phosphorylation of Vav that activates Cdc42 or Rac, the phosphorylation of PI5K that increases the level of PI(4,5)P_2 and the phosphorylation of WASP [118]. Even though the phosphorylation of WASP is significantly decreased in Btk-deficient mouse B cells, whether Btk directly phosphorylates WASP or indirectly through activating another kinase is not known. The stronger effects of WASP and N-WASP double knockout (with N-WASP as B cell-specific conditional knockout) on B cell spreading on a CD44-coated surface, peripheral B cell development, and B cell-mediated antibody responses suggest an involvement of the ubiquitously expressed WASP homologue, N-WASP[170].

1.11 Hypothesis

Previous studies from our lab have shown that Btk can activate actin remodeling via activating WASP in response to antigenic stimulation. Btk is a key stimulatory kinase in BCR signaling pathway, and its activity is negatively controlled by the inhibitory phosphatase SHIP after BCR signaling activation. These lead to the central hypothesis of this thesis: Btk and SHIP positively and negatively regulate actin reorganization by activating and inhibiting the activation of WASP, and signaling controlled actin remodeling modulates B cell morphology and BCR clustering at the B cell surface, consequently providing positive and negative feedback to BCR signaling. Further, both WASP and its ubiquitous homolog N-WASP are required for antigen induced actin reorganization and optimal activation of BCR signaling.

1.12 Significance

Antigen binding to the BCR induces the activation of BCR signaling and actin reorganization. However, the underlying mechanism that links BCR signaling and actin reorganization is still unknown. This thesis focuses on the key positive and negative regulators of BCR signaling, Btk and SHIP-1 and studies their role in the initiation and regulation of actin remodeling. These studies will help us to understand the molecular mechanisms by which BCR signaling regulates B cell morphology, surface BCR dynamics and B cell activation via modulating actin dynamics. Our studies on the actin regulators, WASP and N-WASP will potentially provide explanations for how actin can provide optimal feedback to the BCR signaling. Overall, the results of these studies could help us to understand how BCR signaling controls actin reorganization and is regulated by actin-mediated feedback at the molecular level. The aberrant BCR signaling is known to lead to immunodeficiency and autoimmune disease, such as the XLA and WAS that are caused by the gene deficiency of Btk and WASP. The molecular mechanisms revealed by the studies presented in this thesis will provide new insights into how Btk and WASP deficiency causes immune deficiency and autoimmune diseases, and enlighten new ideas for development of immunotherapies for treating these two diseases and related immune diseases.

Chapter 2: A balance of Bruton's tyrosine kinase and SHIP activation regulates B cell receptor cluster formation by controlling actin remodeling

2.1 Abstract

The activation of the B-cell receptor (BCR), which initiates B-cell activation, is triggered by antigen-induced self-aggregation and clustering of receptors at the cell surface. While antigen-induced actin reorganization is known to be involved in BCR clustering in response to membrane-associated antigen, the underlying mechanism that links actin reorganization to BCR activation remains unknown. Here we show that both the stimulatory Bruton’s tyrosine kinase (Btk) and the inhibitory SH2-containing inositol-5 phosphatase-1 (SHIP-1) are required for efficient BCR self-aggregation. In Btk-deficient B cells, the magnitude of BCR aggregation into microclusters and B-cell spreading on antigen-tethered lipid bilayers are drastically reduced compared to wild type B-cells. In SHIP-1-deficient B-cells, surface BCRs aggregate into microclusters, but the centripetal movement and growth of BCR clusters are inhibited and B-cell spreading is increased. The persistent BCR microclusters in SHIP-deficient B-cells exhibit higher levels of signaling than merged BCR clusters. In contrast to the inhibition of actin remodeling in Btk-deficient B-cells, SHIP-1 deficiency enhances actin polymerization, F-actin accumulation, and WASP phosphorylation in a Btk-dependent manner. Thus, a balance between positive and negative signaling regulates the spatiotemporal organization of the BCR at the cell surface by controlling

actin remodeling, which potentially regulates the signal transduction of the BCR. This study suggests a novel feedback loop between BCR signaling and the actin cytoskeleton.

2.2 Introduction

The B-cell receptor (BCR) induces signaling cascades and antigen processing and presentation in response to antigen binding. These BCR-induced cellular activities combine with signals from the microenvironment to determine the fate of B-cells. Biochemical and genetic studies in the last two decades [66,171,172] have shown that upon cross-linking by antigen, surface BCRs aggregate and associate with lipid rafts [64], where they are phosphorylated by Src kinases, such as Lyn. The binding of tyrosine kinase Syk to phosphorylated immunoreceptor tyrosine-based activation motifs (ITAMs) in the cytoplasmic tails of the BCR activates Syk, which in turn activates downstream signaling components including phospholipase Cγ2 (PLCγ2), Ras, phosphatidylinositol 3-kinases (PI3K), and Bruton's tyrosine kinase (Btk). Antigen binding to the BCR also activates negative signaling components, in particular, SH2-containing inositol-5 phosphatase-1 (SHIP-1) [112,116,173] eliminating the docking sites of PLCγ2, Btk, and Akt at the plasma membrane and turning down BCR signaling [55,116].

Recent studies utilizing advanced cell imaging technologies have begun to reveal the molecular details of the initiation events in BCR activation [68,75,174]. Antigen binding induces conformational changes of the BCR, which expose the Cμ4 domain of membrane IgM for BCR self-aggregation [71] and ITAMs for signaling molecules to bind [61]. Self-aggregation reduces the lateral mobility of the BCR and induces the formation of BCR microclusters [71]. Newly formed BCR microclusters reside in lipid rafts [72] and recruit signaling molecules, including Lyn, Syk [61], PLCγ2, Vav [74], and the co-stimulatory receptor CD19 [53]. BCR microclusters grow in size by trapping more BCRs and merging into each other. This leads to the formation of a polarized central cluster, similar to the immunological synapse formed between T-cells and antigen presenting cells [175]. Therefore, the control of BCR mobility and self-aggregation is essential for signal initiation and transduction.

The surface mobility and aggregation of the BCR has been shown to require antigen-induced actin reorganization. The actin cytoskeleton is known to control cell morphology [144,176] and lateral diffusion of transmembrane proteins [176]. Recent studies have shown that membrane-associated antigens induce B-cell spreading, which is followed by cell contraction. These morphological changes of B-cells enhance the formation of BCR clusters. Disrupting the actin cytoskeleton inhibits this enhanced BCR cluster formation [76]. However, in the absence of antigen, actin disruption increases the lateral diffusion rate of surface BCRs and induces spontaneous signaling in B-cells [149]. These findings suggest that antigen-induced actin remodeling can regulate BCR self-aggregation by controlling B-cell morphology and BCR lateral mobility at the cell surface.

Antigen-induced actin reorganization, BCR microcluster formation and B-cell spreading all are signaling dependent processes. Multiple BCR signaling molecules, including CD19, PLCγ2, Vav, and Rac2, promote BCR cluster formation and B-cell spreading [53,74,177]. In contrast, co-engagement of the BCR and FcγRIIB, which activates SHIP-1, inhibits the formation of BCR clusters and BCR signaling [63,77]. We have previously shown that Btk can relay BCR signaling to the actin cytoskeleton by activating an actin nucleation promoting factor, Wiscott Aldrich symptom protein (WASP), via Vav and PtdIns [118]. These findings point to an intimate cooperativity between BCR signaling and the actin cytoskeleton. However, the underlying mechanism for the signaling-actin interplay during BCR activation remains unknown.

In this study, we used live cell imaging, total internal reflection fluorescence microscopy (TIRFm), interference reflection microscopy (IRM), and genetically altered mice to examine the molecular mechanism by which the actin cytoskeleton cooperates with early BCR signaling at the cell surface during BCR activation. Our results show that the positive and negative downstream signaling molecules of the BCR, Btk and SHIP-1, have distinct roles in self-aggregation and cluster formation of surface BCRs, B-cell morphology, and actin reorganization. The activation of Btk promotes B-cell spreading, BCR microcluster formation, and actin polymerization and accumulation. In contrast, SHIP-1 promotes the merger of BCR microclusters and B-cell contraction, but inhibits actin polymerization and accumulation. Our results suggest a balance of Btk and SHIP-1 activation controls the nature of actin reorganization, which in turn regulates the spatiotemporal organization of surface BCRs.

2.3 Materials and Methods

2.3.1 Mice and cells

Wild type (wt) (CBA/CaJ), xid (CBA/CaHN*Btkxid*/J) and CD19$^{Cre/+}$ (B6.129P2(C)-*Cd19*$^{tm1(cre)Cgn}$/J) mice were purchased from Jackson Laboratories (Bar Harbor, ME). B-cell specific SHIP-1 knockout mice CD19$^{Cre/+}$SHIP-1$^{Flox/Flox}$ were generated by crossing CD19$^{Cre/+}$ with CD19$^{+/+}$ SHIP-1$^{Flox/Flox}$ mice [178]. WASP$^{-/-}$ mice on a 129 SvEv background were kindly provided by Dr. Scott Snapper (Harvard Medical School, MA) [179] and 129 SvEv wt mice were from Jackson Laboratories. Splenic B-cells were isolated as previously described [118]. All animal work was reviewed and proved by the Institutional Animal Care and Usage Committee of University of Maryland.

2.3.2 Preparation of mono-biotinylated Fab' antibody

Mono-biotinylated Fab' fragment of anti-mouse IgM+G antibody (mB-Fab'-anti-Ig) was generated from the F(ab')$_2$ fragment (Jackson ImmunoResearch, West Grove, PA) using a published protocol [180]. The disulfide bond that links the two Fab' was reduced using 20 mM 2-mercaptoethylamine, and the reduced cysteine was biotinylated by maleimide activated biotin (Thermo Scientific, Odessa, TX). Fab' was further purified using Amicon Ultra centrifugal filters (Millipore, Temecula, CA). One biotin per Fab' was confirmed by a biotin quantification kit (Thermo Scientific). Fab' was labeled with Alexa Fluor (AF) 546 (Invitrogen, Carlsbad, CA).

2.3.3 Preparation of antigen-tethered planar lipid bilayers

The planar lipid bilayer was prepared as described previously [72,181]. Liposomes were made by sonicating 1,2-dioleoyl-sn-glycero-3-phosphocholine and 1,2-dioleoyl-sn-glycero-3-phosphoethanolamine-cap-biotin (Avanti Polar Lipids, Alabaster, AL) in a 100:1 molar ratio in PBS at a lipid concentration of 5 mM. Aggregated liposomes were removed by ultracentrifugation and filtration. Coverslip chambers (Nalge Nunc International, Rochester, NY) were coated with the planar lipid bilayer by incubating with the liposomes (0.05 mM) for 10 min. After extensive washes, the coated coverslip chamber was incubated with 1 μg/ml streptavidin (Jackson ImmunoResearch), followed by 2 μg/ml AF546-mB-Fab'-anti-Ig mixed with 8 μg/ml mB-Fab'-anti-Ig antibody. As a non-specific antigen, the coated coverslip was incubated with 1 μg/ml streptavidin (Invitrogen), followed by 10 μg/ml AF546 labeled biotinylated Fab-anti-rabbit IgG antibody. For a non antigenic control, surface BCRs were labeled by incubating with AF546-Fab-anti-Ig (2 μg/ml) on ice for 30 min. The labeled B-cells were then incubated with biotinylated holo-transferrin (Tf, 16 μg/ml, which gave an equal molar concentration of 10 μg/ml mB-Fab'-anti-Ig, Sigma-Aldrich, St. Louis, MO) tethered to lipid bilayers by streptavidin.

2.3.4 Total internal reflection fluorescence microscopy

Images were acquired using a Nikon laser TIRF system on an inverted microscope (Nikon TE2000-PFS), equipped with a 60X, NA 1.49 Apochromat TIRF objective (Nikon Instruments Inc., Melville, NY), a Coolsnap HQ2 CCD camera (Roper

Scientific, Sarasota, FL), and two solid-state lasers of wavelength 491 nm and 561 nm. For live cell imaging, time lapse images were acquired at the rate of one frame every 3 sec. Image acquisition started upon the addition of B-cells onto antigen-tethered lipid bilayers and continued for 5 to 10 min at 37°C. Interference refection images (IRM), AF488, and AF546 images were acquired sequentially.

To image intracellular molecules, B-cells were incubated with antigen-tethered lipid bilayers at 37°C for varying lengths of time. Cells were then fixed with 4% paraformaldehyde, permeabilized with 0.05% saponin, and stained for phosphotyrosine (Millipore), phosphorylated Btk (Y551, BD Bioscience, San Jose, CA), Akt (S473, Cell Singling Technology, Inc., Danvers, MA), and WASP (S483/S484, Bethyl Laboratory, Inc., Montgomery, TX). F-actin was stained using AF488-phalloidin. In the case of Btk inhibition, splenic B-cells were pretreated with LFM A-13 (50 or 400 μg/ml, EMD Bioscience, Gibbstown, NJ) for 1 h at 37°C before incubation with lipid bilayer-tethered antigen. The inhibitor was also included in the incubation media. The B-cell contact area was determined using IRM images and MATLAB software (The MathWorks, Inc., Natick, MA). The total fluorescence intensity (TFI) and mean fluorescence intensity (MFI) of each staining in the B-cell contact zone and relative fluorescence and IRM intensity along a line across cells were determined using Andor iQ software (Andor Technology, Belfast, UK). Background fluorescence generated by antigen tethered to lipid bilayers in the absence of B-cells or secondary antibody controls, was subtracted. For each set of data, more than 20 individual cells from two or three independent experiments were analyzed.

2.3.5 Analysis of the mobility and fluorescence intensity of BCR clusters

To analyze the mobility of BCR microclusters, Kymographs of time lapse images by TIRFm were generated using Andor iQ software (Andor Technology). The moving velocity of BCR microclusters were calculated using the slope of moving streaks of individual clusters in kymographs. The length of time that each emerging microcluster required to merge with the central cluster was calculated as life span.

The TFI of BCR and phosphotyrosine staining in individual BCR clusters was determined using TIRFm images of B-cells that were incubated with antigen-tethered lipid bilayer for 3 and 7 min, using Andor iQ software. The data were plotted as the TFI ratio of phosphotyrosine to the BCR in individual BCR clusters versus the TFI of the BCR in individual clusters. Stimulation curves of the plot were generated using a nonparametric regression method, LOWESS (locally weighted scatterplot smoothing) [182,183], by Stata software (StataCorp LP, College Station, Texas). The bwidth or the smoothing factor used for the LOWESS analysis is 0.8.

2.3.6 Analysis of actin nucleation sites

Actin nucleation sites were detected as previously described [184]. B-cells were incubated with AF546-mB-Fab'-anti-Ig tethered to lipid bilayers in the presence of AF488-G-actin (Invitrogen) and 0.025% saponin at 37°C. Time lapse images were acquired for 5 min using TIRFm. The total fluorescence intensity (TFI) and mean fluorescence intensity (MFI) of incorporated AF488-G-actin in the B-cell contact zone and relative fluorescence and IRM intensity along a line across cells were determined using Andor iQ software (Andor Technology).

2.3.7 Statistical analysis

Statistical significance was assessed using the Mann-Whitney test by Prism software (GraphPad Software, San Diego, CA). *p* values were determined in comparison with wt or control B-cells.

2.4 Results

2.4.1 Btk and SHIP-1 regulate B-cell spreading and BCR aggregation

Antigen engagement of the BCR induces the activation of both Btk [171,185] and SHIP-1 [112,116,173], the key positive and negative signaling molecules downstream of the BCR. To determine how BCR signaling regulates the organization of surface BCRs, we used xid mice, which express inactive Btk that has a point mutation in its PH domain [186], and B-cell-specific SHIP-1 knockout mice [178]. We examined the effects of Btk or SHIP-1 deficiency on BCR aggregation at the cell surface and B-cell spreading in response to membrane associated antigen in the absence of adhesion molecules. The model antigen consisted of fluorescently labeled, mono-biotinylated Fab' fragment of anti-mouse IgG+M (mB-Fab'-anti-Ig) tethered to planar lipid bilayers by streptavidin. Total internal reflection fluorescence microscopy (TIRFm) was used to evaluate the aggregation of surface BCRs, and interference reflection microscopy (IRM) to identify and determine the areas of B-cells contacting antigen-tethered lipid bilayers (B-cell contact zone).

Upon incubation with antigen-tethered lipid bilayer, the contact zone of wt and CD19$^{Cre/+}$ SHIP-1$^{+/+}$ control B-cells rapidly expanded, peaked at ~6 min and ~3 min respectively, and then slightly decreased (Fig. 2.1A-D). Concurrently, surface BCRs formed microclusters, appearing as puncta, in the first few minutes, which then merged into each other, forming a central cluster in the B-cell contact zone (Fig. 2.1A-B). The total fluorescence intensity (TFI) of antigen in the contact zone of wt and control B-cells increased over time and reached a plateau at

FIGURE 2.1. Both Btk and SHIP-1 regulate B-cell spreading and BCR cluster formation and accumulation in response to membrane associated antigen. Splenic B-cells from wt CBA, xid, CD19$^{Cre/+}$SHIP-1$^{+/+}$ (Control), CD19$^{Cre/+}$SHIP-1$^{Flox/Flox}$ (SHIP ko) mice were incubated with AF546-mB-Fab'-anti-Ig (Ag) tethered to lipid bilayers at 37^{o}C. As a non-antigen control, splenic B-cells were labeled with AF546-Fab-anti-Ig for the BCR before incubation with biotinylated transferrin (Tf) tethered to lipid bilayers. As a non-specific antigen control (NS-Ag), splenic B-cells from wt CBA or xid mice were incubated with biotinylated AF546-Fab-anti-rabbit IgG tethered to lipid bilayers. Time lapse images were acquired using TIRFm and IRM. The B-cell contact area and the total fluorescence intensity (TFI) of antigen in the contact zone were quantified. Shown are representative images of cells at 7 min (A-B) and the average values (±SD) of the contact area (C and D) and the TFI (E and F) from ~20 cells of three independent experiments. Scale bar, 2.5 μm.

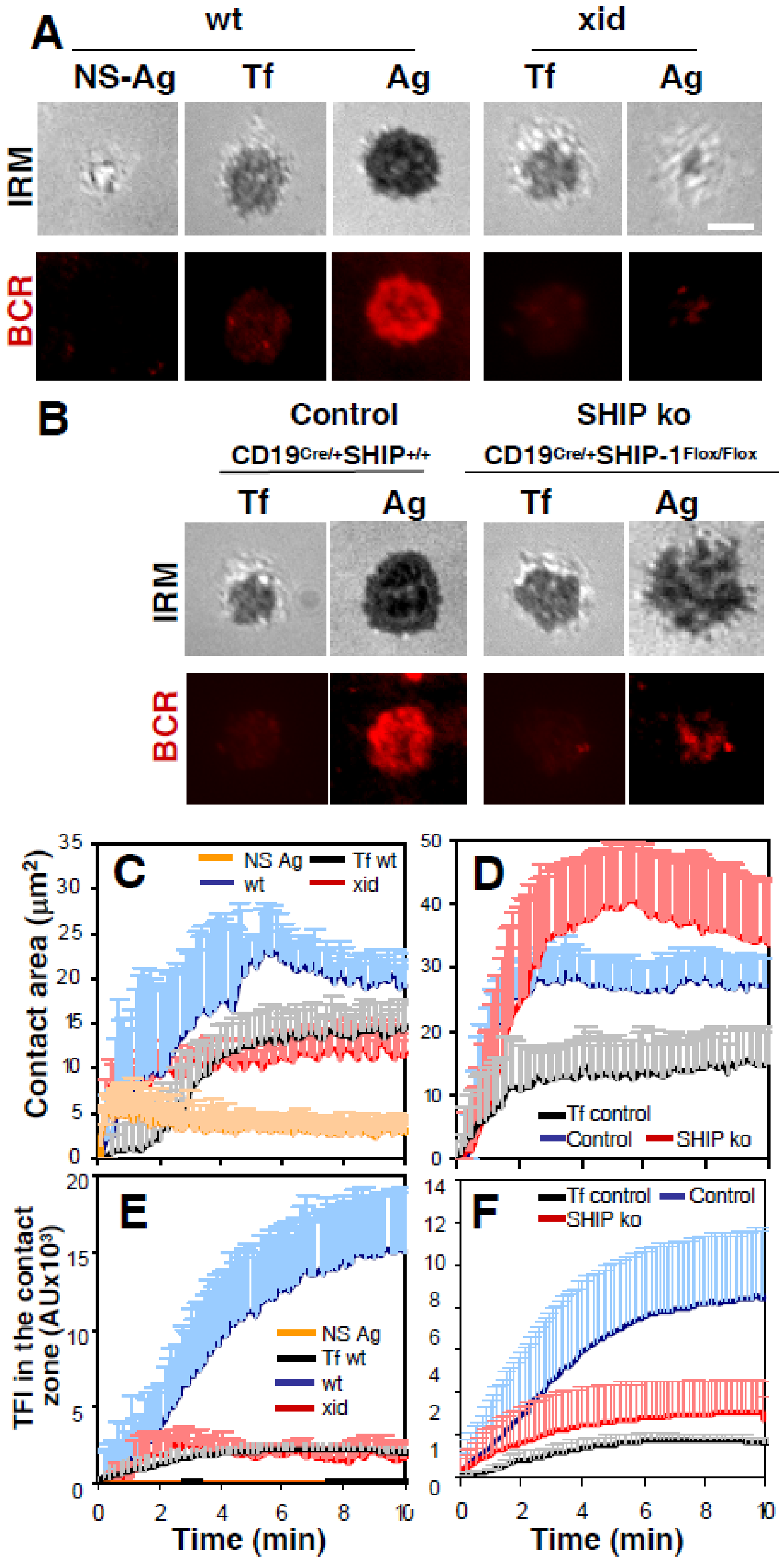
A
wt
xid
NS-Ag
Tf
Ag
Tf
Ag
IRM
BCR
B
Control
CD19Cre/+SHIP+/+
SHIP ko
CD19Cre/+SHIP-1Flox/Flox
Tf
Ag
Tf
Ag
IRM
BCR
C
NS Ag
Tf wt
wt
xid
Contact area (µm²)
35
30
25
20
15
10
5
0
D
50
40
30
20
10
0
Tf control
Control
SHIP ko
E
NS Ag
Tf wt
wt
xid
TFI in the contact zone (AUx10³)
20
15
10
5
0
F
Tf control
Control
SHIP ko
14
12
10
8
6
4
2
1
0
0
2
4
6
8
10
Time (min)
0
2
4
6
8
10
Time (min)

~7 or 5 min respectively (Fig. 2.1A-B, 2.1E-F). Fab-anti-rabbit-tethered to lipid bilayers was used as a non-specific antigen (NS-Ag) control, and transferrin (Tf) tethered to lipid bilayers, which binds to Tf receptor (TfR) on the B-cell surface, was used as a non-antigenic control. For the non-specific antigen control, wt B-cells established limited contact with lipid bilayers, but neither spread further nor recruited the Fab to the B-cell contact zone (Fig. 2.1A, 2.1C, and 2.1E). For the non-antigenic control, the B-cell contact area was larger than that observed with non-specific Fab, but smaller than that observed with specific antigen (Fig. 2.1A-D). Similarly, BCR staining in the contact zone on Tf-tethered lipid bilayer was much lower than that on antigen-tethered lipid bilayer (Fig. 2.1A-B and 2.1E-F). Since only BCR-specific antigen induces cluster formation, the antigen accumulation shown here reflects the aggregation of surface BCRs. Therefore, BCR cluster formation and B-cell spreading are events induced by specific antigen.

When incubated with antigen-tethered lipid bilayer, the xid splenic B-cells only established loose attachment to the lipid bilayer and failed to spread (Fig. 2.1A, 2.1C,). Compared to that of wt B-cells, the amount of the BCR accumulated in the contact zone of xid B-cells was reduced drastically (Fig. 2.1A and 2.1E). The behavior of xid B-cells was similar to that of wt when interacting with Tf-tethered lipid bilayer (Fig. 2.1A, 2.1C, and 2.1E). This indicates that Btk deficiency inhibits antigen induced BCR cluster formation and B-cell spreading, but not Tf induced B-cell spreading. In contrast to xid B-cells, SHIP-1$^{-/-}$ B-cells spread more extensively than CD19$^{Cre/+}$ SHIP-1$^{+/+}$ control B-cells (Fig. 2.1B, 2.1D). Despite the increase in the contact area, the amount of the BCR in the contact zone of SHIP-1$^{-/-}$ B-cells was substantially reduced (Fig. 2.1B, 2.1F,), showing that BCR aggregation efficiency is disassociated from the B-cell spreading process. Moreover, the BCR at the contact zone of SHIP-1$^{-/-}$ B-cells appeared as punctate clusters and failed to form a central cluster as in control B-cells (Fig. 2.1B).

To determine whether B-cell developmental defects caused by Btk mutation affect BCR microcluster formation and B-cell spreading, we sorted mature and immature B cells from the spleens of wt and xid mice based on their CD93 expression. When incubated with antigen-tethered lipid bilayers, mature (CD93^{-}) and immature (CD93^{+}) B cells spread and accumulated the BCR in the contact zone in a similar kinetics and to a similar magnitude. Furthermore, Btk-deficiency inhibited BCR microcluster formation and B-cell spreading in both mature and immature B cells (Fig. 2.2). Furthermore, B-cell specific SHIP-1 knockout did not generate major alterations in splenic B cell subsets[187]. This indicates that the effect of Btk and SHIP-1 deficiency on BCR microcluster formation and cell spreading are not due to alterations of B cell subsets in the spleens of xid and SHIP-1 knockout mice.

Taken together, these results indicate that both positive and negative signaling mediated by Btk and SHIP-1 are involved in regulating antigen-induced B-cell spreading and BCR cluster formation and accumulation. Btk induces B-cell spreading and BCR microcluster formation, and SHIP-1 inhibits B-cell spreading and promotes the formation of the central cluster.

FIGURE 2.2 The effect of Btk deficiency on BCR cluster formation and B-cell spreading is not due to B-cell developmental defect in xid mice. Splenic B cells from wt CBA and xid mice were sorted into B220+AA4.1+ (immature) and B220+AA4.1- (mature) using a cell sorter. Sorted B-cells were incubated with AF546-mB-Fab'-anti-Ig tethered to lipid bilayers at 37°C. Time lapse images were acquired using TIRFm and IRM. The B-cell contact area and the total fluorescence intensity (TFI) of the BCR in the contact zone were quantified. Shown are representative images of cells at 7 min (A-B) and the average values (±SD) of the contact area (C) and the TFI (D) from ~20 cells of two independent experiments. Scale bar, 2.5 μm.

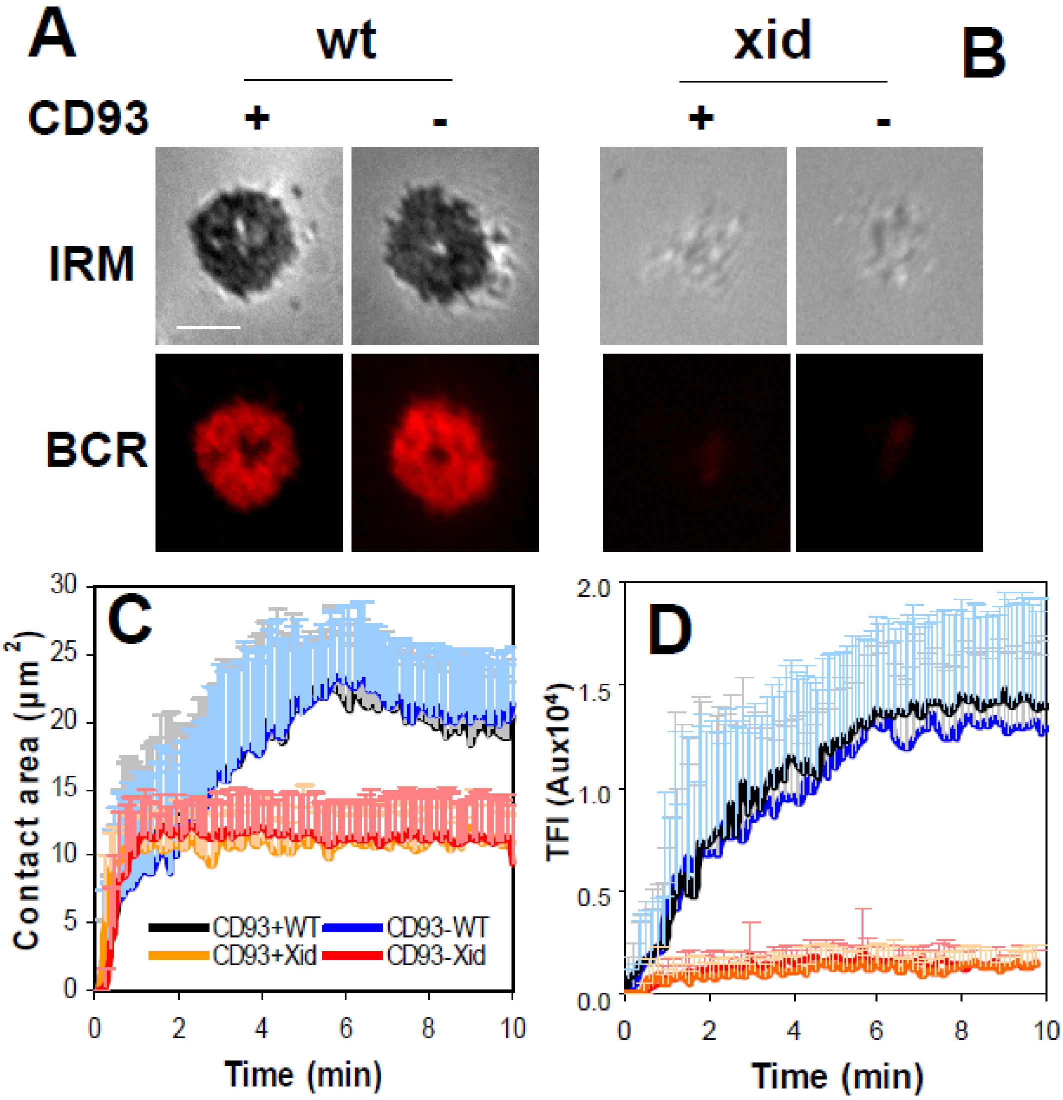
A
wt
xid
B
CD93
+
-
+
-
IRM
BCR
C
Contact area (µm²)
30
25
20
15
10
5
0
0
2
4
6
8
10
Time (min)
CD93+WT
CD93-WT
CD93+Xid
CD93-Xid
D
TFI (Aux10⁴)
2.0
1.5
1.0
0.5
0.0
0
2
4
6
8
10
Time (min)

2.4.2 SHIP-1 deficiency inhibits the centripetal movement of BCR microclusters

To understand why SHIP-$1^{-/-}$ B-cells fail to form BCR central clusters, we analyzed the lateral movement of BCR microclusters using kymographs. Kymographs generated from time lapse images by TIRFm provide graphical representations of spatial positions of BCR microclusters in the B-cell contact zone. Using kymographs, we determined the mobility of individual BCR microclusters and the timespan that an emerging BCR microcluster takes to merge with the central cluster (life span). The results show that in CD$19^{Cre/+}$ SHIP-$1^{+/+}$ control B-cells, BCR microclusters moved at an average mobility of ~10 nm/sec or ~0.6 μm/min towards the center of the B-cell contact zone (Fig. 2.3A-B). It took about 1 min for emerging BCR microclusters to merge with central clusters (Fig. 2.3C). In SHIP-$1^{-/-}$ B-cells, the mobility of BCR microclusters was reduced to 1.2 nm/sec or 0.072 μm/min, and therefore they took six times longer to merge into the central cluster (Fig. 2.3). These data demonstrate a critical role for SHIP-1 in the centripetal movement of BCR microclusters and the merger of BCR microclusters into the central cluster.

FIGURE 2.3 SHIP-1 deficiency inhibits the centripetal movement of BCR microclusters. Splenic B-cells from CD19$^{Cre/+}$SHIP-1$^{+/+}$ (Control), CD19$^{Cre/+}$SHIP-1$^{Flox/Flox}$ (SHIP ko) mice were incubated with AF546-mB-Fab'-anti-Ig tethered to lipid bilayers at 37^{o}C. Time lapse images were acquired using TIRFm. Kymographs of individual clusters were generated using time lapse images. Shown are two representative kymographs depicting movement of BCR microclusters (A). Arrowheads point to individual moving microclusters. The moving velocity of BCR microclusters was calculated using the slope of the moving streak in kymographs. The timespan that each emerging microcluster required to merge with a central cluster was calculated as life span. Shown are the average velocity (±SD) (B) and life span (±SD) (C) calculated from 30 BCR microclusters of three independent experiments. Scale bar, 2.5 μm. * $p<0.01$.

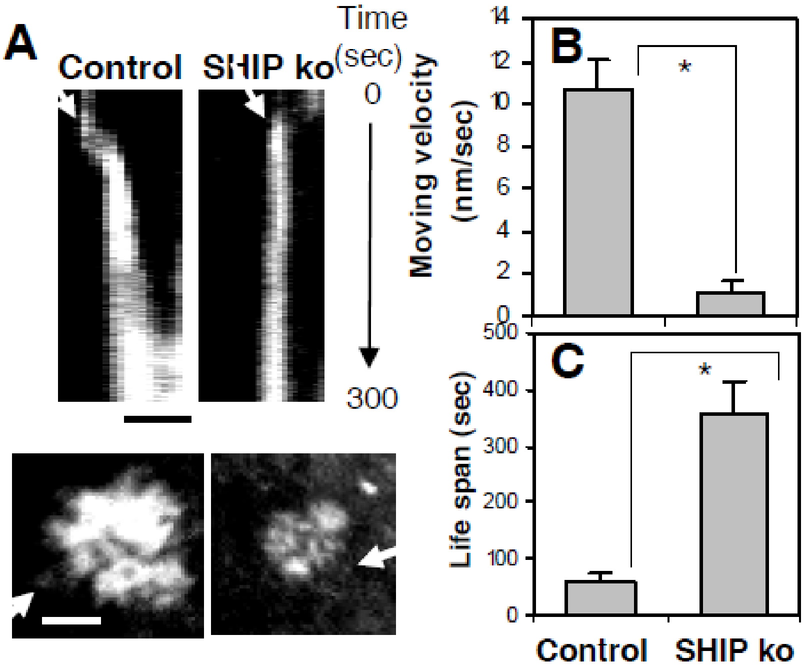
A
Control
SHIP ko
Time (sec)
0
300
B
Moving velocity (nm/sec)
14
12
10
8
6
4
2
0
*
C
Life span (sec)
500
400
300
200
100
0
*
Control
SHIP ko

2.4.3 SHIP-1 deficiency inhibits the growth but enhances the signaling capability of BCR microclusters

BCR self-aggregation is essential for receptor activation. While the contribution of SHIP-1 to BCR signaling via its phosphatase activity is well known, the effects of SHIP-1 deficiency on surface BCR aggregation suggest a role for SHIP-1 beyond its enzymatic activity. To investigate this hypothesis, we examined the levels and distribution of tyrosine phosphorylation (pY) and Btk phosphorylation (pBtk), and Akt phosphorylation (pAkt) in relation to BCR microclusters in the B-cell contact zone. In CD19$^{+/+}$ SHIP-1$^{Flox/Flox}$ control B-cells, the level of pY staining in the contact zone increased over time and peaked at ~3 min (Fig. 2.4A). As the pY level rose, the pY staining largely colocalized with BCR microclusters (Fig. 2.4D and 2.4F). After 3 min, the pY level in the B-cell contact zone decreased (Fig. 2.4A). Concurrent with this decrease, BCR microclusters merged into a central cluster, and the pY staining redistributed away from BCR clusters to the outer edge of the B-cell contact zone (Fig. 2.4D and 2.4F). Similarly, the levels of pBtk and pAkt in the contact zone of control B-cells peaked ~3 min and reduced afterwards (Fig. 2.4B-C). This suggests a negative correlation between signaling activity and the merger of BCR microclusters at the cell surface. In SHIP-1$^{-/-}$ B-cells, the pY level in the contact zone increased at a rate similar to that of control B-cells, but the peak level was sustained ~2 min longer than that in the control B-cells (Fig. 2.4A). The higher level of pY in the contact zone was not simply due to an increase in cell spreading, since the mean fluorescence intensity (MFI) of phosphotyrosine staining in the contact zone of SHIP-1$^{-/-}$ B-cells was also higher than that in control B-cells (data not shown). In addition, the levels of pBtk and pAkt in the contact zone of SHIP-1$^{-/-}$ B-cells were markedly higher than those in control B-cells (Fig. 2.4B-C). Moreover, the pBtk level in the contact zone of SHIP-1$^{-/-}$ B-cells continuously increased until ~ 5 min (Fig. 2.4B), and the high level of pAkt persisted rather than returning to the basal level like in the control B-cells (Fig. 2.4C). The surface distribution of pY was also altered by SHIP-1 deficiency, appearing as puncta and colocalizing with BCR clusters at all the time points tested (Fig. 2.4E and 2.4G).

To further investigate the relationship between the growth of BCR clusters and their signaling activities, we determined the relative size of BCR clusters based on the total fluorescence intensity of BCR labeling in individual clusters and the relative signaling levels of BCR clusters based on the fluorescence intensity ratio of the phosphotyrosine to the BCR in individual clusters. We used a nonparametric regression method, LOWESS, to analyze the trend of the data. In CD19$^{+/+}$ SHIP-1$^{Flox/Flox}$ control B-cells, we found a two phase correlation between the sizes of BCR clusters and their tyrosine phosphorylation activity. First, when the sizes of BCR clusters were relatively small, the pY to BCR ratio increased as emerging microclusters grew (Fig. 2.4H). However, after the sizes of the BCR clusters reached a certain level, the pY to BCR ratio decreased as BCR clusters further expanded, likely via the merger of BCR microclusters (Fig. 2.4H). In contrast, BCR clusters formed in the contact zone of SHIP-1$^{-/-}$ B-cells were limited to smaller sizes, in comparison with those in control B-cells (Fig. 2.4I). The fluorescence intensity ratio of pY to BCR in individual microclusters of SHIP-$1^{-/-}$ B-cells was much higher than those of control B-cells. These results suggest that SHIP-1 promotes the growth of BCR clusters, which contributes to signaling down regulation.

FIGURE 2.4 SHIP-1 deficiency increases the signaling capability but inhibits the growth of BCR microclusters. Splenic B-cells from CD19$^{+/+}$ SHIP-1$^{Flox/Flox}$ (Control) and CD19$^{Cre/+}$SHIP-1$^{Flox/Flox}$ (SHIP ko) mice were incubated with AF546-mB-Fab'-anti-Ig tethered to lipid bilayers at 37^{o}C for indicated times. Cells were fixed, permeabilized, and stained for phosphotyrosine (pY), phosphorylated Btk (pBtk) and Akt (pAkt). Cells were analyzed using TIRFm. The TFI (A-C) of pY, pBtk, and pAkt in the B-cell contact zone was quantified. The average TFI (±SD) were determined from 34-87 cells of two independent experiments. Shown are representative images (D-E) and the relative intensity of IRM, BCRs, and pY across the cells (blue lines) (F-G). Green dashed lines indicate the major peaks of pY and red arrows point to BCR peaks in histograms. The TFI of the BCR and the fluorescence intensity ratio of pY to the BCR in individual BCR clusters were determined (H-I). Each open symbol represents a BCR cluster, and solid symbols represent the LOWESS curve that was generated by Stats software. The data were generated from 40 cells of each strain of mice and two independent experiments. Scale bars, 2.5 μm.

* *$p<0.01$.*

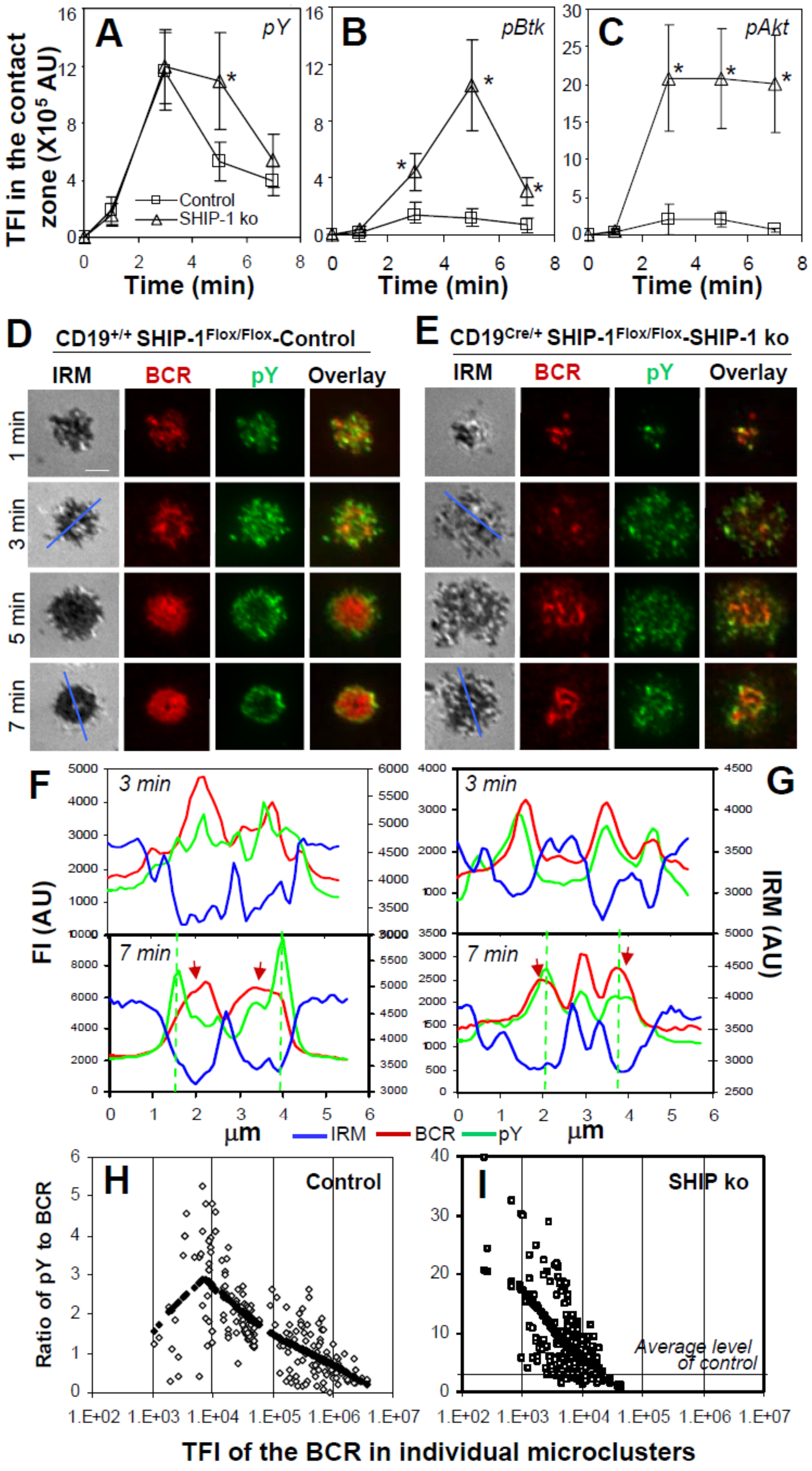
A
pY
B
pBtk
C
pAkt
TFI in the contact zone (X10^5 AU)
Control
SHIP-1 ko
*
0
2
4
6
8
12
16
5
10
15
20
25
30
Time (min)
D
CD19$^{+/+}$ SHIP-1$^{Flox/Flox}$-Control
E
CD19$^{Cre/+}$ SHIP-1$^{Flox/Flox}$-SHIP-1 ko
IRM
BCR
pY
Overlay
1 min
3 min
5 min
7 min
F
G
3 min
7 min
FI (AU)
IRM (AU)
µm
IRM
BCR
pY
H
Control
I
SHIP ko
Ratio of pY to BCR
Average level of control
1.E+02
1.E+03
1.E+04
1.E+05
1.E+06
1.E+07
TFI of the BCR in individual microclusters

2.4.4 Btk and SHIP-1 play opposing roles in actin reorganization

Both BCR aggregation and B-cell spreading are shown to depend on the actin cytoskeleton. The effects of Btk and SHIP-1 deficiency on BCR cluster formation and B-cell spreading imply a role for these signaling molecules in regulating actin dynamics. We have previously shown that Btk deficiency inhibits actin polymerization and WASP activation in response to soluble antigen [118]. Here, we examined the effect of SHIP-1 deficiency on the levels and distribution of F-actin and actin polymerization sites in the contact zone. While the level of F-actin in the contact zone of both CD19$^{+/+}$SHIP-1$^{Flox/Flox}$ control and SHIP-1$^{-/-}$ B-cells increased in response to antigen-tethered lipid bilayer, the increase was significantly greater in SHIP-1$^{-/-}$ B-cells (Fig. 2.5A-C). In the contact zone of control B-cells, F-actin was largely colocalized with BCRs upon B-cell interaction with antigen-tethered lipid bilayer (Fig. 2.5A). When BCR microclusters merged into each other, F-actin moved away from BCR clusters to BCR poor regions and the outer edge of the contact zone (Fig. 2.5A and 2.5D). For SHIP-1$^{-/-}$ B-cells, F-actin did redistribute away from BCR clusters, but it formed a wide ring in the middle of the contact zone and did not accumulate at the outer edge of the contact zone (Fig. 2.5B and 2.5E).

F-actin accumulation suggests an increase in actin polymerization. To compare actin polymerization activity of Btk and SHIP-1 deficient B-cells with wt and CD19$^{+/+}$ SHIP-1$^{Flox/Flox}$ control B-cells, we used G-actin incorporation assay. In this assay, the incorporation of fluorescently labeled G-actin to the polymerizing end of F-actin indicates the location and level of actin polymerization [184]. We found that in xid

B-cells, the MFI of incorporated AF488-G-actin in the contact zone was significantly decreased, compared to that in wt B-cells. In contrast, G-actin incorporation was significantly increased in the contact zone of SHIP-1$^{-/-}$ B-cells, compared to that in control B-cells (Fig. 2.5F). Despite the enhanced actin polymerization in SHIP-1$^{-/-}$ B-cells, actin polymerization sites were distributed in a pattern similar to that was seen in control B-cells (Fig. 2.5G-H).

FIGURE 2.5 Btk and SHIP-1 have opposing roles in antigen-induced actin reorganization. (A-E) Splenic B-cells from CD19$^{Cre/+}$SHIP-1$^{+/+}$ (Control) and CD19$^{Cre/+}$SHIP-1$^{Flox/Flox}$ (SHIP-1 ko) mice were incubated with AF546-mB-Fab'-anti-Ig tethered to lipid bilayers at 37°C for indicated times. Cells were fixed, permeabilized, and stained for F-actin. Cells were analyzed by TIRFm. Shown are representative images (A-B), the MFI of F-actin in the contact zone (C), and the relative intensity of IRM, F-actin, and the BCR across the cells (blue lines) (D-E). Green dashed lines indicate the major peaks of F-actin and red arrows point to BCR peaks in histograms. The average values (±SD) of the MFI were generated from 20-90 cells of three independent experiments. (F-H) Splenic B-cells were incubated with AF546-mB-Fab'-anti-Ig tethered to lipid bilayers at 37°C for 5 min in the presence of AF488-G-actin and 0.025% saponin. Cells were fixed and analyzed using TIRFm. Shown are representative images (G-H) and the average MFI (±SD) of incorporated AF488-G-actin in the contact zone (F), generated from 22-24 cells of two or three independent experiments. Scale bar, 2.5 μm. * $p<0.01$.

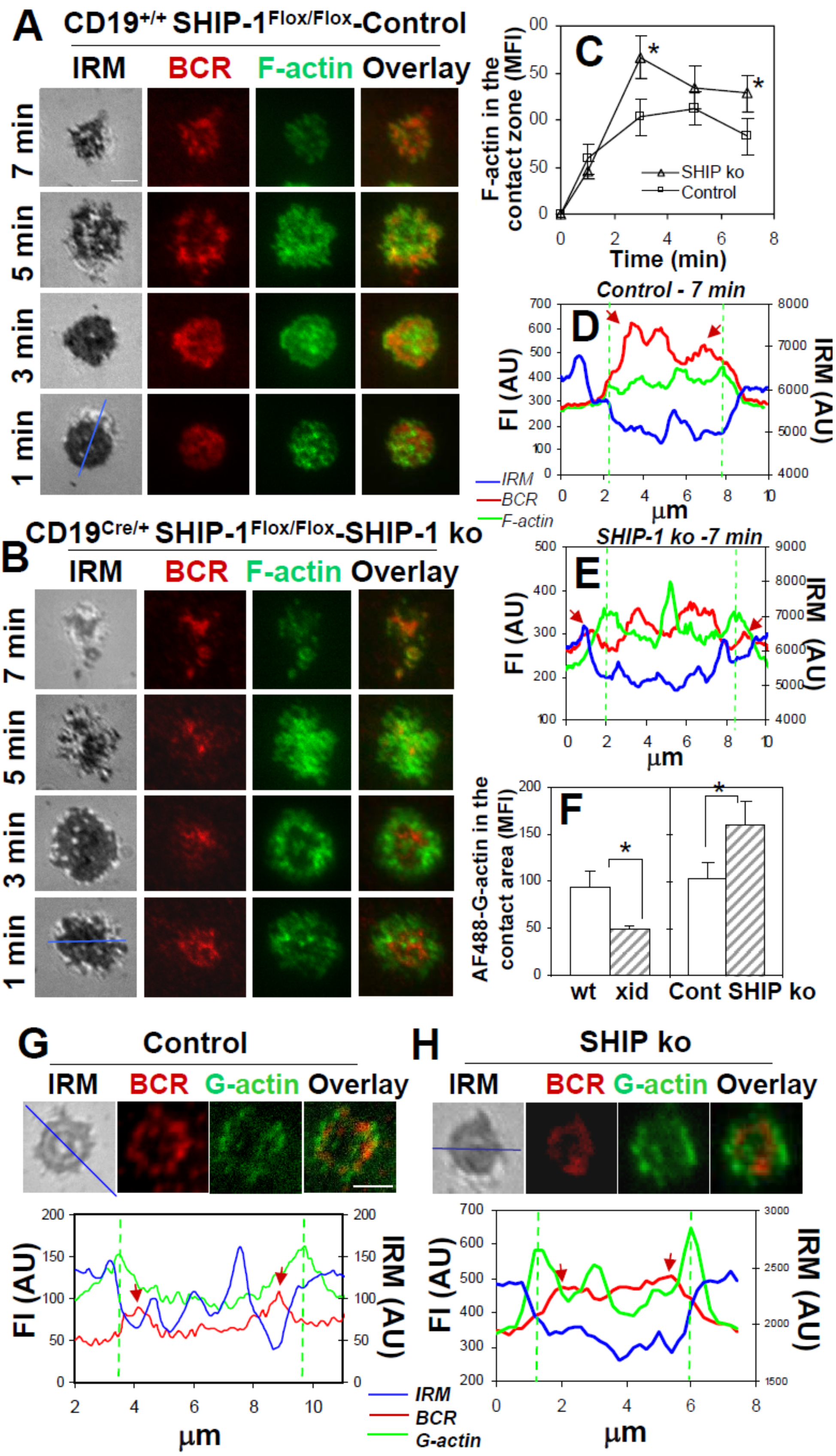
A
CD19+/+ SHIP-1Flox/Flox-Control
IRM
BCR
F-actin
Overlay
7 min
5 min
3 min
1 min
B
CD19Cre/+ SHIP-1Flox/Flox-SHIP-1 ko
IRM
BCR
F-actin
Overlay
7 min
5 min
3 min
1 min
C
F-actin in the contact zone (MFI)
00
50
00
50
0
*
*
SHIP ko
Control
0
2
4
6
8
Time (min)
Control - 7 min
D
700
600
500
400
300
200
100
0
FI (AU)
8000
7000
6000
5000
4000
IRM (AU)
IRM
BCR
F-actin
0
2
4
6
8
10
µm
SHIP-1 ko -7 min
E
500
400
300
200
100
FI (AU)
9000
8000
7000
6000
5000
4000
IRM (AU)
0
2
4
6
8
10
µm
F
AF488-G-actin in the contact area (MFI)
200
150
100
50
0
*
*
wt
xid
Cont
SHIP ko
G
Control
IRM
BCR
G-actin
Overlay
200
150
100
50
0
FI (AU)
200
150
100
50
0
IRM (AU)
2
4
6
8
10
µm
IRM
BCR
G-actin
H
SHIP ko
IRM
BCR
G-actin
Overlay
700
600
500
400
300
200
FI (AU)
3000
2500
2000
1500
IRM (AU)
0
2
4
6
8
µm

Actin polymerization is activated by actin nucleation promoting factors. Our previous study shows that Btk promotes actin polymerization by activating the hematopoietic specific actin nucleation promoting factor, WASP [118]. Here we determined the effect of SHIP-1 deficiency on WASP activation using an antibody specific for the phosphorylated WASP (S483/S484, pWASP). Similar to F-actin, the level of pWASP in the contact zone of CD19$^{+/+}$SHIP-1$^{Flox/Flox}$ control B-cells increased over time in response to antigen-tethered lipid bilayer and reached a peak at ~5 min (Fig. 2.6A and 2.6F). SHIP-1-deficiency significantly increased the pWASP level in the B-cell contact zone, especially at 1-3 min (Fig. 2.6B, top panels, and 2.6F). The pWASP staining in the contact zone of both control and SHIP-1$^{-/-}$ B-cells appeared as puncta and colocalized with BCR microclusters early during the stimulation (Fig. 2.6A, 2.6C, and data not shown). As BCR microclusters merged into each other, pWASP in control B-cells redistributed away from BCR clusters to the outer edge of the contact zone and to BCR poor regions (Fig. 2.6A and 2.6D), but pWASP in SHIP-1$^{-/-}$ B-cells failed to do so (Fig. 2.6B, top panels, and 2.6E).

These results collectively indicate that Btk and SHIP-1 positively and negatively regulate actin reorganization, respectively. Btk induces while SHIP-1 inhibits WASP activation, actin polymerization, and F-actin accumulation in the B-cell contact zone.

FIGURE 2.6 SHIP-1 regulates WASP activation, B-cell spreading, and BCR cluster formation and accumulation in a Btk dependent manner. Splenic B-cells from CD19$^{+/+}$SHIP-1$^{Flox/Flox}$ (control) and CD19$^{Cre/+}$SHIP-1$^{Flox/Flox}$ (SHIP ko) mice were pretreated with or without LFM A-13 (A-13) for 1 h and incubated with AF546-mB-Fab'-anti-Ig tethered to lipid bilayers at 37^{o}C for indicated times in the presence or absence of A-13. Cells were fixed, permeabilized, and stained for phosphorylated WASP (pWASP). Cells were analyzed by TIRFm. Shown are representative images (A-B) and the relative intensity of IRM, pWASP, and the BCR across the cells (blue lines) (C-E). Green dashed lines indicate the major peaks of pWASP and red arrows point to BCR peaks in histograms. The MFI of pWASP (F), the B-cell contact area (G) and the TFI of the BCR (H) in the contact zone were quantified. Shown are average values (±SD) of 20-90 cells from three independent experiments. Scale bar, 2.5 μm. * indicates the *p* value ($p<0.01$) in comparison with controls.

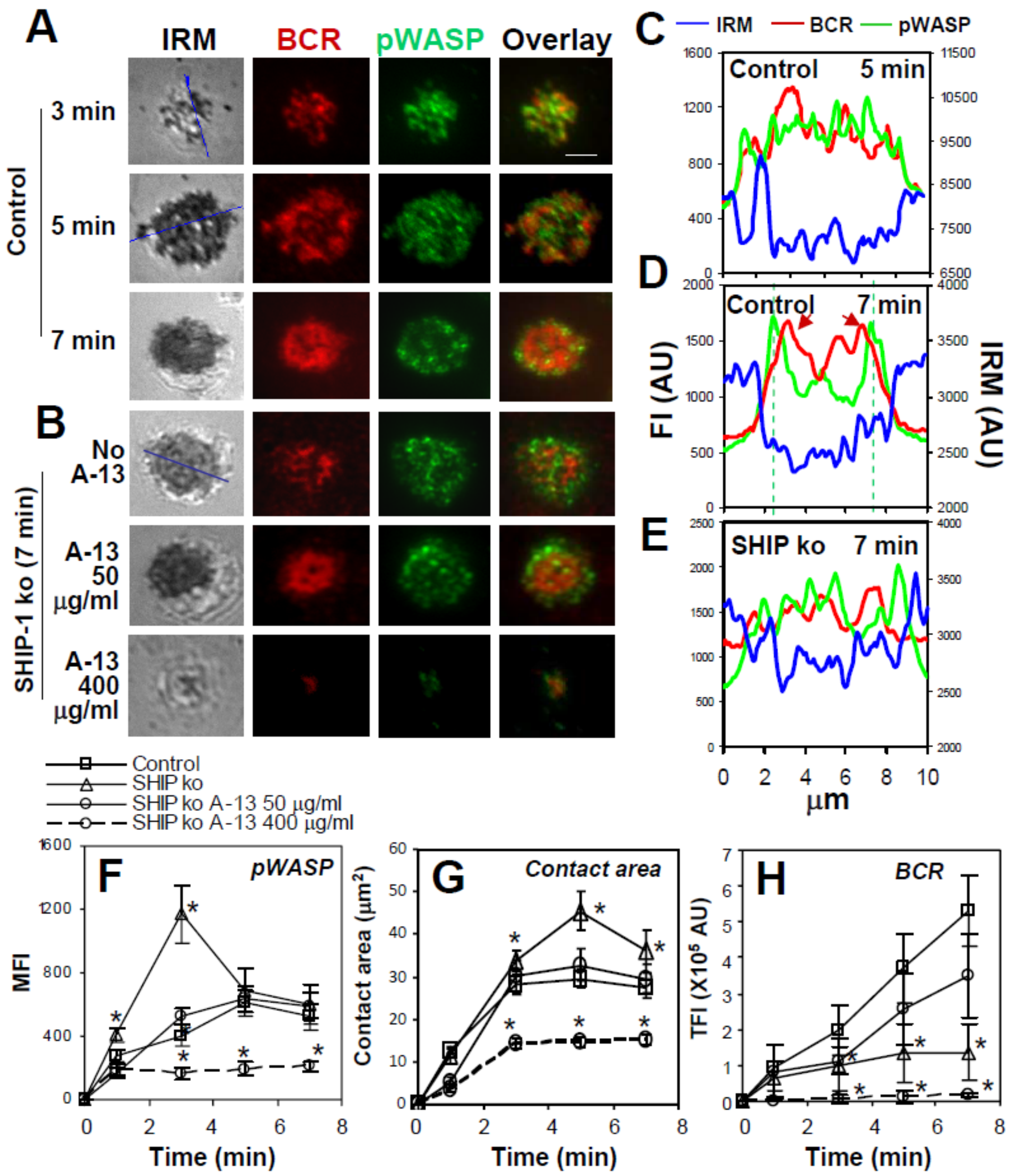
A
IRM
BCR
pWASP
Overlay
Control
3 min
5 min
7 min
B
No A-13
A-13 50 µg/ml
A-13 400 µg/ml
SHIP-1 ko (7 min)
C
IRM
BCR
pWASP
Control 5 min
1600
1200
800
400
0
11500
10500
9500
8500
7500
6500
D
Control 7 min
2000
1500
1000
500
0
4000
3500
3000
2500
2000
FI (AU)
IRM (AU)
E
SHIP ko 7 min
2500
2000
1500
1000
500
0
4000
3500
3000
2500
2000
0 2 4 6 8 10
µm
Control
SHIP ko
SHIP ko A-13 50 µg/ml
SHIP ko A-13 400 µg/ml
F
pWASP
MFI
1600
1200
800
400
0
*
Time (min)
0 2 4 6 8
G
Contact area
Contact area (µm²)
60
50
40
30
20
10
0
Time (min)
0 2 4 6 8
H
BCR
TFI (X10⁵ AU)
7
6
5
4
3
2
1
0
Time (min)
0 2 4 6 8

2.4.5 SHIP-1 regulates WASP activation, B-cell spreading, and BCR cluster formation in a Btk-dependent manner

Btk is one of the downstream targets of SHIP-1. SHIP-1 dephosphorylates PtdIns(3,4,5)P_3 at its 5 position, removing the docking site of Btk at the plasma membrane. Therefore, SHIP-1 deficiency increases Btk activation (Fig. 2.4B) [55]. To examine the functional interrelationship between SHIP-1 and Btk in initiation steps of BCR activation, we reduced Btk activity in SHIP-1$^{-/-}$ B-cells using a Btk specific inhibitor, LFM A-13 (A-13). Our previous study shows that this inhibitor causes reductions in BCR and WASP activation similar to Btk deficiency [118]. An intermediate and a high concentration of A-13 were used to manipulate the level of the kinase activity of Btk. At an intermediate concentration, the Btk inhibitor restored the magnitudes of B-cell spreading (Fig. 2.6G), BCR cluster formation (Fig. 2.6H) and WASP phosphorylation (Fig. 2.6B and 2.6F) in the contact zone of SHIP-1$^{-/-}$ B-cells to levels similar to those in CD19$^{+/+}$ SHIP-1$^{Flox/Flox}$ control B-cells. At a high concentration, the Btk inhibitor reduced B-cell spreading (Fig. 2.6G), BCR cluster formation (Fig. 2.6H), and WASP phosphorylation in the contact zone (Fig. 2.6B and 2.6F) to levels close to those in Btk-deficient B-cells. These data indicate that SHIP-1 can regulate actin reorganization, B-cell spreading, and BCR cluster formation via inhibiting Btk.

2.4.6 WASP-deficiency reduces B-cell spreading, BCR cluster formation, and tyrosine phosphorylation in the B-cell contact zone

Our finding that WASP activation is regulated by both Btk and SHIP-1 suggests that

WASP contributes to BCR activation. To determine the role of WASP in the early event of BCR activation, we compared B-cell spreading, BCR cluster formation and tyrosine phosphorylation in WASP$^{-/-}$ B-cells with those in wt B-cells. WASP deficiency significantly reduced the magnitude of B-cell spreading, the extent of BCR clustering, and the level of tyrosine phosphorylation in the B-cell contact zone (Fig. 2.7). However, the inhibitory effects of WASP deficiency were less remarkable than those of Btk deficiency and Btk inhibition (Fig. 2.1 and 2.6). These results suggest that WASP is important, but not essential, for B-cell spreading and BCR aggregation in response to membrane-associated antigen.

2.5 Discussion

In this study, we have examined the underlying mechanism for the functional interplay between signaling and the actin cytoskeleton during BCR activation. Our results show that the stimulatory kinase Btk promotes B-cell spreading, BCR microcluster formation, and actin polymerization and recruitment, in response to membrane associated antigen. In contrast, the inhibitory phosphatase SHIP-1 inhibits B-cell spreading and actin polymerization and recruitment, but promotes the centripetal movement and merger of BCR microclusters. These results suggest that a balance between positive and negative signaling regulates the dynamics and magnitude of BCR self-aggregation at the B-cell surface, via controlling actin reorganization. The unique finding of this study is that positive and negative signals have distinct roles in regulating BCR aggregation. Previous studies show that the activation of proximal

FIGURE 2.7 WASP deficiency inhibits BCR cluster formation, B-cell spreading, and tyrosine phosphorylation. Splenic B-cells from wt and WASP$^{-/-}$ mice were incubated with AF546-mB-Fab'-anti-Ig tethered to lipid bilayers at 37^{o}C for indicated times. Cells were fixed, permeabilized, and stained for phosphotyrosine (pY). Cells were analyzed using TIRFm. Shown are representative images (A-B) and the average values (±SD) of the B-cell contact area (C), the TFI of the BCR (D), and the MFI of the pY (E) in the contact zone. The data were generated using 20-90 cells from three independent experiments. Scale bar, 2.5 μm. * $p<0.01$.

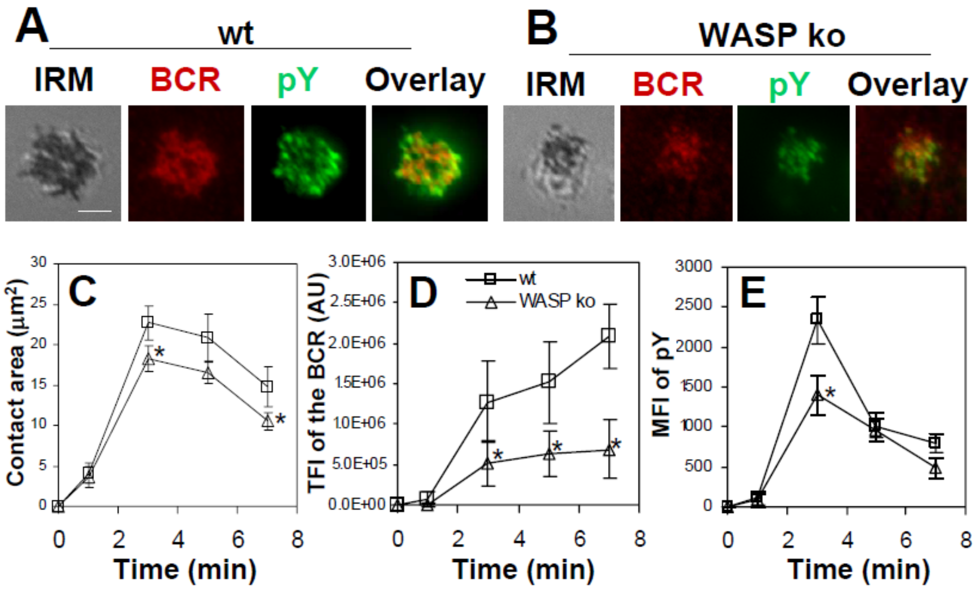
A
wt
IRM
BCR
pY
Overlay
B
WASP ko
IRM
BCR
pY
Overlay
C
Contact area (µm²)
30
25
20
15
10
5
0
0
2
4
6
8
Time (min)
*
*
D
TFI of the BCR (AU)
3.0E+06
2.5E+06
2.0E+06
1.5E+06
1.0E+06
5.0E+05
0.0E+00
wt
WASP ko
0
2
4
6
8
Time (min)
*
*
*
E
MFI of pY
3000
2500
2000
1500
1000
500
0
0
2
4
6
8
Time (min)
*

signaling molecules, including PLCγ2, Vav, Rac2, and costimulatory molecule CD19 [53,74,177], can have significant impact on BCR aggregation on the cell surface. Consistent with these findings, we show here that Btk, a downstream molecule of CD19 and an upstream molecule of Vav and Rac, is required to induce the formation of BCR microclusters in response to membrane-associated antigen. However, the inhibitory phosphatase SHIP-1 is not essential for the formation of BCR microclusters, but it is involved in the centripetal movement and merger of BCR microclusters after their formation. Our results suggest that the relative activation levels and timing of stimulatory kinases, such as Btk, and inhibitory phosphatases, such SHIP-1, can control the formation and growth of BCR microclusters. Therefore, signaling triggered by antigen induced aggregation of BCRs in turn regulates the kinetics and magnitude of BCR self-aggregation, providing feedbacks to signal initiation.

BCR activation is triggered by self-aggregation of surface receptors into microclusters. The formation and growth of BCR microclusters has been positively linked to the signaling capability of the receptor [188]. Contrary to this positive link, proximal signaling molecules have been shown to be primarily recruited to TCR microclusters in the periphery but not the center of the immunological synapse [189]. In line with the previous study, we detected tyrosine phosphorylation primarily at BCR microclusters and the outer edge of the BCR central cluster. This supports the notion that signal initiation occurs at receptor microclusters rather than the central cluster. By analyzing the ratio between the amount of BCRs and the level of tyrosine phosphorylation in individual clusters, our results suggest a two phase relationship between the size and signaling capability of BCR clusters. In the first phase, the tyrosine phosphorylation level increases as BCR microclusters emerge and undergo initial growth, which can be considered as the signal activation phase. In the second phase, the tyrosine phosphorylation level decreases as the size of the BCR clusters further expand, which can be considered as the signal transitional or down regulation phase. We found that SHIP-1 deficiency inhibited the growth but not the formation of BCR microclusters, which seems to limit the size of BCR microclusters to the signal activation phase and to prevent BCR microclusters from moving to the signal down regulation phase. Therefore, Btk plays a dominant role in the signal activation phase and SHIP-1 in the signal down regulation phase of BCR clusters. This suggests that in addition to their enzymatic activity, Btk and SHIP-1 could up and down regulate BCR activation by promoting the formation of BCR microclusters or the growth and merger of BCR microclusters into the central cluster. How the merger of BCR microclusters contributes to signaling down regulation remains to be elucidated.

The effects of Btk and SHIP-1 deficiency on the organization of the actin cytoskeleton suggest that these signaling molecules can regulate BCR aggregation by controlling actin dynamics. In addition to determine cell morphology, the actin cytoskeleton also creates a barrier for the lateral movement of transmembrane proteins whose cytoplasmic tails are extended into the cortical actin network [176]. Perturbing this barrier has been shown to increase the lateral mobility of surface BCRs and to induce signaling without antigen [149]. We found here that Btk and SHIP-1 had opposite roles in actin reorganization. Btk and SHIP-1 deficiency decrease and increase actin polymerization activity and F-actin accumulation in the B-cell contact zone, respectively. The decreased actin polymerization in Btk-deficient B-cells is associated with a marked reduction in B-cell spreading and surface BCR cluster formation. This indicates that Btk-induced actin polymerization is required for BCR aggregation and B-cell spreading. The inhibition of BCR aggregation in Btk-deficient B-cells is likely caused by the reduction in B-cell spreading, since B-cell spreading has been shown to enhance the formation of BCR microclusters by increasing the number of surface BCRs engaging antigen [76]. In SHIP-1$^{-/-}$ B-cells, enhanced actin polymerization and F-actin recruitment are concurrent with increased B-cell spreading and reduced centripetal movement and merger of BCR microclusters. This suggests that in response to antigenic stimulation, SHIP-1-suppressed actin polymerization is important for preventing B-cells from further spreading and for driving the centripetal movement of BCR microclusters. The timing and level of SHIP-1 activation may negatively control the magnitude of B-cell spreading and the mobility of BCR aggregates by altering the dynamics and organization of the actin cytoskeleton. Therefore, a balance of positive and negative signals can regulate the nature of actin reorganization, which in turn controls the morphology of B-cells and the mobility and growth of BCR aggregates.

How the proximal signaling molecules regulate actin dynamics is not fully understood. Here we show that WASP, an actin nucleation promoting factor, is a common downstream target of Btk and SHIP-1 during antigenic activation of the BCR. WASP has been shown to be involved in the formation of immunological synapses in both B- and T-cells [190,191,192]. We have previously shown that Btk can induce the activation of WASP via increasing the phosphorylation of Vav and the level of PtdIns(4,5)P_2 [118]. This study shows that SHIP-1 inhibits WASP phosphorylation, counteracting against Btk. The opposing effect of Btk and SHIP-1 on WASP activation is consistent with their opposite impact on actin polymerization. Moreover, phosphorylated WASP and F-actin were found to exhibit similar distribution patterns in the B-cell contact zone. These results suggest that WASP controls de novo actin polymerization induced by BCR activation. Our finding that the SHIP-1-mediated inhibition of WASP depends on its ability to inhibit Btk indicates that SHIP-1 prevents WASP from activating by turning off the kinase that induces WASP activation. Therefore, BCR signaling can regulate actin reorganization by controlling the activity of actin regulators like WASP.

In support of a role for WASP in BCR activation, this study found that B-cell spreading, BCR cluster formation and tyrosine phosphorylation in the contact zone induced by membrane-associated antigen were inhibited by WASP deficiency. However, the inhibition was only partial, suggesting that there are additional actin regulators that have overlapping functions with WASP in the process of signal initiation. WASP belongs to a family of proteins [193]. The other members of WASP family proteins, such as N-WASP and WAVE, may compensate for the function of WASP in WASP$^{-/-}$ B-cells. Such compensational roles could explain the partial inhibition observed here, as well as the mild defects in B-cell activation and B-cell responses in WASP$^{-/-}$ mice reported previously [179,190]. It is also noted that the inhibitory effects of WASP deficiency on B-cell spreading and BCR clustering are less dramatic than those of Btk deficiency. This suggests that Btk can regulate these processes through multiple downstream molecules, in addition to WASP. Identification of additional actin regulators downstream of Btk and SHIP-1 that are involved in actin remodeling during BCR activation is a subject of our future investigation.

In summary, this study demonstrates a close cooperation between signaling and the actin cytoskeleton during BCR activation. Positive and negative signals mediated through Btk and SHIP-1 regulate B-cell membrane dynamics and spatiotemporal organization of surface BCRs, via controlling actin reorganization. The magnitude of BCR aggregation and the mobility of BCR aggregates regulate the signaling capability of the receptor. This interplay between actin reorganization with signaling forms a mechanistic basis for feedback regulation of BCR signaling. Such a feedback is potentially a general regulatory mechanism of receptor signaling. Further studies are required to identify additional molecular linkers and define the molecular nature of the interaction between the actin cytoskeleton and BCR signaling pathway. (Copy right 2011. The American Association of Immunologists, Inc)

Chapter 3. Actin reorganization is required for the formation of polarized BCR signalosomes in response to both soluble and membrane associated antigen

3.1 Abstract

B-cells encounter both soluble (sAg) and membrane-associated antigens (mAg) in the secondary lymphoid tissue, yet how the physical form of Ag modulates B-cell activation remains unclear. This study compares actin reorganization and its role in BCR signalosome formation in mAg- and sAg-stimulated B-cells. Both mAg and sAg induce F-actin accumulation and actin polymerization at BCR microclusters and at the outer rim of BCR central clusters, but the kinetics and magnitude of F-actin accumulation in mAg-stimulated B-cells are greater than those in sAg-stimulated B-cells. Accordingly, the actin regulatory factors, cofilin and gelsolin, are recruited to BCR clusters in both mAg- and sAg-stimulated B-cells but with different kinetics and patterns of cellular redistribution. Inhibition of actin reorganization by stabilizing F-actin inhibits BCR clustering and tyrosine phosphorylation induced by both forms of Ag. Depolymerization of F-actin leads to unpolarized microclustering of BCRs and tyrosine phosphorylation in BCR microclusters without mAg and sAg, but in much slower kinetics than those induced by Ag. Therefore, actin reorganization, mediated via both polymerization and depolymerization, is required for the formation of BCR signalosomes in response to both mAg and sAg.

3.2 Introduction

Mature B-cells encounter their cognate antigen (Ag) when they circulate through the secondary lymphoid organs, where they are attracted into follicles through a CXCL13 gradient generated by follicular dendritic cells and fibroblastic reticular cells [194,195,196]. The binding of Ag to the clonally specific B-cell receptor (BCR) initiates B-cell activation. In contrast to the T-cell receptor, the BCR can bind Ag in diverse forms. Two broad forms of Ag that B-cells commonly encounter in the secondary lymphoid organs are soluble (sAg) and membrane-associated Ag (mAg). Recent studies using multiphoton intravital microscopy have shown that sAg with relatively small molecular weight (≤60 kDa), when injected subcutaneously, rapidly reach B-cell follicles in the drainage lymph node, probably via gaps in the sinus floor [197] or the collagen-rich conduit network [198,199]. The conduits, which are secreted by fibroblastic reticular cells, passively deliver small molecules, like Ag and the B-cell chemokine CXCL13 [198,199]. Macrophages lining the lymph node subcapsular sinus capture and transport particulate Ag and immune complexes to follicles [200,201,202]. Dendritic cells in the medullary sinus capture Ag and transport Ag to the B-cell compartment. Moreover, follicular dendritic cells can capture sAg in complexes with complement factors or antibody (Ab) and retain them for long term presentation [198,203,204]. Ag captured by macrophages and dendritic cells is presented to B-cells in a membrane-associated form.

While *in vitro* B-cells readily bind both sAg and mAg, how B-cells are activated by different forms of Ag *in vivo* is not completely clear. Ag binding to the BCR can induce signaling cascades as well as Ag uptake, processing and presentation. The cellular activities triggered by BCR-Ag interaction and signals from the microenvironment of B-cells collectively determine the fate of B-cells. The activation of B-cells by both sAg and mAg has been studied extensively *in vitro* [66,68,75,172,174]. Early studies, starting from the 1970s, mainly focused on sAg. These studies show that multivalent but not monovalent sAg induces the aggregation of surface BCRs into a central cluster at one pole of a B-cell, which was called a BCR cap [142,205,206]. Later, Chen *et al.* [64] found that aggregated BCRs associated with lipid rafts, where Src kinases, such as Lyn, are constitutively present. The phosphorylation of the immunoreceptor tyrosine-based activation motifs in the cytoplasmic tails of the BCR by Src kinases leads to the activation of signaling cascades [66,207]. The requirement of multivalent sAg for BCR activation indicates the importance of Ag-induced BCR aggregation in BCR activation.

Recent studies utilizing total internal reflection fluorescence microscopy (TIRFM) provide high resolution live cell images of BCR signaling initiation events at the surface of B-cells interacting with Ag tethered to planar lipid bilayers. Ag tethered to lipid bilayers is a widely used model for mAg. The binding of mAg, even monovalent mAg, to the BCR induces conformational changes and self aggregation of surface BCRs [61,71]. The newly formed BCR microclusters reside in lipid rafts [72] and recruit signaling molecules, including Lyn, Syk [61], PLCγ2, Vav [74] and co-stimulatory receptor CD19 [53]. BCR microclusters increase in size over time by trapping more BCRs and eventually merge together to form a central cluster at the surface zone contacting Ag-tethered membrane, similar to the BCR cap. When the adhesion molecule ICAM is present on Ag-tethered membranes, the BCR central cluster is surrounded by ICAM, forming a surface macromolecular structure (SMAC) similar to the immunological synapse between T-cells and Ag presenting cells [175]. Unlike T-cells, ICAM facilitates, but is not required for the formation of BCR signalosomes in response to mAg [175,208].

Concurrent with BCR aggregation, mAg also induces B-cell spreading and contraction on the Ag tethered membrane [76]. Such morphological changes have been shown to increase Ag gathering and BCR aggregation at the B-cell surface. B-cell morphological changes and amplified BCR aggregation are dependent on BCR signaling mediated by CD19, Btk, Vav and Rac2 [53,74,177], suggesting that BCR proximal signaling induced by mAg provides a positive feedback for the BCR signalosome formation. Similar to the B-cell response to mAg, morphological changes have been also observed in sAg-stimulated B-cells, where these B-cells form membrane protrusions in the vicinity of the BCR central cluster [206].

The actin cytoskeleton has been shown to be an important factor in B-cell activation [209]. It was first observed more than thirty years ago that sAg induced F-actin accumulation at the BCR cap [143,151,210,211]. A link between the actin cytoskeleton and BCR signaling was first suggested by Baeker *et al.* who showed that disrupting the actin cytoskeleton by cytochalaisin D induced Ca^{2+} flux [212]. Later studies reported that perturbation of the actin cytoskeleton delayed the attenuation of protein tyrosine phosphorylation [134] and enhanced activation of the MAP kinase, ERK, and the transcription factors, SRF, NF-κB and NFAT, induced by sAg [213]. The underlying mechanism by which the actin cytoskeleton contributes to sAg-induced BCR activation remains to be elucidated. Recent studies using TIRFM show that the cortical actin network secured to the B-cell membrane by ezrin controls the lateral movement of surface BCRs [70,149]. Disrupting the cortical actin network inhibits surface BCR aggregation and B-cell spreading in response to mAg [76]. However, in the absence of mAg, perturbation of cortical actin increases the lateral diffusion of surface BCRs and induces spontaneous signaling [149,214]. Our recent study demonstrates that the BCR proximal signaling molecule Btk and its negative regulator SH2-containing inositol-5 phosphatase-1 (SHIP-1) positively and negatively regulate actin reorganization induced by mAg, respectively. Btk activates actin nucleation promoting factor, Wiskott Aldrich symptom protein (WASP), promoting BCR aggregation and B-cell spreading [118,155]. In contrast, SHIP-1 inhibits the activation of Btk and WASP, promoting the contraction of B-cells and the merger of BCR microclusters into a central cluster [155]. These data collectively reveal a critical role for the actin cytoskeleton in BCR activation induced by mAg. It remains unclear whether the actin cytoskeleton plays a similar role in sAg-induced BCR activation.

In this study, we compared the role of the actin cytoskeleton in BCR activation induced by sAg and mAg. Our results show that both mAg and sAg induce F-actin accumulation, actin polymerization, and the recruitment of the actin regulatory factors to BCR clusters, even though the kinetics and magnitude of these events are different in the two cases. Inhibition of actin reorganization by stabilizing F-actin blocks BCR clustering and tyrosine phosphorylation induced by both forms of Ag. Depolymerization of F-actin leads to unpolarized microclustering of BCRs and tyrosine phosphorylation in BCR microcluster without sAg and mAg. Our results demonstrate a similar role for the actin cytoskeleton in the initiation of BCR activation induced by mAg and sAg.

3.3 Materials and Methods

3.3.1 Mice and Cells.

Mice (CBA/CaJ) (Jackson Laboratories, Bar Harbor, ME) of 6-12 weeks old were used. To purify splenic B-cells, mononuclear cells isolated using Ficoll density-gradient centrifugation (Sigma-Aldrich, St Louis, MO) were treated with anti-Thy1.2 mAb (BD Biosciences, San Jose, CA) and guinea pig complement (Rockland Immunobiochemicals, Gilbertsville, PA) to remove T-cells and panned for 1 h to remove monocytes and dendritic cells.

3.3.2 Model antigens

Alexa Fluor 546 conjugated mono-biotinylated Fab'-anti-mouse IgM+G antibody (AF546-mB-Fab'-anti-Ig) was used to label the BCR. It is generated from the F(ab')$_2$ fragment (Jackson ImmunoResearch, West Grove, PA) using a published protocol [180]. To activate B-cells with soluble Ag (sAg), splenic B-cells were incubated with AF546-mB-Fab'-anti-Ig (2 μg/ml) mixed with mB-Fab'-anti-Ig (8 μg/ml) for 30 min and streptavidin (1 μg/ml) for 10 min at 4°C. As a control, streptavidin was omitted. The cells were washed and warmed up to 37°C for varying lengths of time. To activate B-cells with membrane-associated Ag (mAg), cells were incubated with AF546-mB-Fab'-anti-Ig and mB-Fab'-anti-Ig tethered to planar lipid bilayers by streptavidin at 37°C for varying lengths of time. As a control for mAg, surface BCRs were labeled with AF546-Fab-anti-mouse IgM+G (2 μg/ml) at 4°C, washed, and then the B-cells were incubated with transferrin (Tf)-tethered lipid bilayers where the molecular density of Tf on lipid bilayers was equivalent to that of AF546-mB-Fab'-anti-Ig.

The planar lipid bilayer was prepared as described previously [72,181]. Briefly, liposomes were made by sonication of 1,2-Dioleoyl-sn-Glycero-3-phosphocholine and 1,2-Dioleoyl-sn-Glycero-3-phosphoethanolamine-cap-biotin (Avanti Polar Lipids, Alabaster, AL) in a 100:1 molar ratio in PBS at a lipid concentration of 5 mM. Aggregated liposomes were removed by ultracentrifugation and filtration. Coverslip chambers (Lab-Tek Nalge Nunc, Rochester, NY) were incubated with the liposomes (0.05 mM) for 10 min. After extensive washes, the coated coverslip chambers were incubated with 1 μg/ml streptavidin (Jackson ImmunoResearch), followed by 2 μg/ml AF546-mB-Fab'-anti-Ig mixed with 8 μg/ml mB-Fab'-anti-Ig antibody or 16 μg/ml biotin-Tf.

3.3.3 Confocal fluorescence microscopy and image analysis

Splenic B-cells were incubated with mAg or sAg at 37°C for varying lengths of time. The cells were fixed with 4% paraformaldehyde (PFA), permeabilized with 0.05% saponin, and stained with anti-cofilin, phosphorylated cofilin, gelsolin (Santa Cruz Biotechnology, CA), or phosphotyrosine (4G10, Millipore, Billerica, Massachusetts) antibodies. F-actin was stained with AF488-phalloidin (Invitrogen) or total actin by anti-actin antibody (Sigma, St. Louis, MO). Cells were analyzed using a confocal microscope (Zeiss LSM 710, Carl Zeiss Microscopy, Thornwood, NY). Series of Z-sections were acquired at 0.4 μm per section and reconstituted into 3-D using Zen software from Zeiss. The 2.5 D images, which show fluorescence intensity profiles of F-actin, cofilin, or gelsolin in relation to the BCR staining, were generate using Zen software. Pearson correlation coefficients between different staining were determined using LSM 510 software [215].

The ratio of fluorescence intensity at the cell pole of BCR aggregation to that at the opposite pole of the cells was determined using z-series of images and Andor iQ software (Andor Technology, Belfast, UK). For mAg-stimulated B-cells, the fluorescence intensity sum of three z-sections close to lipid bilayers and that at the top of the cell were determined. For sAg-stimulated B-cells, only B-cells with the BCR central cluster located at the top of the cells were selected for the analysis. The fluorescence intensity sum of three z-sections close to the BCR central cluster and that close to the coverslip were determined. The level of tyrosine phosphorylation in individual mAg-stimulated B-cells was determined by adding up the fluorescence intensity of phosphotyrosine staining in all z-sections of a cells using Andor iQ software. For each time point, the average fluorescence intensity was generated from ~50 individual cells from two or three independent experiments.

3.3.4 Total internal reflection microcopy and image analysis

Images were acquired using a Nikon laser TIRF system on an inverted microscope (Nikon TE2000-PFS), equipped with a 60X, 1.49 NA Apochromat TIRF objective (Nikon Instruments Inc., Melville, NY), a Coolsnap HQ2 CCD camera (Roper Scientific, Sarasota, FL), and two solid-state lasers of wavelength 491 nm and 561 nm. For live cell imaging, time lapse images were acquired at the rate of one frame every 3 sec. Image acquisition started upon the addition of B-cells onto Ag-tethered lipid bilayer and continued for 5 to 10 min at 37°C. Interference reflection microscopy (IRM) images and fluorescence images at 491 nm excitation (for AF488) and 561 nm excitation (for AF546) were acquired sequentially.

To image intracellular molecules, B-cells were incubated with mAg at 37°C for varying lengths of time, and then fixed with 4% PFA, permeabilized with 0.05% saponin, and stained for cofilin, gelsolin, phosphotyrosine, and F-actin as described above. The B-cell contact area was determined using IRM images and MATLAB software (The MathWorks, Inc., Natick, MA). The total fluorescence intensity (TFI) of each staining in the B-cell contact zone was determined using Andor iQ software. Background fluorescence generated by Ag tethered to lipid bilayers in the absence of B-cells or secondary antibody controls was subtracted. For each set of data, more than 20 individual cells from two or three independent experiments were analyzed.

3.3.5 Analysis of actin nucleation sites

Actin nucleation sites were labeled as previously described [184]. For B-cells that were incubated with sAg, cells were treated with 0.45 μM AF488-G-actin (Invitrogen) in the presence of 0.025% saponin during the last minute of incubation. For B-cells that were activated by mAg, B-cells were incubated with mAg in the presence of AF488-G-actin and 0.025% saponin for 5 min at 37°C. The cells were fixed and analyzed using Zeiss 710 confocal microscope to generate 3-D images and/or

TIRFM.

3.3.6 Treatment of latrunculin B and Jasplakinolide

B-cells were pretreated with latrunculin B (Lat, 10 μM) or Jasplakinolide (Jas, 2 μM) (Calbiochem, Gibbstown, NJ) for 30 min at 37°C before the incubation with Ag in the presence of Lat or Jas. When B-cells were treated with Lat alone, the time course started at the addition of Lat.

3.3.7 Flow cytometry analysis

The tyrosine phosphorylation levels of sAg-stimulated B-cells were determined using flow cytometry. B-cells were incubated with sAg, Lat, or Jas plus sAg for varying lengths of time at 37°C. Then cells were fixed by 4% PFA, permeabilized by 0.05% saponin, and stained with anti-phosphotyrosine mAb. After post-fix with 2% PFA, the cells were analyzed using BD Canto II flow cytometer.

3.3.8 Statistical Analysis

Statistical significance was assessed by the Mann-Whitney test using Prism software (GraphPad Software, San Diego, CA).

3.4 Results

3.4.1 Both soluble and membrane-associated antigens induce the recruitment of F-actin to BCR aggregates

To compare actin reorganization induced by mAg and sAg, we chose a pseudo Ag system that can be applied as both soluble and membrane-associated forms. Alexa Fluor 546-conjugated, mono-biotinylated Fab' fragment of goat-anti-mouse IgG+M (AF546-mB-Fab'-anti-Ig) was used to label surface BCRs. Labeled BCRs were aggregated either with soluble streptavidin (sAg) or streptavidin tethered onto lipid bilayers (mAg). The reorganization of the actin cytoskeleton and surface BCRs in B-cells stimulated with sAg was examined using 3-dimentional (3-D) confocal fluorescence microscopy (CFM) and those in B-cells stimulated with mAg using both 3-D CFM and total internal reflection fluorescence microscopy (TIRFM). The surface area contacting Ag-tethered lipid bilayer (B-cell contact zone) was visualized by interference reflection microscopy (IRM). Upon incubation with mAg- but not with transferrin (Tf)-tethered lipid bilayers, surface BCRs on splenic B-cells aggregated into small clusters (3 min) and then formed a centralized cluster (7 min) at the B-cell contact zone, while the B-cell contact zone rapidly increased first (1-6 min) and then reduced (7 min) (Fig. 3.1A-C). During BCR aggregation, the actin cytoskeleton underwent a dramatic redistribution, from a uniform distribution at the periphery of unstimulated cells to accumulation at the contact zone (Fig. 3.1A-C). By 7 min, the actin cytoskeleton was primarily concentrated at the outer edge of centralized BCR clusters and did not colocalize with BCR clusters extensively (Fig. 3.1A-B and 3.1D).

In B-cells stimulated with sAg, surface BCRs also formed microclusters at 3 min and then a polarized BCR central cluster at 7 min (Fig. 3.1E), which was similar to what was seen in mAg-stimulated B-cells. However, BCR clusters induced by sAg appeared less dense than those induced by mAg (Fig. 3.1A and 3.1E, bottom panels). Soluble Ag also induced the recruitment of F-actin to BCR clusters. F-actin accumulated not only at the periphery but also the center of the BCR central cluster (Fig. 3.1E), colocalizing with the BCR extensively (Fig. 3.1D). In order to compare the kinetics and magnitude of actin redistribution in mAg- and sAg-stimulated cells, the ratio of F-actin fluorescence intensity in the CFM image slices at the BCR central cluster to that at the opposite pole of the BCR central cluster was determined. The two pole ratio of F-actin was about 1 in unstimulated B-cells that interacted with polylysine-coated glass or Tf-tethered lipid bilayers, and it increased over time in both mAg- and sAg-stimulated B-cells (Fig. 3.1F). This indicates a redistribution of F-actin from unpolarized to polarized distribution towards BCR clusters. The two pole ratio in mAg-stimulated B-cells increased faster and was two fold higher than that in sAg-stimulated B-cells at all the tested time points (Fig. 3.1F). Taken together, these results indicate that both mAg and sAg induce the recruitment of the actin cytoskeleton to BCR clusters in accompany of BCR aggregation. Membrane-associated Ag appears to induce a greater degree of polarized actin redistribution than sAg.

3.4.2 Both soluble and membrane-associated antigens induce actin polymerization at BCR aggregates

Figure 3.1 The recruitment of F-actin to BCR aggregates in B-cells stimulated by membrane associated or soluble antigen. (A-C) To mimic mAg, splenic B-cells were incubated with AF546-mB-Fab'-anti-Ig tethered to lipid bilayers at 37°C for varying lengths of time. As controls, splenic B-cells were labeled with AF546-Fab-anti-Ig for the BCR before incubation with biotinylated transferrin (Tf)-tethered lipid bilayers. (E) To mimic sAg, splenic B-cells were incubated with AF546-mB-Fab'-anti-Ig for 10 min at 37°C to label the BCR. Then the cells were either incubated with streptavidin or with the medium alone (- or 0 min) as a control at 37°C for varying lengths of time. After fixation and permeabilization, the cells were stained for F-actin by AF488-phalloidin and analyzed using CFM. Series of Z-section images were acquired and reconstituted into 3-D images (A and E). The B-cell membrane contacting lipid bilayers was analyzed using TIRFM (B). The B-cell contact area and the total fluorescence intensity (TFI) of mAg and F-actin in the contact zone were quantified using Andor iQ software, and the data were plotted versus time (C). The distribution of F-actin in relation to BCR central clusters in B-cells stimulated with sAg and mAg for 7 min was analyzed by Zen software and is shown as 2.5-D fluorescence intensity profile (D), where yellow indicates colocalization. The fluorescence intensity ratios of F-actin at the BCR central cluster and at the opposite pole of the BCR central cluster (FI two pole ratio) in mAg- or sAg-stimulated B-cells were quantified using Andor iQ software (F). Shown are representative images and average values (±SD) from ~50 cells of three or four independent experiments. Scale bars, 2.5 μm. * $p<0.01$ compared to sAg in F.

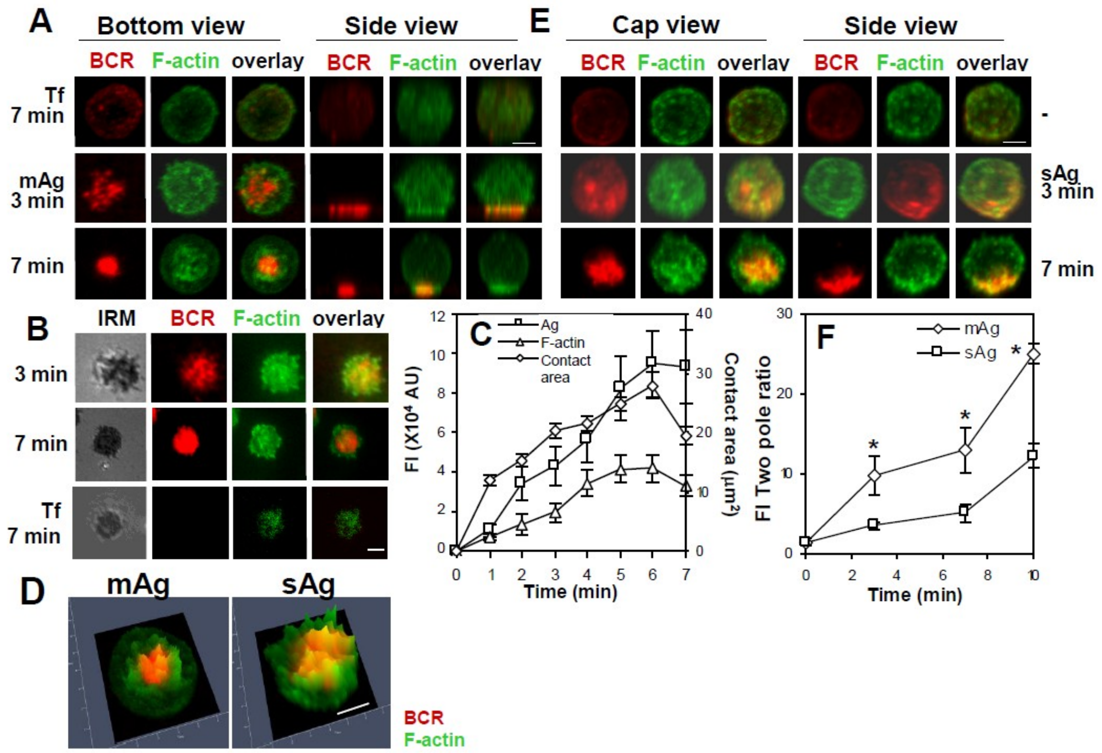
A
Bottom view
Side view
BCR
F-actin
overlay
Tf 7 min
mAg 3 min
7 min
E
Cap view
Side view
sAg 3 min
7 min
B
IRM
BCR
F-actin
overlay
3 min
7 min
Tf 7 min
C
Ag
F-actin
Contact area
FI (X10⁴ AU)
Contact area (μm²)
Time (min)
0
1
2
3
4
5
6
7
8
10
12
20
30
40
D
mAg
sAg
BCR
F-actin
F
mAg
sAg
FI Two pole ratio
Time (min)
*
0
2
4
6
8
10
20
30

The actin cytoskeleton is reorganized by rapid polymerization and depolymerization. To further compare actin remodeling induced by mAg with that induced by sAg, we analyzed the cellular distribution of *de novo* actin polymerization sites in relation to surface BCRs. Actin polymerization sites were detected by the incorporation of AF488-G-actin into polymerizing ends of actin filaments. AF488-G-actin was introduced into cells in the presence of a low concentration of non-ionic detergent during the last minute of incubation with sAg or during the entire incubation time with mAg. Intracellular incorporation of AF488-G-actin was significantly increased in splenic B-cells stimulated by mAg compared to B-cells incubated with Tf-tethered lipid bilayer (Fig. 3.2A). Both 3-D CFM (Fig. 3.2A) and TIRFM (Fig. 3.2B) analysis showed that actin polymerization sites were preferentially located at the outer edge of BCR clusters after a 5 min-incubation with mAg. Similarly, actin polymerization was undetectable in the absence of sAg (Fig. 3.2C, top panels). After sAg stimulation, *de novo* actin polymerization sites were first colocalized with BCR microclusters and later were exclusively found at the outer rim of BCR central clusters as they were forming (Fig. 3.2C). These results show that both sAg and mAg induce actin polymerization, and actin polymerization occurs at BCR microclusters and at the outer edge of the BCR central cluster.

Figure 3.2 Both membrane-associated and soluble antigens trigger actin polymerization at BCR aggregates. Splenic B-cells were incubated with AF546-mB-Fab'-anti-Ig tethered to lipid bilayers (mAg) in the presence of AF488-G-actin and 0.025% saponin at 37°C for 5 min, followed by fixation. 3-D images were acquired using a confocal microscope (A). The B-cell contact zone was imaged using TIRFM (B). Splenic B-cells were incubated with AF546-mB-Fab'-anti-Ig for 10 min and continued without (-) or with streptavidin (sAg) at 37°C for indicated times. In the last minute of the stimulation, cells were incubated with AF488-G-actin in the presence of 0.025% saponin. Cells were fixed and analyzed by CFM (C). Shown are representing 2-D, 3-D CFM and TIRFM images from three independent experiments. Scale bars, 2.5 μm.

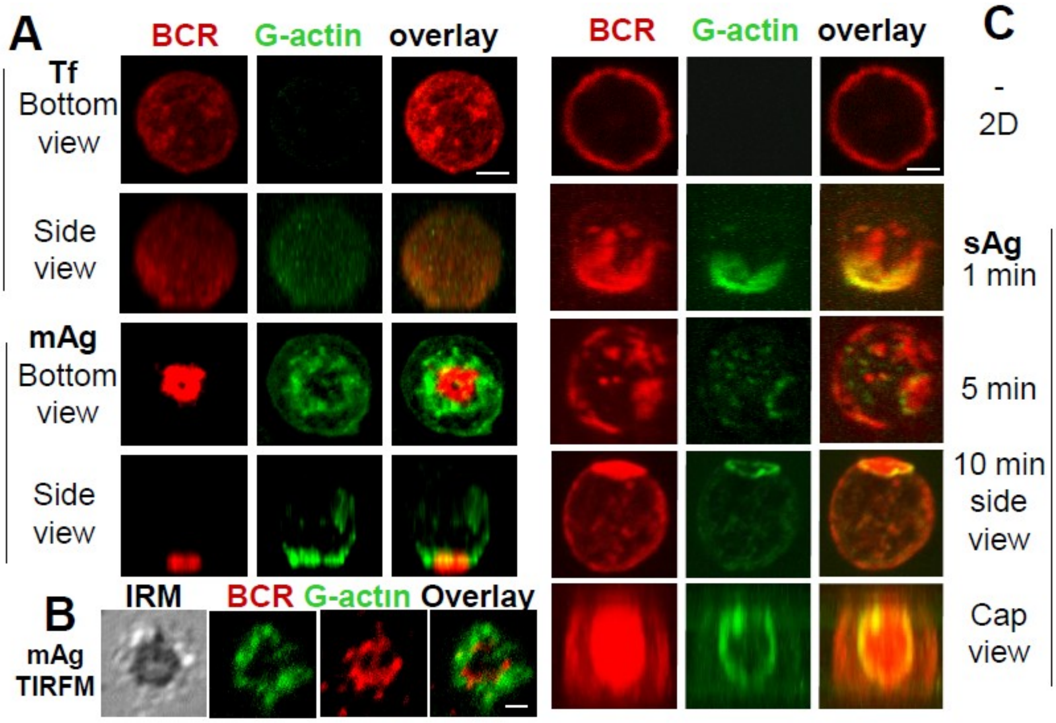
A
BCR
G-actin
overlay
Tf
Bottom view
Side view
mAg
Bottom view
Side view
B
mAg
TIRFM
IRM
BCR
G-actin
Overlay
BCR
G-actin
overlay
C
-
2D
sAg
1 min
5 min
10 min side view
Cap view

3.4.3 Both sAg and mAg induce the mobilization of actin regulators cofilin and gelsolin

Actin reorganization induced by Ag indicates that antigenic stimulation triggers the activation of actin regulators. Our previous studies have demonstrated that both mAg and sAg can induce Btk-dependent activation of WASP, an actin nucleation promoting factor [118,155]. Here we compared the effects of mAg and sAg on the cellular redistribution of actin regulators, cofilin and gelsolin. Cofilin can either stabilize or destabilize F-actin depending on its concentration in the cytoplasm, and its F-actin binding activity is inhibited by phosphorylation [216]. Gelsolin severs F-actin in a calcium dependent manner [217]. The cellular distribution of cofilin and gelsolin in splenic B-cells was analyzed using specific antibodies. In the control conditions where splenic B-cells interact with Tf-tethered lipid bilayers (Fig. 3.3A, top panels) or with polylysine-coated glass slides (Fig. 3.3C, top panels), cofilin distributed evenly at the cell periphery. Reconstituted 3-D CFM images showed that in mAg-stimulated B-cells, cofilin was recruited to BCR clusters as early as 3 min, surrounding the BCR central cluster (Fig. 3.3A, bottom panels). However, TIRFM did not detect a significant amount of cofilin at the B-cell contact zone (Fig. 3.3B), suggesting that recruited cofilin does not associate with the plasma membrane and is at least 200 nm away from the contact zone. Reconstituted 3-D CFM images showed that cofilin was primarily located at the top of the BCR central cluster (Fig. 3.3A, bottom panels). In sAg-stimulated splenic B-cells, cofilin was clearly recruited to BCR aggregates at early times and the central clusters at later times (Fig. 3.3C, bottom panels). Reconstituted 3-D images and 2.5-D fluorescence intensity profiles showed extensive colocalization of cofilin with the BCR central cluster (Fig. 3.3C-D), distinct from the distribution of cofilin in mAg-stimulated B-cells (Fig. 3.3A). The colocalization of cofilin with the BCR in sAg-stimulated B-cells, as quantified by Pearson's correlation coefficients, increased over time for 10 min and decreased by 30 min as the BCR was internalized (Fig. 3.3E).

To determine whether cofilin recruitment is dependent on signaling, B-cells were pretreated with the Src kinase inhibitor PP2. This treatment inhibited BCR central cluster formation and reduced the colocalization of cofilin with the BCR to the basal level in sAg-stimulated B-cells (Fig. 3.3E-F). To determine whether the cofilin recruited to BCR clusters is activated, we stained for phosphorylated cofilin (p-cofilin) which is incapable of binding to F-actin in sAg-stimulated B-cells [218]. In mAg-stimulated B-cells, p-cofilin was neither recruited to the B-cell contact zone (Fig. 3.3G) nor the region above the contact zone in response to mAg (Fig. 3.3H) in comparison with B-cells interating with Tf tethered lipid bilayers. In sAg-stimulated B-cells, p-cofilin was largely excluded from BCR clusters (Fig. 3.3I) and did not colocalize with the BCR (Fig. 3.3J). The differential distribution of total cofilin and p-cofilin suggests that most of cofilin that co-clustered with surface BCRs is active. Similar to F-actin recruitment, the fluorescence intensity ratio of cofilin at the BCR central cluster to that at the opposite pole increased over time in both mAg- and sAg-stimulated B-cells, but it increased much faster and reached higher levels in mAg-stimulated cells than in sAg-stimulated cells (Fig. 3.3K). Incubation with either mAg or sAg led to the redistribution of gelsolin to BCR clusters in splenic B-cells, where gelsolin staining appeared punctate (Fig. 3.4A and 3.4C). Similar to cofilin, gelsolin surrounded the BCR central cluster in mAg-stimulated B-cells (Fig. 3.4A), but colocalized with the BCR through the central cluster in sAg-stimulated B-cells (Fig. 3.4C-D).

Figure 3.3 Both membrane-associated and soluble antigens induce the recruitment of cofilin in a signaling-dependent manner. Splenic B-cells were incubated with AF546-mB-Fab'-anti-Ig tethered to lipid bilayers (mAg) at 37°C for indicated times. Cells were fixed, permeabilized, stained for cofilin and phosphorylated cofilin (p-cofilin), and analyzed by 3-D CFM (A and H) and TIRFM (B and G). Splenic B-cells pretreated without (C and I) or with PP2 (F) were incubated with AF546-mB-Fab'-anti-Ig without (-) or with streptavidin (sAg) at 4°C, washed, and warmed to 37°C for varying lengths of time. After fixation and permeabilization, the cells were stained for cofilin (C and F) or p-Cofilin (I), and analyzed using CFM. Fluorescence intensity profiles (2.5-D) of cofilin and BCRs in B-cells stimulated by mAg and sAg for 10 min were generated using Zen software (D). The Pearson's correlation coefficients between BCR and cofilin (E) or p-cofilin (J) staining were determined. The fluorescence intensity ratio of cofilin at the BCR central cluster to that at its opposite pole (FI two pole ratio) in B-cells stimulated by mAg and sAg were determined using Andor iQ software (K). Shown are representative 2-D, 2.5-D, 3-D CFM and TIRFM images at 10 min and the average values (±SD) of ~50 cells from three independent experiments. Scale bars, 2.5 μm. * *$p<0.01$* compared to PP2 treatment in E and compared to sAg in I.

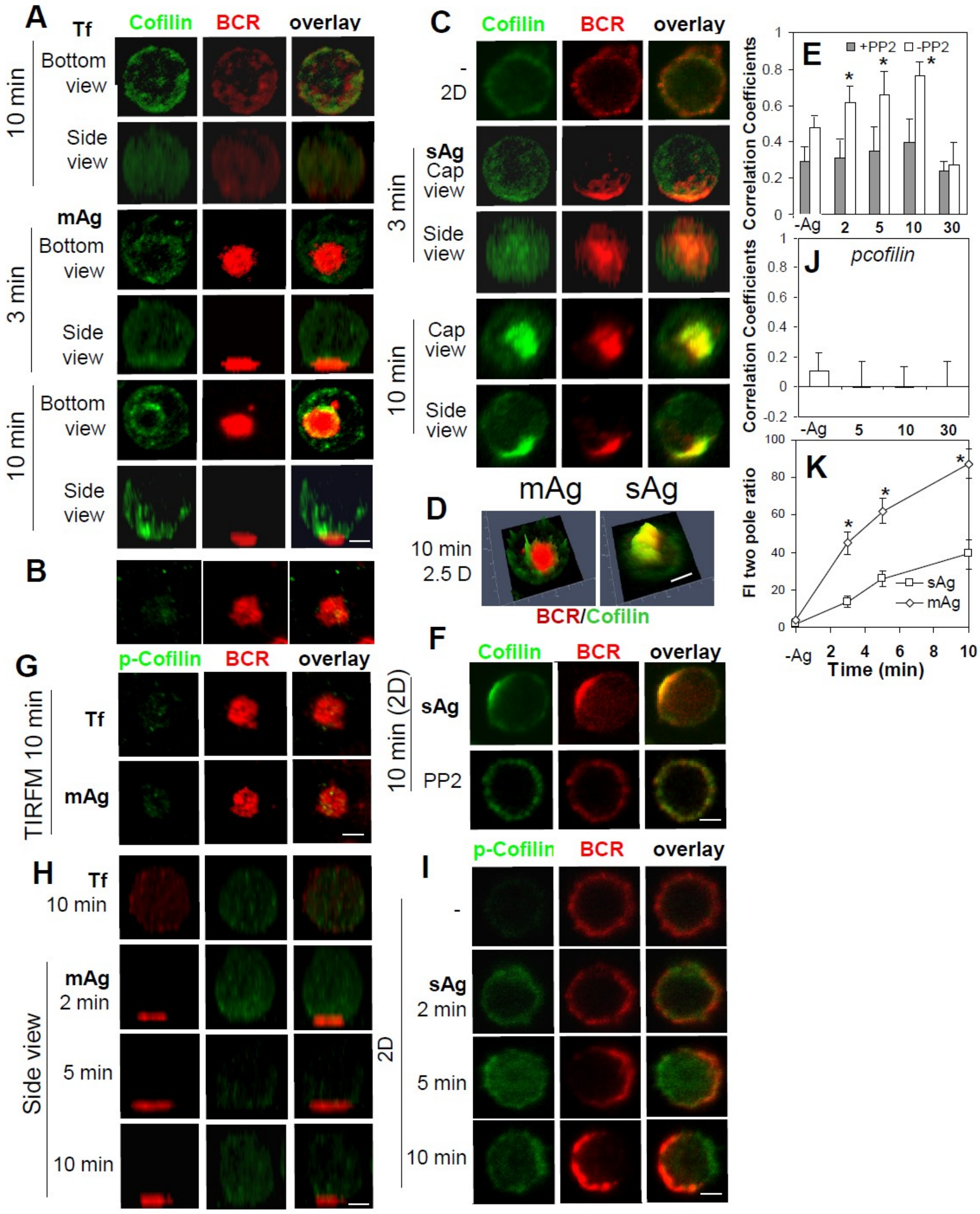
A
Tf
Cofilin
BCR
overlay
10 min
Bottom view
Side view
mAg
3 min
Bottom view
Side view
10 min
Bottom view
Side view
B
C
Cofilin
BCR
overlay
-
2D
3 min
sAg
Cap view
Side view
10 min
Cap view
Side view
D
mAg
sAg
10 min
2.5 D
BCR/Cofilin
E
+PP2
-PP2
Correlation Coefficients
1
0.8
0.6
0.4
0.2
0
-Ag
2
5
10
30
J
pcofilin
Correlation Coefficients
1
0.8
0.6
0.4
0.2
0
-0.2
-Ag
5
10
30
K
FI two pole ratio
100
80
60
40
20
0
sAg
mAg
-Ag
2
4
6
8
10
Time (min)
G
p-Cofilin
BCR
overlay
TIRFM 10 min
Tf
mAg
F
Cofilin
BCR
overlay
10 min (2D)
sAg
PP2
H
Tf
10 min
Side view
mAg
2 min
5 min
10 min
I
p-Cofilin
BCR
overlay
2D
-
sAg
2 min
5 min
10 min

There was no significant amount of gelsolin detected in the contact zone of mAg-stimulated B-cells by TIRFM (Fig. 3.4B). The Pearson's correlation coefficients showed a similar increase in the colocalization of gelsolin with the BCR over time as cofilin (Fig. 3.4E). The two pole ratio of gelsolin fluorescence intensity increased over time and was much higher (~4 fold) in mAg-stimulated cells than that in sAg-stimulated cells (Fig. 3.4F).

Taken together, these results show that both mAg and sAg induce the recruitment of cofilin and gelsolin to BCR clusters; however their recruitment kinetics and magnitude and their distribution are different in mAg- and sAg-stimulated B-cells.

Figure 3.4 The recruitment of gelsolin to BCR clusters in B-cells stimulated by soluble or membrane-associated Ag. Splenic B-cells were incubated with AF546-mB-Fab'-anti-Ig tethered to lipid bilayers (mAg) at 37°C for indicated times. Cells were fixed, permeabilized, stained for gelsolin, and analyzed by CFM (A) and by TIRFM (B). Splenic B-cells were incubated with AF546-mB-Fab'-anti-Ig without (-) or with streptavidin (sAg) at 4°C, washed, and warmed to 37°C for varying lengths of time. After fixation and permeabilization, the cells were stained for gelsolin and analyzed using CFM (C). The 2.5-D fluorescence intensity profiles of BCRs and gelsolin were generated using Zen software (D). The Pearson's correlation coefficients between BCR and gelsolin staining in sAg-stimulated cells were determined using Zen software (E). The two pole ratio of gelsolin fluorescence intensity was determined using Andor iQ software (F). Shown are representative 2-D, 2.5-D, and 3-D images at 10 min and the average values (±SD) of ~50 cells from three independent experiments. Scale bars, 2.5 μm. * $p<0.01$ compared to no streptavidin (-) in E and compared to sAg in F.

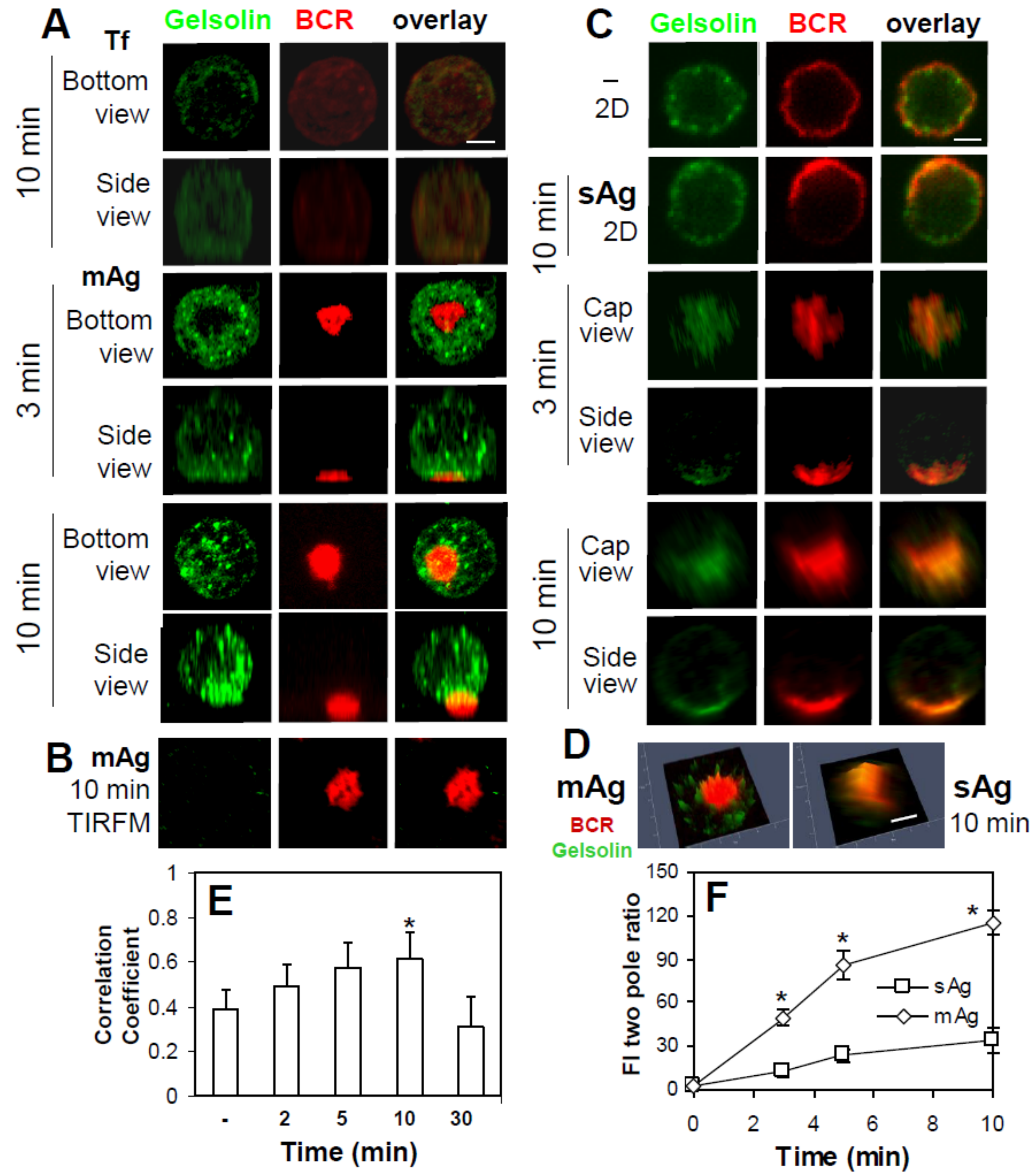
A
Gelsolin
BCR
overlay
Tf
10 min
Bottom view
Side view
mAg
3 min
Bottom view
Side view
10 min
Bottom view
Side view
B
mAg
10 min
TIRFM
C
Gelsolin
BCR
overlay
–
2D
10 min
sAg
2D
3 min
Cap view
Side view
10 min
Cap view
Side view
D
mAg
BCR
Gelsolin
sAg
10 min
E
Correlation Coefficient
1
0.8
0.6
0.4
0.2
0
*
-
2
5
10
30
Time (min)
F
FI two pole ratio
150
120
90
60
30
0
*
*
*
sAg
mAg
0
2
4
6
8
10
Time (min)

3.4.4 Disruption of the actin cytoskeleton alters BCR activation in response to both soluble and membrane-associated antigens as well as antigen-independent BCR signaling

To compare the role of the actin cytoskeleton in BCR activation induced by mAg and sAg, we disrupted the actin cytoskeleton using a pharmacological approach using latrunculin B (Lat) and jasplakinolide (Jas). Lat promotes actin depolymerization by sequestering G-actin [219], and in contrast, Jas stabilizes F-actin and binds F-actin at the same site as phalloidin [220]. We used these two reagents at concentrations that abolished most phalloidin staining, which indicates that Lat depolymerizes and Jas binds most F-actin in B-cells at these concentrations. Using both 3-D CFM and TIRFM, we found that at these concentrations, both the pretreatment of Lat and Jas dramatically reduced BCR aggregation at the B-cell contact zone (Fig. 3.5A-B and Fig. 3.6A-C) as well as B-cell spreading on Ag-tethered lipid bilayers (Fig. 3.5A and 3.5C). Similarly, Jas pretreatment inhibited the formation of BCR clusters induced by sAg (Fig. 3.6F-H). These data indicate that BCR aggregation induced by both mAg and sAg requires actin reorganization.

Figure 3.5 Inhibition of actin reorganization blocks BCR aggregation and cell spreading in membrane-associated antigen-stimulated B-cells. Splenic B-cells were pretreated with or without latrunculin B (Lat, 10 μM) or jasplakinolide (Jas, 2 μM) for 30 min and then incubated with AF546-mB-Fab'-anti-Ig or non-specific antibody (Control Ag) tethered to lipid bilayers at 37°C. Time lapse images were acquired using TIRFM (A). The B-cell contact area (C) and the total fluorescence intensity (TFI) of AF546-mB-Fab'-anti-Ig in the contact zone (B) were quantified using Andor iQ software, and the data were plotted versus time. Shown are representative images of cells at 7 min (A) and the average contact area (C) and Ag TFI (+SD) (B) from ~ 20 cells of three independent experiments. Scale bars, 2.5 μm.

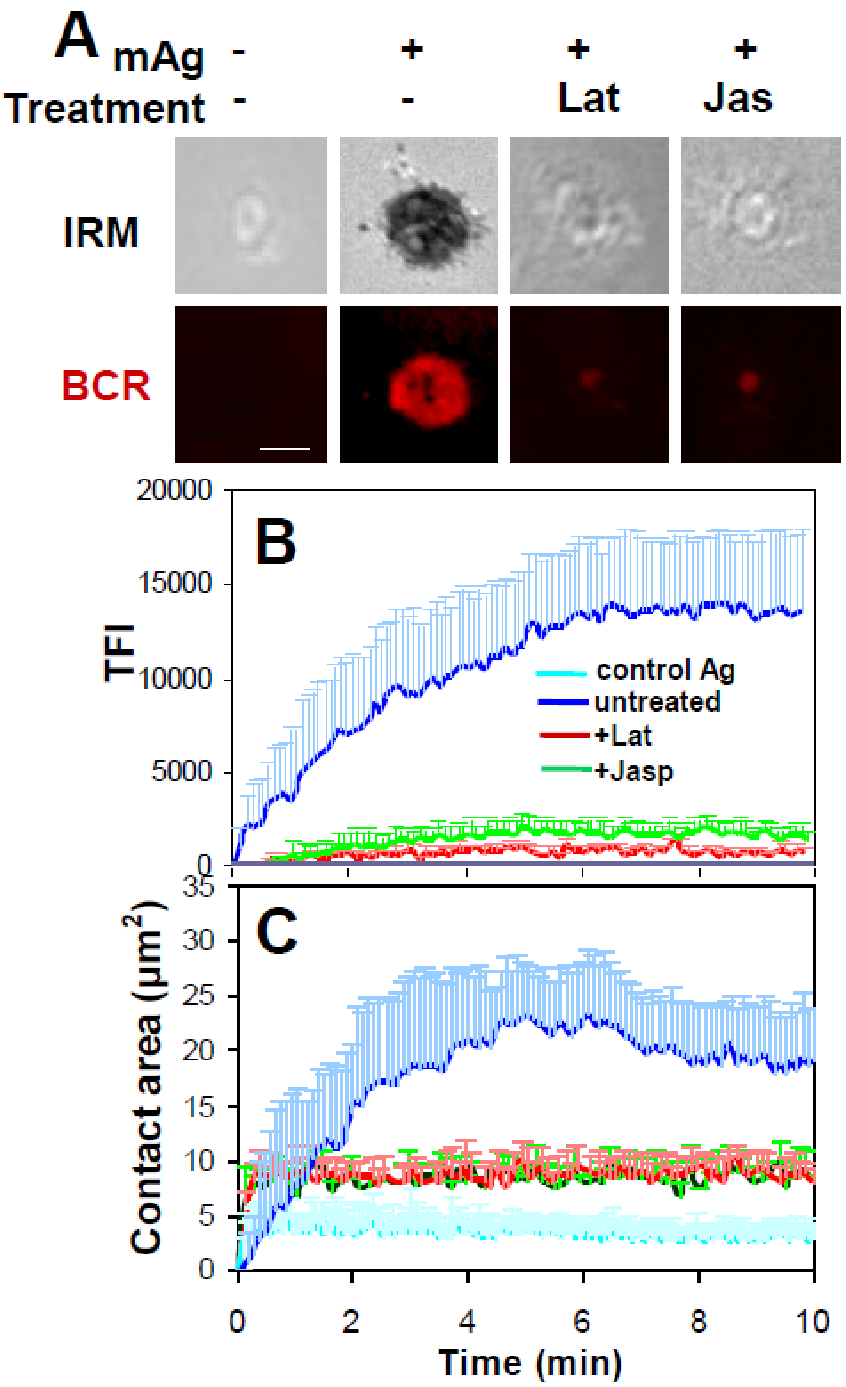
A
mAg - + + +
Treatment - - Lat Jas
IRM
BCR
B
TFI
20000
15000
10000
5000
0
control Ag
untreated
+Lat
+Jasp
C
Contact area (µm²)
35
30
25
20
15
10
5
0
2
4
6
8
10
Time (min)

In order to investigate whether the effect of Jas and Lat on BCR aggregation has any impact on BCR signaling, we examined the distribution and level of tyrosine phosphorylation (pY) using phosphotyrosine mAb by both microscopy and flow cytometry approaches. The staining of pY was detected at BCR clusters in response to both mAg and sAg, but appeared in different distribution patterns in relation to the BCR central cluster (Fig. 3.6A-B and 3.6F-G). It was primarily located at the outer edge of the BCR central cluster in mAg-stimulated B-cells (Fig. 3.6B, 3.6E, and 3.6J), but colocalized extensively with the BCR through the central cluster in sAg-stimulated B-cells (Fig. 3.6G and 3.6J). The pY levels in splenic B-cells dramatically increased in response to both mAg and sAg, peaking at ~2 min and returning to the basal level by 10 min (Fig. 3.6K-L). Pretreatment with Jas blocked tyrosine phosphorylation induced by both mAg and sAg (Fig. 3.6C, 3.6H, and 3.6K-L).

The actin cytoskeleton has been shown to regulate Ag-independent signaling in B-cells by controlling BCR lateral mobility [149]. To understand how actin is involved in signaling regulation in resting B-cells, we determined the effect of Lat and Jas at the concentrations that eliminate or bind most F-actin on BCR aggregation and tyrosine phosphorylation in unstimulated B-cells attached to lipid bilayers by Tf or attached to polylysine-coated glass slides. The reconstituted 3-D CFM analysis showed that when B-cells were treated with Lat in absence of Ag, surface BCRs formed microclusters in a non-polarized manner (Fig. 3.6D and 3.6I). There were very few numbers of BCR microclusters detected by TIRFM in the B-cell membrane zone contacting Tf-tethered lipid bilayers (Fig. 3.6E, bottom panels). BCR microclusters in

Figure 3.6 Disruption of the actin cytoskeleton alters signal activation in response to both membrane-associated and soluble antigens and antigen-independent signal activation. For mAg stimulation, splenic B-cells that were pretreated without (B and E top panels) or with Jas (C) were incubated with AF546-mB-Fab'-anti-Ig tethered lipid bilayers at 37°C for indicated times. For a negative control of mAg, splenic B-cells were stained with AF546-Fab-anti-Ig first and then incubated with Tf-tethered lipid bilayer at 37°C for indicated times (A). For Lat treatment, B-cells labeled with AF546-Fab-anti-Ig were incubated with Lat and Tf-tethered lipid bilayer at the same time (D and E, bottom panels). For sAg stimulation, splenic B-cells that were pretreated without (G) or with Jas (H) were incubated with AF546-mB-Fab'-anti-IgG plus streptavidin at 37°C for indicated times. For a negative control of sAg, splenic B-cells were labeled with AF546-mB-Fab'-anti-Ig for the BCR first and then incubated with medium at 37°C for indicated times (F). For Lab treatment, B-cells labeled with AF546-mB-Fab'-anti-Ig were incubated with Lat (I). After fixation and permeabilization, the cells were stained for phosphotyrosine (pY) and analyzed using CFM (A-D and F-J) and TIRFM (E). Shown are representative 3-D CFM images (A-D and F-I), 2.5-D FI profiles (J), and TIRFM images (E) from three independent experiments. Scale bars, 2.5 μm. The total fluorescence intensity of pY in individual cells stimulated by mAg was determined by summing the fluorescence intensity of all z-sections of a cell, and shown are the average fluorescence intensity (FI) (±SD) of ~50 cells from three individual experiments (K). The MFI of pY in sAg-stimulated cells was quantified using flow cytometry, and shown are the average MFI (±SD) of pY staining of three

independent experiments (L). * $p<0.01$ compared to cells treated with mAg (K) or sAg (L) without Lat or Jas.

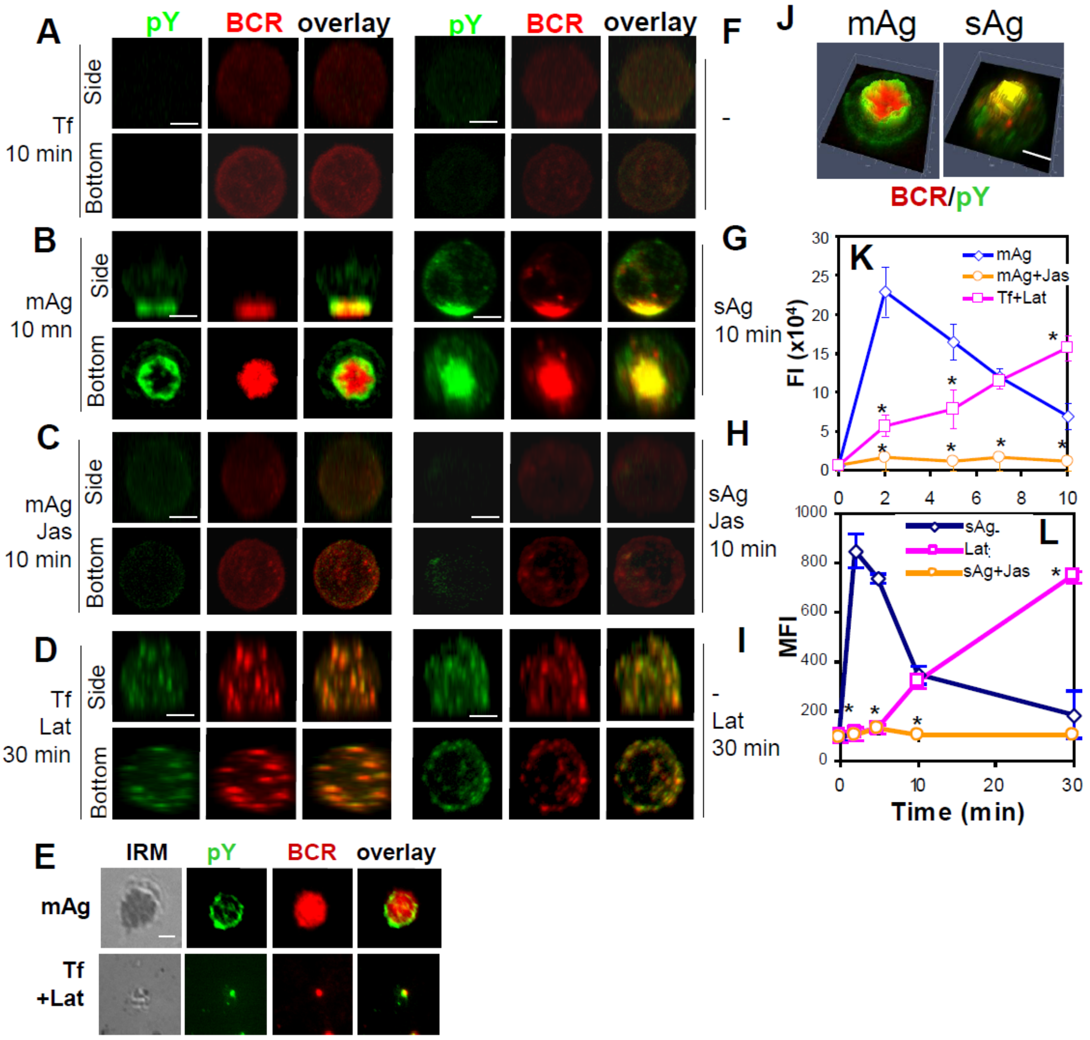
A
pY
BCR
overlay
pY
BCR
overlay
F
Side
Bottom
Tf
10 min
-
B
mAg
10 mn
G
sAg
10 min
C
mAg
Jas
10 min
H
sAg
Jas
10 min
D
Tf
Lat
30 min
I
-
Lat
30 min
J
mAg
sAg
BCR/pY
K
mAg
mAg+Jas
Tf+Lat
FI (x10⁴)
0
5
10
15
20
25
30
0
2
4
6
8
10
*
L
sAg
Lat
sAg+Jas
MFI
0
200
400
600
800
1000
0
10
20
30
Time (min)
E
IRM
pY
BCR
overlay
mAg
Tf
+Lat

Lat-treated cells were formed at 10 min, which is later than those induced by mAg and sAg (data not shown), and remained randomly distributed at 30 min (Fig. 3.6D and 3.6I). These BCR microclusters were positive for pY staining (Fig. 3.6D and 3.6I), suggesting that tyrosine phosphorylation occurs at these BCR microclusters. Quantitative analysis showed that Lat treatment alone increased the pY level in unstimulated B-cells. However, this Lat-induced pY increase had a much slower kinetics than that induced by Ag and did not show any sign of attenuation for at least 30 min (Fig. 3.6K-L). In contrast, Jas treatment induced neither BCR aggregation nor tyrosine phosphorylation (data not shown).

These results collectively suggest that actin depolymerization itself is sufficient for BCR self aggregation into microclusters and signal induction in BCR aggregates; however actin polymerization may be essential for the fast kinetics of BCR aggregation and signal activation and the merger of BCR microclusters into the central cluster as well as signaling attenuation induced by both mAg and sAg.

3.5 Discussion

Two of the common physical forms of Ags that B-cells encounter in the draining lymph node and spleen are soluble Ag and Ag presented on the surface of dendritic cells and macrophages [196]. How the physical presentation of Ag modulates BCR signaling has not been well studied. Previous studies have shown a role for the actin cytoskeleton in mAg-induced BCR activation [209]. This study reveals that actin reorganization is equally important for BCR signaling triggered by sAg. Both mAg and sAg induce actin reorganization and recruitment of actin regulators to BCR aggregates. Inhibition of actin reorganization by stabilizing F-actin blocks BCR aggregation and tyrosine phosphorylation induced by both mAg and sAg. Elimination of most F-actin by depolymerization leads to the unpolarized formation of BCR microclusters and tyrosine phosphorylation in the BCR microcluster in the absence of Ag. These data indicate an essential role for the actin cytoskeleton in BCR activation, despite of the nature of Ag presentation.

Because of their different physical forms, sAg and mAg have distinct modes of interaction with surface BCRs. While sAg can bind BCRs on the entire surface of B-cells at the same time in a non-polarized fashion, mAg can only bind BCRs at the surface zone contacting the Ag-tethered membrane, which provides a polarized stimulation. Although both sAg and mAg can induce BCR self-aggregation into microclusters and central clusters by cross-linking BCRs, in the case of sAg, surface BCRs have to identify a pole of the cell to laterally migrate towards in order to form the BCR central cluster. In addition, mAg induces more dramatic morphological changes to B-cells than sAg. These lead to the hypothesis that the actin cytoskeleton plays distinct roles in mAg- and sAg-stimulated BCR activation. This study shows that while both mAg and sAg induce actin reorganization in splenic B-cells, the magnitude of F-actin and actin regulator recruitment in mAg-stimulated cells is generally greater than that in sAg-stimulated cells, which was revealed by comparing the fluorescence intensity ratio between the pole where the BCR central cluster forms and its opposite pole. In addition, mAg-induce BCR redistribution appears to lead to the formation of more compact BCR central clusters than sAg. Because we formulated mAg and sAg using the same reagents with the same concentrations and examined both using the same approach, the observed differences suggest that the physical form of Ag has an impact on actin reorganization and surface BCR aggregation, and mAg appears to be more potent in triggering these events compared to sAg.

In addition to differences in the recruitment levels, the distribution patterns of F-actin, cofilin and gelsolin differ in mAg- and sAg-stimulated B-cells. F-actin, cofilin and gelsolin are preferentially localized at the outer edge of the contact zone in mAg-stimulated B-cells, but colocalized with the BCR throughout the central cluster in sAg-stimulated B-cells. Their differential distribution likely is linked to the distinct mechanisms by which BCR aggregates grow and merge with each other in mAg- and sAg-stimulated cells. In mAg-stimulated B-cells, after initial contacting with mAg, B-cells undergo rapid spreading against Ag-tethered membrane, which is followed by contraction [76]. B-cell spreading has been shown to enhance BCR self-aggregation by allowing more surface BCRs to engage Ag, and B-cell contraction after spreading facilitates the merger of small BCR aggregates into the central cluster [76,155]. The co-accumulation of WASP, cofilin and gelsolin with F-actin at the outer edge of the contact membrane suggests that actin polymerization (by WASP), severing and/or depolyermization (by cofilin and gelsolin) occur at the leading edge of the spreading membrane. This study also finds that in contrast to WASP [155], cofilin and gelsolin are not concentrated in the B-cell contact zone, but localized more than 200 nm above the BCR central cluster. This indicates that F-actin severing and/or polymerization mediated by cofilin and gelsolin occurs above the BCR central cluster, which potentially promotes actin depolymerization at the cytoplasmic side of the actin cytoskeleton and provides G-actin monomers for WASP-mediated act polymerization at the B-cell contact zone. Such a coordination of cofilin and gelsolin with WASP and other actin regulators potentially leads to actin reorganization in a unique mannor that generates both lateral force for B-cell spreading and contraction and vertical force for the adherence of B-cells to Ag-tethered membrane. A recent study by Freeman et al. [69] shows that Rap GTPase-dependent activation of cofilin leads to actin severing, which is required for efficient B cell spreading and BCR aggregation, which confirms a role for cofilin in BCR activation in response to mAg.

In contrast to mAg-stimulated B-cells, sAg-stimulated B-cells do not have a target surface to adhere to and do not dramatically change their morphology. The persisted colocalization of F-actin, cofilin and gelsolin with surface BCR aggregates in sAg-stimulated B-cells provides two indications. First, the lateral movement of BCR aggregates and the actin cytoskeleton is functionally linked with each other. Second, both WASP activated actin polyermization and cofilin- and gelsolin-mediated actin severing and/or depolymerization occur at the plasma membrane, which potentially induces lateral mobilization of actin filaments for the later movement of BCR but not for the formation of lamellipodia for morphological changes. Further studies are required to test these hypotheses.

The differences in distribution of F-actin and actin regulators in mAg- and sAg-stimulated B-cells raise the question of how these two types of Ags induce distinct actin reorganization. Ag-triggered actin reorganization has been shown to depend on BCR signaling. We have recently shown that the recruitment and activation of WASP are positively and negatively regulated by Btk and SHIP-1 respectively [118,155]. This study shows that cofilin and gelsolin, two actin regulators involved in actin severing and depolymerization, also co-clustered with surface BCRs in response to both mAg and sAg. Furthermore, the co-clustered cofilin is primarily in the active form that is unphosphorylated and capable of binding F-actin, and the co-clustering of cofilin with the BCR depends on BCR signaling. Freeman et al. [69] recently show that cofilin in B-cells is activated in a Rap GTPase-dependent manner in response to Ag stimulation. These results indicate that the activation and recruitment of cofilin and gelsolin is an additional route for BCR signaling to regulate actin reorganization. Gelsolin is known to be activated by calcium flux [221]. The activity of cofiin has been shown to be regulated via a growing number of cellular pathways, including its phosphorylation and dephosphorylation by LIM kinases and phosphotases chronophin and slingshot 1L, its binding to phosphatidylinositides, and its local concentration relative to the level of F-actin [222]. The physical presentation of Ags may regulate the spatiatemporal organization of BCR signaling microsomes, consequently leading to differential activation or distribution of these actin regulators.

How the physical presentation of Ag, soluble and membrane bound, impacts the initiation event of BCR signaling remains to be addressed. Association with membrane transforms Ag stimulation from a non-polarized into a polarized, concentrated one, which could cause physical restrain to the Ag-BCR interaction. This increased physical restraint potentially enhances the ability of Ag to induce conformational changes to the BCR, thereby facilitating BCR self-aggregation. Tolar *et al.* [71] showed that a mono-valent Ag, which cannot induce BCR activation as a soluble form, induced BCR aggregation and signaling when it was tethered to lipid bilayers. This mono-valent mAg induces BCR self-aggregation probably by inducing conformational changes of the BCR, exposing the Cμ4 domain of membrane IgM that has been shown to be involved in BCR self-aggregation. Therefore, the physical form of Ag potentially modulates BCR activation via their ability to induce conformational change. This study shows that the phosphotyrosine stain has different distribution patterns in mAg- and sAg-stimulated B-cells, at the outer edge of the central cluster in mAg-stimulated B-cells and throughout the central cluster in sAg-stimulated B-cells. This result suggests that mAg- and sAg-induced signalosomes differ in their spatial organization. Our finding that the distribution pattern of phosphotyrosine staining in mAg- and sAg-stimulated cells are similar to those of F-actin and actin regulators, cofilin and gelsolin supports the notion that differential actin remodeling contributes the distinct spatial organization of BCR signalosomes in mAg- and sAg-stimulated B cells.

Actin reorganization has been shown to be involved in the initiation of BCR signaling and the regulation of tonic signaling in resting B-cells [70,149,209,214]. How actin dynamics regulate BCR signaling at different activation stages in response to different forms of Ag remains to be elucidated. Similar to previous findings [76,149], this study found that elimination of most F-actin by Lat induced tyrosine phosphorylation in the absence of Ag. Our study further shows that actin depolymerization by Lat induces BCR aggregation and that the BCR aggregates are positive for tyrosine phosphorylation. This suggests that actin depolymerization alone is sufficient for the induction of BCR aggregation and BCR aggregation is able to initiate BCR signaling. In addition, our study found two distinct properties of Lat-induced BCR aggregates. First, Lat-induced BCR aggregation is slow, random and unpolarized compared to BCR aggregates induced by mAg and sAg, which is concurrent with a slow increase in tyrosine phosphorylation. Second, Lat-induced BCR aggregates persist as microclusters and are unable to merge into a polarized central cluster, which is associated with a lack of attenuation of Lat-induced tyrosine phosphorylation. The second property of Lat-induced BCR aggregates is similar to what we previously found in SHIP-1-deficient B-cells where BCR aggregates persist as microclusters and signaling attenuation is inhibited [155]. This finding further supports the notion that the merger of BCR microclusters into the central cluster is associated with signal attenuation. These results collectively suggest that while actin depolymerization can induce BCR aggregation and BCR signaling, actin polymerization, in coordination with actin depolymerization, is important for the fast kinetics of BCR aggregation and activation as well as the merger of BCR aggregates into a central cluster and signaling attenuation.

Our studies demonstrate that actin remodeling is required for BCR activation in response to both mAg and sAg. In both cases, actin remodeling, including both polymerization and depolymerization, is essential for early and rapid BCR aggregation and the later growth and merger of these aggregates into the polarized central cluster. Actin remodeling induced by sAg and mAg exhibits different magnitude and spatial organization, which provides distinct feedback to the formation of BCR signalosomes. Future studies are required to define the molecular detail underlying the functional interaction between the actin cytoskeleton and BCR signaling during B-cell activation. (Copy right 2012. The American Association of Immunologists, Inc)

Chapter 4: Unique roles of neuronal Wiskott-Aldrich syndrome protein in the negative regulation of B cell receptor signaling and autoimmunity

4.1 Abstract

Negative regulation of receptor signaling is essential for controlling cell activation and differentiation. In B-lymphocytes, the down regulation of B cell antigen receptor (BCR) signaling is critical for suppressing the activation of self reactive B cells; however the mechanism underlying the signaling negative regulation remains elusive. Using genetic manipulated mouse models and total internal reflection fluorescence microscopy, we demonstrate that neuronal Wiskott-Aldrich syndrome protein (N-WASP), which is coexpressed with WASP in all immune cells, is a critical negative regulator of B cell signaling. B cell specific N-WASP gene deletion causes enhanced and prolonged BCR signaling and elevated levels of autoantibodies in the mouse serum. N-WASP negatively regulates signaling by rearranging F-actin from the B cell surface, which inhibits B cell spreading on antigen-associated membrane and promotes B cell contraction, the coalescence of signaling active BCR microclusters into signaling inactive central clusters, and BCR internalization. Upon BCR activation, WASP is activated first, followed by N-WASP in mouse and human primary B cells. The activation of N-WASP is suppressed by Bruton's tyrosine kinase-induced WASP activation, and is released from the WASP suppression by the activation of SH2 domain-containing inositol 5-phosphatase that inhibits WASP activation. Our results reveal a new mechanism for the negative regulation of BCR signaling and broadly

suggest an actin-mediated mechanism for signaling down regulation.

4.2 Introduction

B lymphocytes are a key component of the immune system and responsible for generating antibody responses against foreign invaders. B cell-mediated antibody responses are activated by signals generated from B cell antigen receptor (BCR) and from T helper cells through antigen presentation. Antigen binding induces self aggregation of BCRs and BCR association with lipid rafts, which lead to the recruitment of signaling molecules to BCRs, first the tyrosine kinases Lyn and Syk followed by phospholipase Cγ2 (PL Cγ2), phosphatidylinositol-3-kinase, Bruton's tyrosine kinase (Btk), and the guanine nucleotide exchange factor Vav for the GTPases Rac and Cdc42, which activate signaling cascades [66,172]. BCR aggregates grow over time and subsequently merging into each other, resulting in the formation of a BCR central cluster at one pole of the cell [68,81,223]. After initial signaling activation, inhibitory signaling molecules, including the tyrosine and phosphatidylinositol phosphatases SHP, SHIP, and PTEN, are activated, down regulating signaling [116,224,225,226]. Defects in the negative regulation of BCR signaling are associated with losses of B cell self tolerance and increases in the susceptibility to autoimmune diseases [227,228]. However, the molecular details of the negative regulation of BCR signaling have not been well defined.

The self aggregation of surface BCRs is an essential event for triggering signaling activation and a target for regulation. Spontaneous formation of BCR clusters induced by actin depolymerization leads to signaling activation in the absence of antigen [149,156,214]. BCRs with high affinity to an antigen aggregate and induce signaling with faster kinetics and to higher levels than those with low affinity to the antigen [76,229]. Conversely, the co-engagement of the BCR with the inhibitory coreceptor FcγRIIB by antigen-antibody complexes inhibits both BCR clustering and signaling [63,77]. We have recently shown that while the formation of BCR microclusters induces signaling, the merger of BCR microclusters into the BCR central cluster is associated with signaling attenuation at the B cell surface. Both the attenuation of BCR signaling and the merger of BCR aggregates into the central cluster are inhibited in B cells where the gene of SH2 domain-containing inositol 5-phosphatase (SHIP-1) is specific deleted [155]. These results suggest that the formation of the BCR central cluster is a down regulatory mechanism for BCR signaling.

BCR self aggregation at the B cell surface depends on actin reorganization. Actin can regulate BCR aggregation by controlling the later mobility of surface receptors and B cell morphology [68,76,149,209]. Perturbing the cortical actin increases the lateral mobility of surface BCRs and facilitates BCR self clustering and BCR signaling [149], while stabilizing the actin network does the opposite [156]. In response to membrane associated antigen, B cells undergo actin dependent spreading and contraction. B cell spreading expands the area of contact between the B cell surface and the antigen tethered membrane, thereby increasing the number of antigen engaged BCRs [76]. The merger of BCR aggregates into the central cluster appears to depend on B cell contraction following spreading since the BCR central cluster fails to form when cell contraction is inhibited [155]. Conversely, BCR aggregation and B cell spreading are regulated by BCR signaling. B cells with genetic deletion of signaling molecules, CD19, PLCγ2, Btk, Vav or Rac, exhibit impaired BCR aggregation and B cell spreading [53,74,177]. We have demonstrated that the stimulatory kinase Btk is essential for the activation of the actin regulator Wiskott Aldrich syndrome protein (WASP), B cell spreading and BCR aggregation. In contrast, the inhibitory phosphatase SHIP-1 inhibits WASP activation by suppressing Btk activation, which promotes B cell contraction and the merger of BCR aggregates into the central cluster [155]. Furthermore, actin reorganization is essential for BCR internalization [134], which is not only the initiation step of antigen processing but also a mechanism for down regulation of receptor signaling. Therefore, actin can provide both positive and negative feedback to BCR signaling.

WASP is an actin nucleation promoting factor that is specifically expressed in hematopoietic cells [158,161]. WASP mutations that ablate its expression cause a severe and complicated X-linked immune disorder, WAS [166,230,231], which demonstrates the critical role of actin in immune regulation. WAS patients suffer from recurrent bacterial infections, which are associated with defective T-independent antibody responses against polysaccharide and impaired maturation of T-dependent antibody responses [165,166,232,233]. In addition, a large portion of WAS patients develop autoimmune diseases, which are associated with a higher risk of leukemia and lymphoma [164,234]. In the WASP knockout (KO) mouse model, there is no significant defect in T and B cell development, except for a reduction in marginal zone

B cells [167,170,190]. The in vitro activation of T cells but not B cells from WASP KO mice is decreased [179]. WASP deficient B cells from both mice and WAS patients exhibit defective migration [170,190,233]. We have found that there were significant reductions in cell spreading, BCR aggregation, surface tyrosine phosphorylation [155] and BCR internalization [168] in WASP KO B cells as compared to those of wild type (wt) B cells. Recent studies have clearly demonstrated a critical and B cell intrinsic role of WASP in controlling B cell self tolerance [167,168]. However the molecular mechanism underlying the lost of self tolerance in WASP deficient B cells has not yet been elucidated.

In addition to hematopoietic specific WASP, B cells, like all immune cells, also express the ubiquitous N-WASP. These two proteins share ~50% sequence homology [235] and are reported to have the same cellular function, activating actin polymerization and branching by binding to Arp2/3 complexes [236,237]. They are capable of linking cell signaling to actin dynamics via their GTPase binding (GBD), proline rich (PRD) and Plenkstrin homology (PH) domains. The binding of GTP-Cdc42 and phosphatidylinositol-4,5-biphosphate ($PI(4,5)P_2$) releases the proteins from an autoinhibitory conformation [193,236,238]. Signaling induced phosphorylation of WASP and N-WASP at tyrosines in the GBD domain and serines in the VCA (verprolin homology, cofilin homology, and acidic) domain is required for their optimal activity [162,163,239]. In B cells, Btk is responsible for activating WASP by activating Vav, a guanine nucleotide exchange factor for Cdc42, stimulating the production of $PI(4,5)P_2$ and inducing the phosphorylation of WASP [118]. While

WASP and N-WASP have been well studied individually, how these two proteins function when coexpressed is largely unknown. Recent studies have demonstrated that both WASP and N-WASP are critical for the development and function of B cells [170]. However, why both WASP and N-WASP are required and how N-WASP and WASP functionally coordinate with each other during BCR activation is not well understood.

In this study, we examined the cellular function of N-WASP and its functional relationship with WASP during BCR activation using WASP KO, B cell specific N-WASP KO, and double KO mice, as well as primary human B cells from WAS patients. We found that while both WASP and N-WASP are required for optimal signaling activation and internalization of the BCR, the two proteins have distinct functions. N-WASP is critical for the down regulation of BCR signaling. N-WASP promotes signaling attenuation by facilitating B cell contraction and coalescence of BCR microclusters into a central cluster and by mediating BCR internalization. Surprisingly, WASP and N-WASP functionally suppress each other and are inversely regulated by stimulatory and inhibitory signals. These results reveal a new function for N-WASP in the negative regulation of receptor signaling and demonstrate a unique functional relationship between N-WASP and WASP during BCR activation.

4.3 Materials and Methods

4.3.1 Mice and Cells

Wild type (wt) (CBA/CaJ), xid (CBA/CaHN*Btkxid*/J) and CD19$^{Cre/+}$

(B6.129P2(C)-*Cd19*$^{tm1(cre)Cgn}$/J) mice were purchased from Jackson Laboratories (Bar Harbor, ME). B cell specific SHIP-1 knockout mice CD19$^{Cre/+}$ SHIP-1$^{Flox/Flox}$ were kindly provided by Dr. Silvia Bolland at NIH [155,240]. Control (CD19$^{Cre/+}$ or N-WASP$^{Flox/Flox}$), WASP knockout (WASP$^{-/-}$, WKO), N-WASP conditional knockout (CD19$^{Cre/+}$ N-WASP$^{Flox/Flox}$, cNKO), WASP and N-WASP double conditional knockout (WASP$^{-/-}$ CD19$^{Cre/+}$ N-WASP$^{Flox/Flox}$, cDKO) mice were previously established [170]. B cell lymphoma A20 IIA1.6 cells (H-2d, IgG2a^{+}, FcγIIBR^{-}) were cultured and splenic B cells were isolated as previously described [118]. Human peripheral blood mononuclear cells (PBMCs) were collected from WAS patients, age matched healthy controls, and healthy adults. B cells were isolated from human PBMCs using a Miltenyi Human B cell negative selection kit by AutoMACS (Miltenyi Biotec Inc., Auburn, CA). Informed consent was obtained from all human subjects. All experiments with mice and primary human cells were performed in accordance with institutional and NIH guidelines and regulations using protocols proved by the institution IACUC and IRB.

4.3.2 Preparation of Antigen-tethered Planar Lipid Bilayers

Mono-biotinylated Fab' fragment of anti-mouse or human IgM+G antibody (mB-Fab'-anti-Ig) was generated from the F(ab')$_2$ fragment (Jackson ImmunoResearch, West Grove, PA) using a published protocol [180]. The planar lipid bilayer was prepared as described previously [72,181]. Liposomes were made by sonicating 1,2-dioleoyl-sn-Glycero-3-phosphocholine and

1,2-dioleoyl-sn-Glycero-3-phosphoethanolamine-cap-biotin (Avanti Polar Lipids, Alabaster, AL) in a 100:1 molar ratio in PBS. Coverslip chambers (Nalge Nunc International, Rochester, NY) were incubated with the liposomes before coating with 1 μg/ml streptavidin (Jackson ImmunoResearch) and 2 μg/ml AF546-mB-Fab'-anti- Ig mixed with 8 μg/ml mB-Fab'-anti-Ig antibody. For a non antigen control, surface BCRs were labeled with AF546-Fab–anti-Ig (2 μg/ml). The labeled B cells were then incubated with biotinylated holo-transferrin (Tf; 16 μg/ml, Sigma, St. Louis, MO) tethered to lipid bilayers by streptavidin.

4.3.3 Total Internal Reflection Microscopy

Images were acquired using a Nikon TE2000-PFS microscope equipped with a 60X, NA 1.49 Apochromat TIRF objective, a Coolsnap HQ2 CCD camera (Roper Scientific), and two solid-state lasers of wavelength 491 and 561 nm. Interference refection images (IRM), AF488, and AF546 were acquired sequentially. B cells were incubated with antigen-tethered lipid bilayers at 37°C, and then were then fixed with 4% paraformaldehyde, permeabilized with 0.05% saponin, and stained for phosphotyrosine (Millipore), phosphorylated Btk (BD Bioscience, San Jose, CA), SHIP-1 (Cell Singling Technology, Inc., Danvers, MA), WASP (S483/S484 or Y290) (Bethyl Laboratory, Inc., Montgomery, TX or Abcam, Cambridge, MA), N-WASP (Y256, Millipore), and AF488-phalloidin. The B cell contact area was determined based on IRM images using MATLAB software (The MathWorks, Inc. Natick, MA). The total and mean fluorescence intensity in the B cell contact zone was determined using Andor iQ software (Andor Technology, Belfast, UK). Background fluorescence generated by antigen or secondary antibody was subtracted. For each set of data, >50 individual cells from three independent experiments were analyzed.

4.3.4 Calcium Flux

The intracellular calcium flux was measured by flow cytometry using the calcium-sensitive dyes Fluo4 AM and Fura Red (Invitrogen) using manufacturer-recommended protocols. The relative levels of intracellular calcium were determined by a ratio of Fluo4 AM to Fura Red emission using FlowJo software (Tree Star, Inc., Ashland, OR).

4.3.5 BCR Internalization

Flow cytometry [135]. B cells were incubated with biotinylated F(ab')$_2$-goat anti-mouse IgG+M (10 μg/ml; Jackson ImmunoResearch) at 4°C and chased at 37°C. Biotin-F(ab')$_2$-anti-IgG+M left on the cell surface after the chase was stained with PE-streptavidin and quantified using a flow cytometer. The data were presented as percentages of the cell surface-associated biotin-F(ab')$_2$-anti-IgG+M at time 0.

Immunofluorescence microscopy [135]. B cells that were labeled and cross-linked as described above were chased fro 30 min. The cells were fixed, permeabilized, stained for LAMP-1 (1D4B; ATCC), and analyzed using a confocal microscope (Zeiss LSM 710). Pearson correlation coefficients were determined using LSM 710 software

[215].

4.3.6 Flow Cytometry Analysis

B cells were incubated with FcR blocking antibodies (BD) and then with PE-Cy7-anti-CD19 (BD) at 4°C. B cells were activated with F(ab')$_2$-anti-Ig(M+G) (10 μg/ml, Jackson ImmunoResearch) at 37°C. The cells were fixed, permeabilized and stained with anti-phosphorylated WASP (S483/S484) and N-WASP (Y256) antibodies for mouse B cells, anti-phosphorylated WASP (Y290) (Abcam, Cambridge, MA) and N-WASP (Y256, Millipore) antibodies for human B cells, and anti-WASP or N-WASP (Santa Cruz, CA) antibody for total protein. Stained cells were analyzed by a BD FACS Canto. Anti-phosphorylated WASP antibody showed no significant staining in B cells from WKO mice and anti-phosphorylated N-WASP antibody showed no staining in B cells from cNKO mice, indicating that there is no cross reactivity of these two antibodies between phosphorylated WASP and N-WASP.

4.3.7 Inhibitors

B cells were pretreated with wiskostatin B (10 μM, EMD Bioscience, Gibbstown, NJ) for 1 h at 37°C. The inhibitor was also included in the incubation media.

4.3.8 Serological Analysis

Anti-nuclear antibody in sera was tested using the ANA slide test kit from MBL-Bion (Des Plaines, IL). The serum levels of anti-dsDNA antibody were quantified by ELISA using a published protocol [168].

4.3.9 Statistical Analysis

Statistical significance was assessed by the Mann-Whitney two-tailed test using Prism software (GraphPad Software, San Diego, CA).

4.4 Results

4.4.1 N-WASP Is Activated Following WASP Activation in Response to BCR Stimulation

To understand the function of N-WASP in BCR activation, we examined the activation status of N-WASP in relation to WASP activation in human peripheral blood (PBMC) and mouse splenic B cells in response to antigen in both soluble (sAg) and membrane associated forms (mAg). These are the most common forms of antigen encountered by B cell in vivo. Active WASP and N-WASP were detected using antibodies specific for their phosphorylated forms that did not show cross reactivity between phosphorylated WASP and N-WASP. Human and mouse B cells were activated with mAg (Alexa Fluor 546-labeled, monobiotinylated Fab' fragment of anti-mouse or human IgG+M antibody [AF546-mB-Fab'-anti-Ig] tethered to planar lipid bilayers by streptavidin) or sAg (mB-Fab'-anti-Ig plus soluble streptavidin) before staining for phosphorylated WASP (pWASP) and N-WASP (pN-WASP). Using total internal reflection fluorescence microscopy (TIRFM), we analyzed the distribution and the relative levels of pWASP and pN-WASP at the surface of B cells in contact with the antigen tethered lipid bilayer (B cell contact zone). We found that both pWASP and pN-WASP were detected in the contact zone of mouse (Figure 4.1A,B) and human B cells (Figure 4.1C,D), and they have a punctate appearance. As antigen-BCR complexes coalesced and merged into a central cluster accompanied by B cell contraction, most of the pWASP staining (Figure 4.1A,C), but not pN-WASP (Figure 4.1B,D), moved away from the center to the edge of antigen-BCR center clusters. The mean fluorescence intensity (MFI) of pN-WASP in the B cell contract zone increased over time similar to that of pWASP. However, the pN-WASP MFI reached its maximal level 2 min later than pWASP, concurrent with the pWASP levels returning to the basal levels (Figure 4.1E,G). Flow cytometry analysis was used to determine the overall levels of pWASP and pN-WASP in response to sAg. We found similar patterns of WASP and N-WASP activation, where the MFI of pN-WASP peaked 3-5 min later than that of pWASP until the pWASP levels decreased (Figure 4.1F,H). These results indicate that N-WASP is transiently activated at locations where BCRs interact with antigen similar to WASP, but its activation does not peak until the level of WASP activation decreases.

Figure 4.1 N-WASP is activated following WASP activation upon antigen stimulation. (A-D) TIRFM and IRM analysis of pWASP and pN-WASP in the B cell contact zone of mouse splenic B cells and human PBMC B cells that were incubated with mAg (Alexa Fluor 546-monobiotinylated Fab'-anti-mouse or human IgG+M) at 37°C for indicated times. (E and G) The MFI of pWASP or pN-WASP in the B cell contact zone was quantified using TIRFM images and Andor iQ software. (F and H) The MFI of pWASP or pN-WASP in mouse splenic and human PBMC B cells incubated with sAg (monobiotinylated Fab'-anti-IgG+M plus streptavidin) at 37°C for indicated times were analyzed by flow cytometry. Shown are representative images and the average MFI (±S.D.) from three independent experiments. Bar, 2.5 μm.

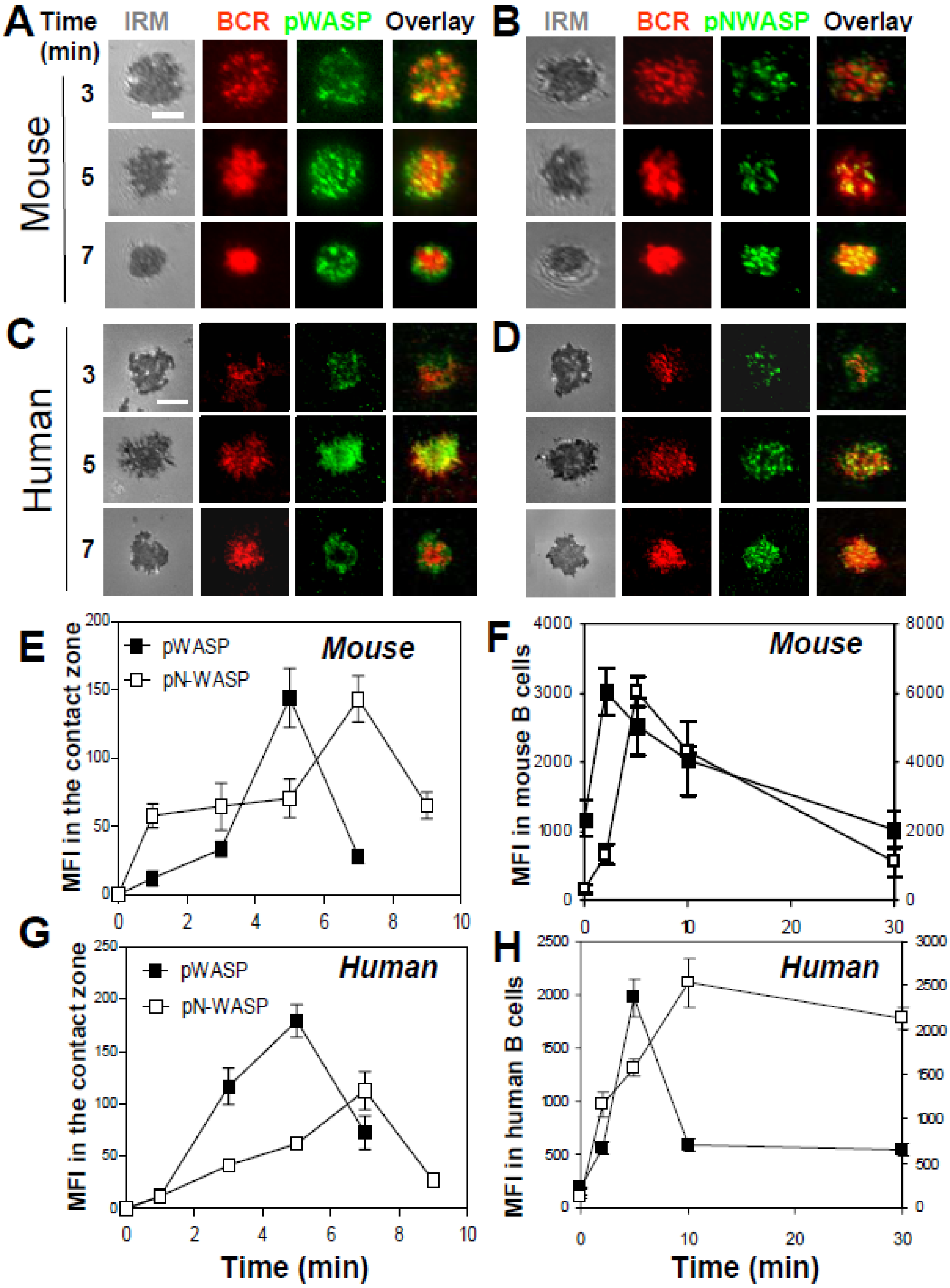
A
Time (min)
IRM
BCR
pWASP
Overlay
Mouse
3
5
7
B
IRM
BCR
pNWASP
Overlay
C
Human
3
5
7
D
E
pWASP
pN-WASP
Mouse
MFI in the contact zone
F
Mouse
MFI in mouse B cells
G
pWASP
pN-WASP
Human
MFI in the contact zone
Time (min)
H
Human
MFI in human B cells
Time (min)

4.4.2 Both WASP and N-WASP Are Critical for Antigen Induced BCR Aggregation and B cell Morphological Changes but the Two Play Distinct Roles

Previous studies have shown that WASP is dispensable for antigen induced BCR aggregation and B cell morphological changes [155,168], implying a compensatory role for N-WASP in WASP KO B cells. To investigate this hypothesis, we utilized WASP KO mice (WKO), B cell specific N-WASP KO mice (cNKO) and double KO mice where N-WASP is selectively deleted in B cells (cDKO), established previously by Westerberg et al. [170]. We examined the effect of WASP and/or N-WASP KO on BCR aggregation and B cell morphology in response to mAg. Surface BCR aggregation was analyzed by TIRFM. As we have shown previously [155,156], upon being bound by the BCR, antigen aggregated, coalesced and formed a polarized central cluster at 7 min (Figure 4.2A), and the total fluorescence intensity (TFI) of mAg in the contact zone of control B cells (CD19$^{Cre/+}$ or N-WASP$^{Flox/Flox}$) increased over time (Figure 4.2D). There was no significant antigen aggregation and accumulation in the contact zone of B cells interacting with transferrin (Tf)-tethered lipid bilayer (Figure 4.2A,D), indicating that antigen aggregation is mediated by the BCR, thereby indicating BCR aggregation. In WKO and cNKO B cells, the TFI of antigen-BCR complexes in the contact zone was significantly decreased compared to that of control B cells (Figure 4.2D). While BCR accumulation in the contact zone of WKO and cNKO B cells was decreased to similar levels, the BCRs showed distinct distribution patterns. BCRs in the contact zone of WKO B cells formed a central cluster smaller than that of control B cells (Figure 4.2A) while in cNKO B cells they appeared punctate, failing to merge into a central cluster (Figure 4.2A). The deletion of both WASP and N-WASP genes caused a further decrease in the BCR TFI in the B cell contact zone to the levels in unstimulated B cells (Figure 4.2A,D). Similarly, treating WKO B cells with the N-WASP inhibitor wiskostatin [241] (Figure 4.2D) or A20 lymphoma B cells with siRNAs targeted to WASP and N-WASP (Figure 4.2B,F) reduced the BCR TFI in the contact zone to levels similar to that in cDKO B cells. Furthermore, the BCR TFI in the contact zone of human B cells was decreased by wiskostatin treatment to a level similar to that of cNKO mouse B cells (Figure 4.2C,H).

We examined the effect of WASP and/or N-WASP KO on B cell morphology by quantifying the changes in the contact area between B cells and antigen tethered lipid bilayer, utilizing interference reflection microscopy (IRM). In control B cells, the contact area increased rapidly during the first 3 min, indicating cell spreading, and then decreased after reaching a maximal spreading area, indicating cell contraction (Figure 4.2A,E). The change of WKO B cell contact area over time was qualitatively similar to that of control B cells, but with a smaller magnitude of increase (Figure 4.2A,E). Both the kinetics and magnitude of the increase in the contact area of cDKO B cells were dramatically slower and smaller than those of control and WKO B cells (Figure 4.2A,E). Surprisingly, the contact area of cNKO B cells was significantly larger and decreased much later (7 min) than that of control B cells (Figure 4.2A,E). Again, treating WKO B cells with the N-WASP inhibitor wiskostatin (Figure 4.2E) or A20 B cells with WASP/N-WASP siRNAs (Figure 4.2B,G) reduced the B cell contact area to sizes similar to that of cDKO B cells. Treating human primary B cells with wiskostatin caused an increase in B cell spreading and a delay of B cell contraction (Figure 4.2C,I), similar to what we observed in cNKO B cells (Figure 4.2A,E).

Taken together, these results indicate that both WASP and N-WASP are indispensable for optimal magnitude of BCR aggregation and B cell spreading, but N-WASP exhibits two opposing functions, supporting BCR aggregation and B cell spreading in the absence of WASP and promoting the merger of BCR aggregates into a central cluster and B cell contraction in the presence of WASP. N-WASP exhibits the similar functions in mouse and human primary B cells.

Figure 4.2 Antigen induced BCR aggregation and B cell spreading depend on both WASP and N-WASP. (A-C) TIRFM and IRM analysis of mouse splenic B cells that were incubated with transferrin (Tf) or mAg (A), A20 B cells that were transfected with control or WASP/N-WASP siRNA (B), and human B cells that were pretreated with or without wiskostatin (Wis) and stimulated with mAg (C). Shown are representative images from 7 min. Bar, 2.5 μm. (D-I) The average values (±SD) of the mAg TFI in the B cell contact zone (D, F and H) and of the B cell contact area (E, G and I) were determined using TIRFM and IRM images from >100 individual cells of three individual experiments. *, $p<0.01$, compared to B cells from control mice, transfected with control siRNA or treated with DMSO.

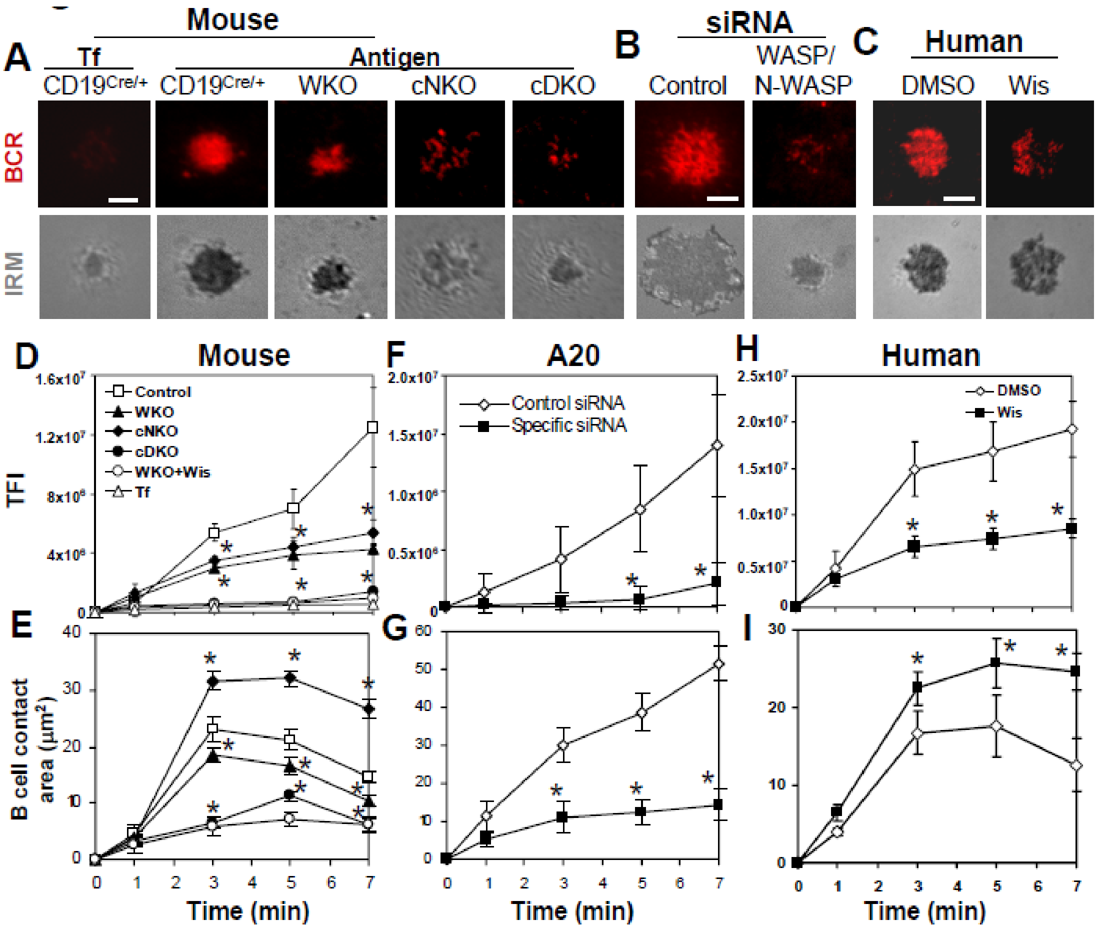
A
Mouse
Tf
Antigen
CD19Cre/+
CD19Cre/+
WKO
cNKO
cDKO
B
siRNA
Control
WASP/ N-WASP
C
Human
DMSO
Wis
BCR
IRM
D
Mouse
TFI
Control
WKO
cNKO
cDKO
WKO+Wis
Tf
F
A20
Control siRNA
Specific siRNA
H
Human
DMSO
Wis
E
B cell contact area (µm²)
G
I
Time (min)
Time (min)
Time (min)

4.4.3 BCR Signaling Is Enhanced and Prolonged in N-WASP KO B cells

The effects of WASP and/or N-WASP KO on BCR aggregation and B cell morphology suggest their involvement in BCR signaling. To test this hypothesis, we analyzed the impact of WASP and/or N-WASP KO on tyrosine phosphorylation (pY) at the cell surface in response to mAg using TIRFM. Similar to what we have shown previously [155], pY was first detected at BCR aggregates at early times during the interaction of control B cells with mAg (~3 min) and then at the outer edge of the BCR central cluster at later times (~7 min) (Figure 4.3A). The MFI of pY staining rapidly increased upon antigen binding, peaked at 3 min and then decreased (Figure 4.3E). The distribution and levels of pY in the contact zone of WKO B cells followed a qualitatively similar pattern as in control B cells, but the increasing magnitude of pY MFI in the contact zone of WKO B cells was significantly smaller than that of control B cells (Figure 4.3B,E). Double KO of WASP and N-WASP caused a further reduction in the levels of pY in the B cell contact zone (Figure 4.3D,E). However, the pY staining in the contact zone of cNKO B cells remained punctate and colocalized with BCR aggregates at 7 min (Figure 4.3C). The peak level of pY in the contact zone of cNKO B cells was similar to that of control B cells, but its attenuation was significantly delayed (Figure 4.3E). These results suggest that N-WASP is involved in both stimulation and attenuation of BCR signaling.

Our previous studies show a two phase relationship between BCR aggregation and signaling, where BCR aggregation into small clusters stimulates signaling activation, but the merger of small clusters into a central cluster leads to signaling attenuation at the cell surface [155]. The effects of cNKO on BCR aggregation and B cell contract led us to hypothesize that N-WASP may regulate signaling via modulating the aggregation of surface BCRs. To investigate this hypothesis, we determined the relative size of BCR clusters based on the TFI of BCR labeling in individual clusters and the relative signaling levels of BCR clusters based on the fluorescence intensity ratio (FIR) of the pY to the BCR in individual clusters. A nonparametric regression method, LOWESS, was used to examine the trend between the size and signaling level of BCR clusters. In control B cells, the FIR of pY to BCR increased as the size of BCR clusters increased when their sizes were relatively small. After the clusters reached a certain size, the FIR decreased as the sizes of BCR clusters further increased (Figure 4.3F). Compared to control B cells, BCR clusters formed in the contact zone of cNKO B cells were limited to smaller sizes, and the FIR of pY to BCR in individual microclusters of cNKO B cells was much higher than that of control B cells (Figure 4.3G). These results show that the delayed attenuation of tyrosine phosphorylation in cNKO B cells is associated with the inhibition of the growth of BCR clusters, suggesting that N-WASP can down regulate BCR signaling via promoting the growth and merger of BCR aggregates into the central cluster.

In order to confirm the roles of WASP and N-WASP in BCR signaling, we determined the effect of WASP and/or N-WASP KO on the phosphorylation of stimulatory kinase Btk (pBtk) and inhibitory phosphatase SHIP-1 (pSHIP-1) in response to mAg by TIRFM and calcium flux in response to sAg by flow cytometry.

Similar to the effect of WASP and/or N-WASP KO on pY, the MFI of pBtk was significantly reduced in the contact zone of WKO B cells and further reduced in that of cDKO B cells, compared to that of control B cells (Figure 4.3H). However, the MFI of pBtk in the contact zone of cNKO B cells was not only significant higher at the 3-min peak time, but the attenuation of pBtk was also significantly delayed, compared to that of control B cells (Figure 4.3H). In contrast, the MFI of pSHIP-1 in the contact zone was significantly increased in WKO B cells but reduced in cNKO B cells (Figure 4.3I). Double KO also caused a decrease in pSHIP-1 level in the B cell contact zone, but the magnitude of the decrease was similar to that in cNKO B cells (Figure 4.3I). Consistent with the changes in levels of pBtk and pSHIP-1 in the contact zone, the level of calcium influx was reduced in both WKO and cDKO B cells, with a much more dramatic reduction in cDKO than WKO B cells. In contrast, calcium influx was increased in cNKO B cells (Figure 4.3J).

These results collectively indicate critical roles for WASP and N-WASP in regulating BCR signaling in response to both mAg and sAg, and suggest dual functions for N-WASP in positive and negative signaling regulation.

Figure 4.3 Differential effects of WASP and/or N-WASP KO on BCR signaling. (A-E) TIRFM and IRM analysis of pY staining in the contact zone of mouse splenic B cells incubated with mAg. Shown are representative images (A-D) and the MFI (±S.D.) of pY in the B cell contact zone (E) from three independent experiments. Bars, 2.5 μm. (F and G) The FIRs of pY to the BCR were plotted versus the TFI of the BCR in individual BCR clusters. Each open symbol represents a BCR cluster. The simulated values (solid symbol) were generated by LOSSE non-linear regression using the Stat software. (H and I) TIRFM analysis of phosphorylated Btk (pBtk) and SHIP-1 (pSHIP) in the contact zone of mouse splenic B cells stimulated with mAg. Shown are the average MFI (±SD) of pBtk and pSHIP in the B cell contact zone from three independent experiments. * $p<0.01$, compared to control B cells. (J) Ca^{2+} flux analysis of splenic B cells activated with sAg using flow cytometry. Shown are representative results from three independent experiments.

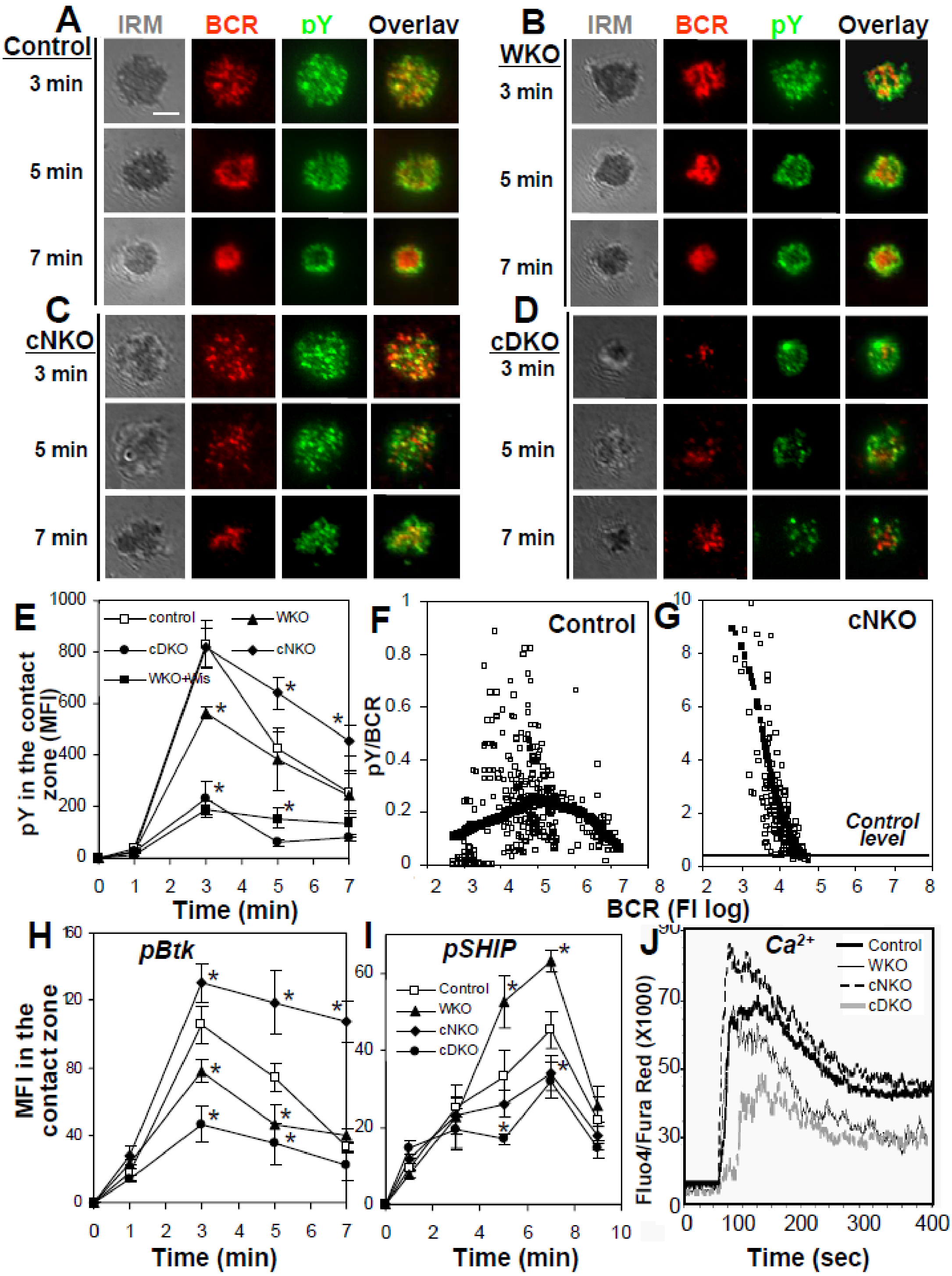
A
Control
IRM
BCR
pY
Overlay
3 min
5 min
7 min
B
WKO
IRM
BCR
pY
Overlay
3 min
5 min
7 min
C
cNKO
3 min
5 min
7 min
D
cDKO
3 min
5 min
7 min
E
pY in the contact zone (MFI)
control
WKO
cDKO
cNKO
WKO+Ms
1000
800
600
400
200
0
0 1 2 3 4 5 6 7
Time (min)
F
Control
pY/BCR
1
0.8
0.6
0.4
0.2
0
2 3 4 5 6 7 8
G
cNKO
10
8
6
4
2
0
Control level
2 3 4 5 6 7 8
BCR (FI log)
H
pBtk
MFI in the contact zone
160
120
80
40
0
0 1 2 3 4 5 6 7
Time (min)
I
pSHIP
Control
WKO
cNKO
cDKO
60
40
20
0
0 2 4 6 8 10
Time (min)
J
Ca^{2+}
Control
WKO
cNKO
cDKO
Fluo4/Fura Red (X1000)
90
70
50
30
0
0 100 200 300 400
Time (sec)

4.4.4 The Level of Autoantibody Is Elevated in Mice with B cell Specific N-WASP Gene Deletion

The negative regulatory function of N-WASP in BCR activation implies a role for N-WASP in controlling B cell self tolerance. To investigate this possibility, we analyzed the serum levels of anti-nuclear and anti-double strand (ds) DNA antibody. Using an immunofluorescence test, we found that the sera of 50% cNKO mice were positive with anti-nuclear antibody (n=4), compared to none of control mice at 6 months age (Figure 4.4A). Consistent with this result, quantitative ELISA analysis detected an elevated level of anti-dsDNA antibody in the sera of cNKO mice, compared to control mice at 6 and 9 months old (Figure 4.4B). Since N-WASP KO is B cell specific, these data indicate a critical role for N-WASP in maintaining B cell tolerance.

Figure 4.4 The serum levels of anti-nuclear and anti-dsDNA antibody are elevated in cNKO mice. (A) Representative images from Immunofluorescence microscopic analysis of anti-nuclear antibody in the serum of control and cNKO mice of 6 months old (n=4). (B) ELISA quantification of anti-dsDNA antibody in the serum of control and cNKO mice of 6 and 9 months old. Each dot represents an individual mouse. *, $p<0.01$.

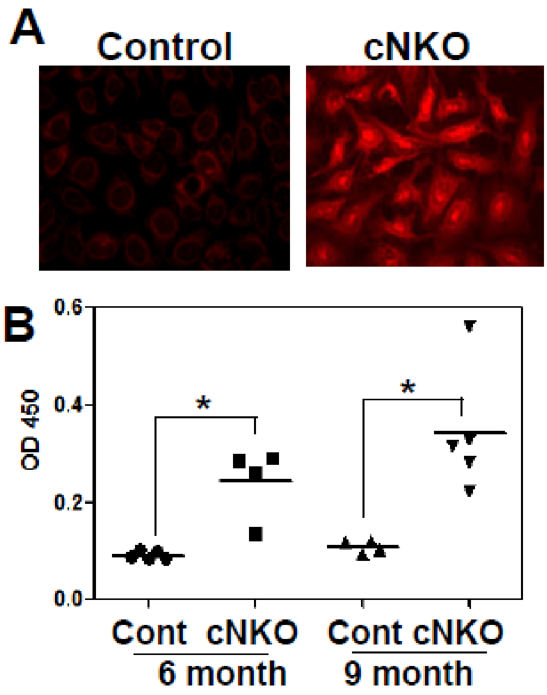
A
Control
cNKO
B
0.6
0.4
0.2
0.0
OD 450
*
*
Cont
cNKO
6 month
Cont
cNKO
9 month

4.4.5 WASP Promotes and N-WASP Inhibits F-actin Accumulation in the B cell Contact Zone

Since the major function of WASP and N-WASP is to activate actin polymerization, we examined the effects of WASP and/or N-WASP KO on the distribution patterns and levels of F-actin in the B cell contact zone using phalloidin staining and TIRFM analysis. When control B cells spread on antigen tethered lipid bilayer, F-actin formed smaller clusters throughout the contact zone and partially colocalized with BCR aggregates. When B cells contracted and BCR aggregates merged into a central cluster, F-actin accumulated at the outer edge of the contact zone (Figure 4.5A). The level of F-actin in the contact zone of control B cells rapidly increased over time and peaked at 3-5 min when B cell spreading reached the maximal magnitude, followed by a significant reduction at 7 min when B cells contracted (Figure 4.2E and 4.5E). Gene KO of WASP or both WASP and N-WASP did not significantly change the distribution pattern of F-actin (Figure 4.5B,D) but reduced the level of F-actin accumulation in the B cell contact zone (Figure 4.5E). The reduction was much more drastic in cDKO B cells and WKO B cells treated with the N-WASP inhibitor wiskostatin than that in WKO B cells (Figure 4.5E). In contrast, the level of F-actin accumulation in the contact zone of cNKO B cells was significantly increased at 5 min and remained high at 7 min (Figure 4.5E). F-actin clusters formed in the contact zone of cNKO B cells appeared much more prominent than those in control B cells, and they displayed sustained colocalization with BCR aggregates (Figure 4.5C) up to 7 min. These results suggest that N-WASP not only synergizes with WASP in generating and mobilizing F-actin to BCR aggregates during signal activation, but also is critical for removing F-actin from the contact zone during B cell contraction and surface signaling attenuation.

Since WASP and N-WASP share the same cellular function, activation of actin polymerization by binding to Arp2/3, we next asked how these two molecules exhibit opposing roles in actin remodeling during BCR activation. We analyzed the behavior of Arp2/3 in response to mAg and its spatial relationship with pWASP and pN-WASP at the B cell surface using TIRFM and Arp2 specific antibody. We found that Arp2 was readily recruited to the contact zone of control B cells, and its recruitment timing, level and distribution patterns were similar to those of F-actin (Figure 4.5F,I). Consistent with the effect of WASP and/or N-WASP KO on F-actin accumulation, the MFI of Arp2 staining decreased slightly in the contact zone of WKO B cells and was significantly reduced in that of cDKO B cells, but increased in that of cNKO (Figure 4.5F,I), This result supports that antigen induced F-actin accumulation in the B cell contact zone is mediated through the activation of Arp2/3 by WASP and N-WASP. The spatial relationship of Arp2 with active WASP and N-WASP were analyzed using Pearson correlation coefficients between the staining of Arp2 and pWASP or pN-WASP in the B cell contact zone. The results showed that pWASP exhibited a significantly higher level of colocalization with Arp2 than pN-WASP in control B cells (Figure 4.5G,H,J). WASP KO caused a significant increase in the colocalization between pN-WASP and Arp2, close to the colocalization level of pWASP with Arp2 in control B cells (Figure 4.5H,J), but N-WASP KO did not change the level of colocalization between pWASP and Arp2 (Figure 4.5G,J). These data suggest that activated WASP predominately colocalizes with Arp2/3 while inhibiting the colocalization of active N-WASP with Arp2/3 at the B cell surface.

4.4.6 N-WASP Plays a Dominant Role in BCR Internalization

BCR activation induces receptor internalization, which attenuates receptor signaling by removing the receptor from the surface signaling microdomain. Since BCR internalization requires actin reorganization [134], we investigated whether WASP and N-WASP are involved in this process. BCR internalization was evaluated qualitatively by the colocalization of surface labeled BCRs with the late endosomal marker LAMP-1 using immunofluorescence microscopy and quantitatively by the amount of surface labeled BCRs remaining at the cell surface after internalization using flow cytometry. In control B cells, 70% of surface labeled BCRs disappeared from the cell surface after internalization (Figure 4.6D), and they colocalized with LAMP-1 labeled late endosomes (Figure 4.6A,C) that coalesced in response to signaling [242]. In WKO B cells, the colocalization of surface labeled BCRs with LAMP-1 was slightly decreased and the amount of the BCR remaining on the cell surface was increased (Figure 4.6A,C,D), indicating a reduction in BCR internalization. In cDKO B cells, the colocalization of the BCR with LAMP-1 was decreased from 0.4 to 0.1 and the amount of the BCR remained at the cell surface increased (~80%), compared to those in control B cells (~30%), showing a dramatic reduction of BCR internalization (Figure 4.6A,C,D). Similarly, double knockdown of WASP and N-WASP by siRNA reduced the colocalization of the BCR with LAMP-1 in

A20 cells (Figure 4.6B-C). Noticeably, cNKO B cells showed a similar level of the reduction in the colocalization of the BCR with LAMP-1 and a similar level of the increase in the surface BCR as those observed in cDKO B cells, indicating that cNKO causes a decrease in BCR internalization to a similar magnitude as cDKO. These results demonstrate that N-WASP plays the major role in this process.

Figure 4.5 WASP promotes and N-WASP inhibits the F-actin accumulation in the B cell contact zone. (A-E) TIRFM analysis of F-actin staining in the contact zone of splenic B cells incubated with mAg. Shown are representative images (A-D) and the average MFI (±S.D.) of F-actin staining in the B cell contact zone (E) from three independent experiments. (F and I) TIRFM analysis of Arp2 staining at the contact zone of splenic B cells incubated with mAg. The MFI of Arp2 staining in the B cell contact zone was quantified. (G, H and J) TIRFM analysis of the spatial relationship of Arp2 with pWASP (G) or pN-WASP (H) in the contact zone of splenic B cells incubated with mAg for 5 min. The colocalization coefficients between Arp2 and pWASP or pN-WASP staining were determined using Zeiss LSM software (J). Shown are representative images (F-H) and the average MFI (I) or colocalization coefficients (±SD) (J) from ~50 individual cells of three independent experiments. Bars, 2.5 μm. *, *p<0.01,* compared to B cells from control mice.

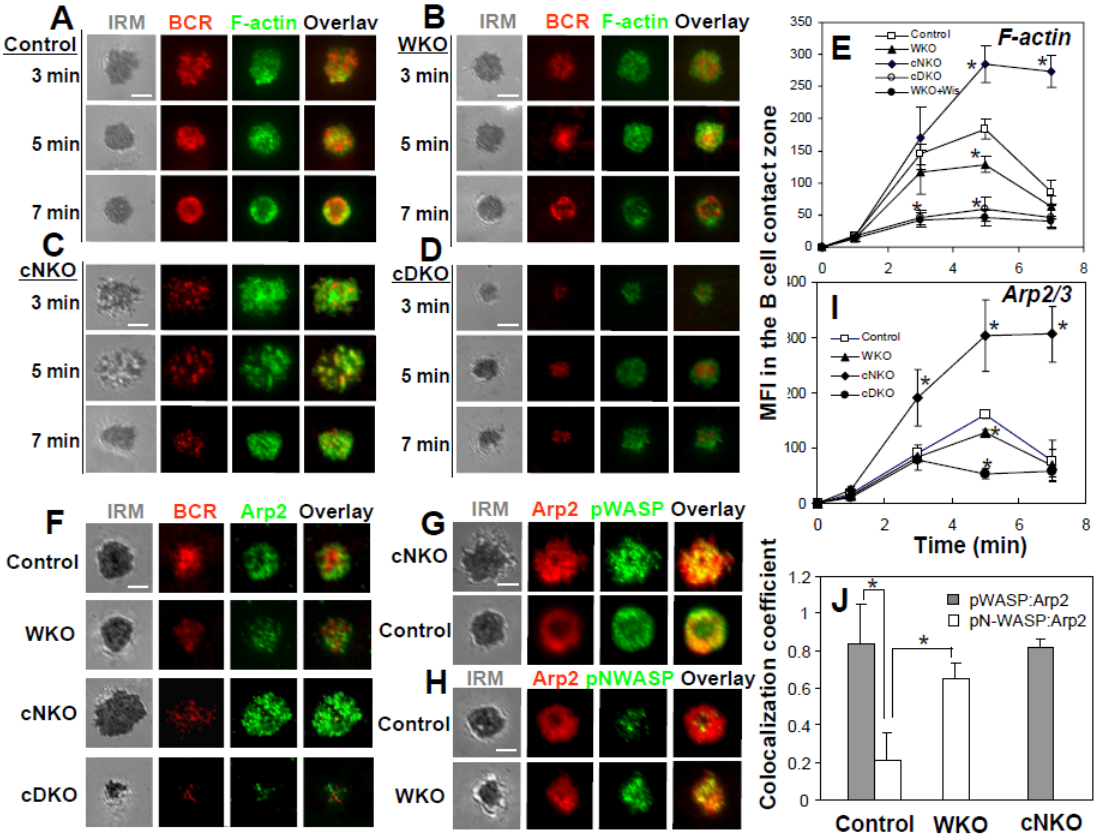
A
IRM
BCR
F-actin
Overlay
Control
3 min
5 min
7 min
B
WKO
C
cNKO
D
cDKO
E
F-actin
Control
WKO
cNKO
cDKO
WKO+Wis
MFI in the B cell contact zone
I
Arp2/3
Time (min)
F
Arp2
G
pWASP
H
pNWASP
J
pWASP:Arp2
pN-WASP:Arp2
Colocalization coefficient
Control
WKO
cNKO
*

Figure 4.6 N-WASP plays a dominant role in BCR internalization. (A-C) Immunofluorescence microscopic analysis of BCR internalization. Colocalization coefficients between the surface labeled BCR with LAMP-1 in splenic B cells (A and C) or A20 B cells transfected with WASP/N-WASP siRNA (B and C) were measured using the Zeiss LSM software. The surface BCR were labeled with sAg and warmed to 37°C for 0 or 30 min. Shown are representative images (A and B) and the average correlation coefficients (±S.D.) (C) from >300 cells of three independent experiments. Bars, 2.5 μm. (D) Flow cytometry analysis of BCR internalization by quantifying the percentage of biotin-F(ab′)$_2$-anti-Ig labeled BCR remaining on the cell surface after the 37^{o}C chase. Shown are the average percentages (±SD) from three independent experiments. *, $p \leq 0.05$, compared to B cells from control mice.

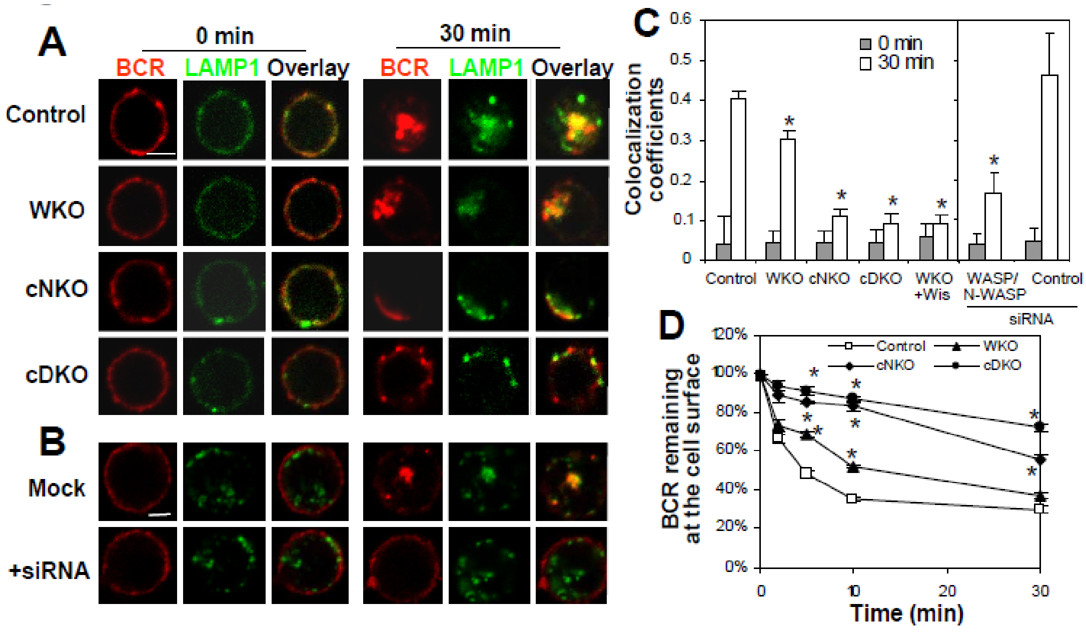
A
0 min
30 min
BCR
LAMP1
Overlay
Control
WKO
cNKO
cDKO
B
Mock
+siRNA
C
Colocalization coefficients
0 min
30 min
0.6
0.5
0.4
0.3
0.2
0.1
0
Control
WKO
cNKO
cDKO
WKO +Wis
WASP/ N-WASP
Control
siRNA
*
D
BCR remaining at the cell surface
120%
100%
80%
60%
40%
20%
0%
Control
WKO
cNKO
cDKO
0
10
20
30
Time (min)

4.4.7 Mutual Regulation between WASP and N-WASP

The involvement of both WASP and N-WASP in BCR activation suggests a functional coordination between these two proteins. To understand their functional relationship, we compared the activation levels and kinetics of one of the two proteins in the presence and absence of the other using TIRFM and flow cytometry. Both the MFI of pWASP in the contact zone of cNKO B cells (Figure 4.7A,C) and the cellular MFI of wiskostatin treated mouse B cells (Figure 4.7E) were increased compared to those in untreated control B cells. Conversely, the pN-WASP levels in the contact zone of WKO B cells (Figure 4.7B,D) and in WKO B cells (Figure 4.7F) were significantly higher than those in control B cells. In both case, the time taken for pN-WASP to peak was not changed. While the levels of pN-WASP and pWASP were changed, the overall protein levels of N-WASP and WASP did not change in WKO and cNKO B cells, indicating that the increased phosphorylation level is not due to an increase in protein expression. Consistent with the data from mouse models, treating human B cells from healthy subjects with the N-WASP inhibitor wiskostatin resulted in an increase in the cellular level of pWASP (Figure 4.7G). Furthermore, the level of pN-WASP was increased in PBMC B cells from WAS patients that did not express or expressed low levels of WASP, compared to that of healthy human controls (Figure 4.7H). These results indicate that WASP and N-WASP negatively regulate each other during BCR activation in both mouse and human B cells.

Figure 4.7 WASP and N-WASP negatively regulates each other. (A-D) TIRFM analysis of pWASP and pN-WASP in the contact zone of splenic B cells stimulated with mAg (A and B). The MFI of pWASP (C) or pN-WASP (D) in the B cell contact zone was quantified. (E-G) Flow cytometry analysis of the cellular MFI of pWASP or pN-WASP in splenic B cells from WKO and control mice (F), and mouse splenic (E) and human PBMC B cells (G) that were treated with or without Wis and sAg. (H) Flow cytometry analysis of the cellular MFI of pN-WASP in PBMC B cells from WAS patients and age matched healthy donors that were incubated with or without sAg for 2 min. Shown are representative images at 7 min and the average MFI (±SD) from three independent experiments. Bars, 2.5 μm. * *p<0.01,* compared to B cells from wt or control mice*,* without Wis treatment or healthy donors.

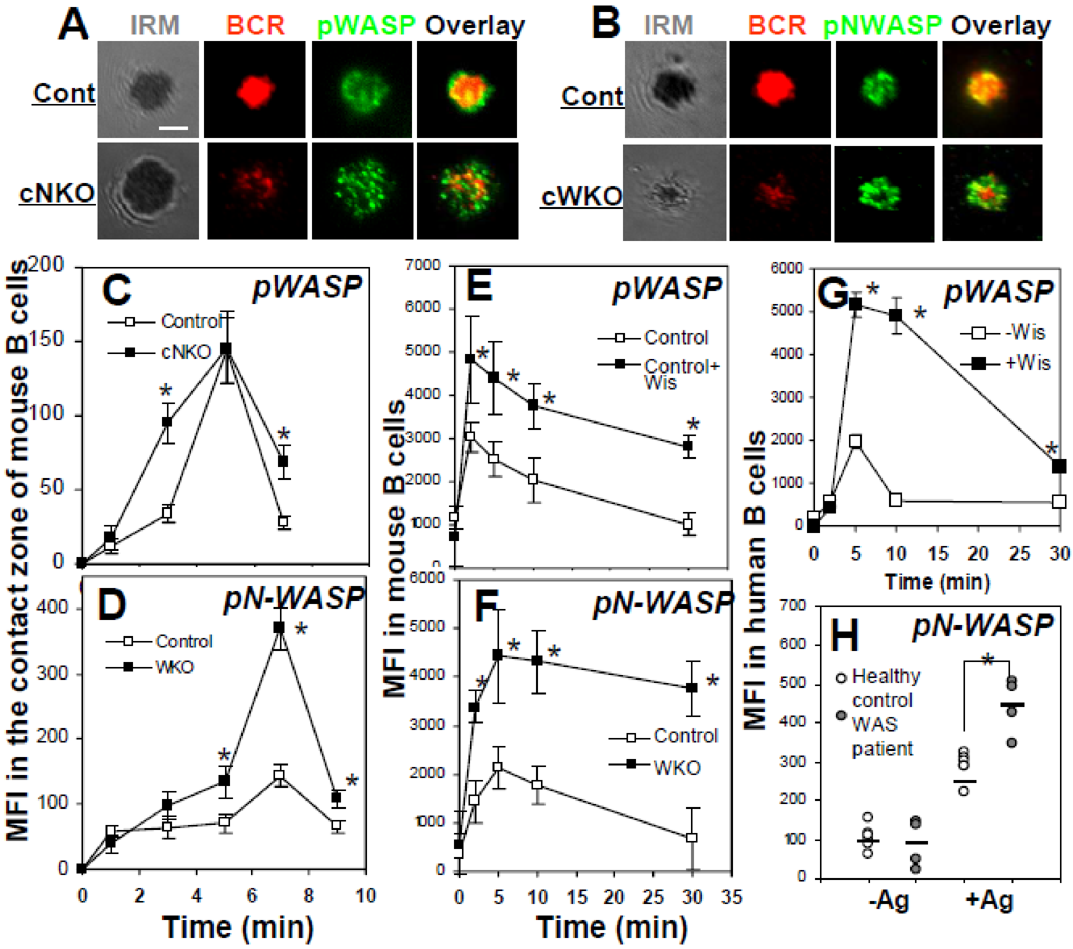
A
IRM
BCR
pWASP
Overlay
Cont
cNKO
B
IRM
BCR
pNWASP
Overlay
Cont
cWKO
C
pWASP
Control
cNKO
D
pN-WASP
Control
WKO
E
pWASP
Control
Control+ Wis
F
pN-WASP
Control
WKO
G
pWASP
-Wis
+Wis
H
pN-WASP
Healthy control
WAS patient
-Ag
+Ag
MFI in the contact zone of mouse B cells
MFI in mouse B cells
MFI in human B cells
Time (min)
*
0
50
100
150
200
300
400
1000
2000
3000
4000
5000
6000
7000
500
600
700
2
4
6
8
10
15
20
25
30
35

4.4.8 The Activation of WASP and N-WASP Is Inversely Regulated by BCR Signaling

The activation of WASP and N-WASP in response to antigen stimulation suggests that BCR signaling triggers their activation. We have previously shown that Btk is responsible for activating WASP while SHIP-1 suppresses WASP activation by inhibiting Btk [155]. To investigate whether N-WASP activation is controlled in the same manner as WASP, we determined the effect of Btk or SHIP-1 deficiency on antigen triggered phosphorylation of N-WASP using xid mice where the PH domain of Btk contains a point mutation that blocks Btk activation [98] and B cell specific SHIP-1 KO mice [155,240]. In sharp contrast with the effect of Btk and SHIP-1 deficiency on WASP activation, the MFI of pN-WASP was increased in the B cell contact zone and B cells from xid mice (Figure 4.8A-C), while it was decreased in the B cell contact zone and B cells from SHIP-1 KO mice (Figure 4.8D-F). These results suggest that the activation of WASP and N-WASP is regulated inversely by BCR signaling: Btk that activates WASP suppresses N-WASP activation while SHIP-1 that inhibits the activation of Btk and WASP promotes N-WASP activation.

Figure 4.8 WASP and N-WASP are inversely regulated by Btk and SHIP-1. (A-B and D-E) TIRFM analysis of pN-WASP in the contact zone of splenic B cells from wt, xid, control, and B cell-specific SHIP-1$^{-/-}$ mice that were incubated with mAg. The MFI of pN-WASP in the B cell contact zone were determined (B and E). (C and F) Flow cytometry analysis of the cellular MFI of pN-WASP in splenic B cells incubated with sAg. Shown are representative images at 7 min and the average MFI (±SD) from three independent experiments. Bars, 2.5 μm. * $p<0.01$, compared to B cells from wt or control mice, without Wis treatment or healthy donors.

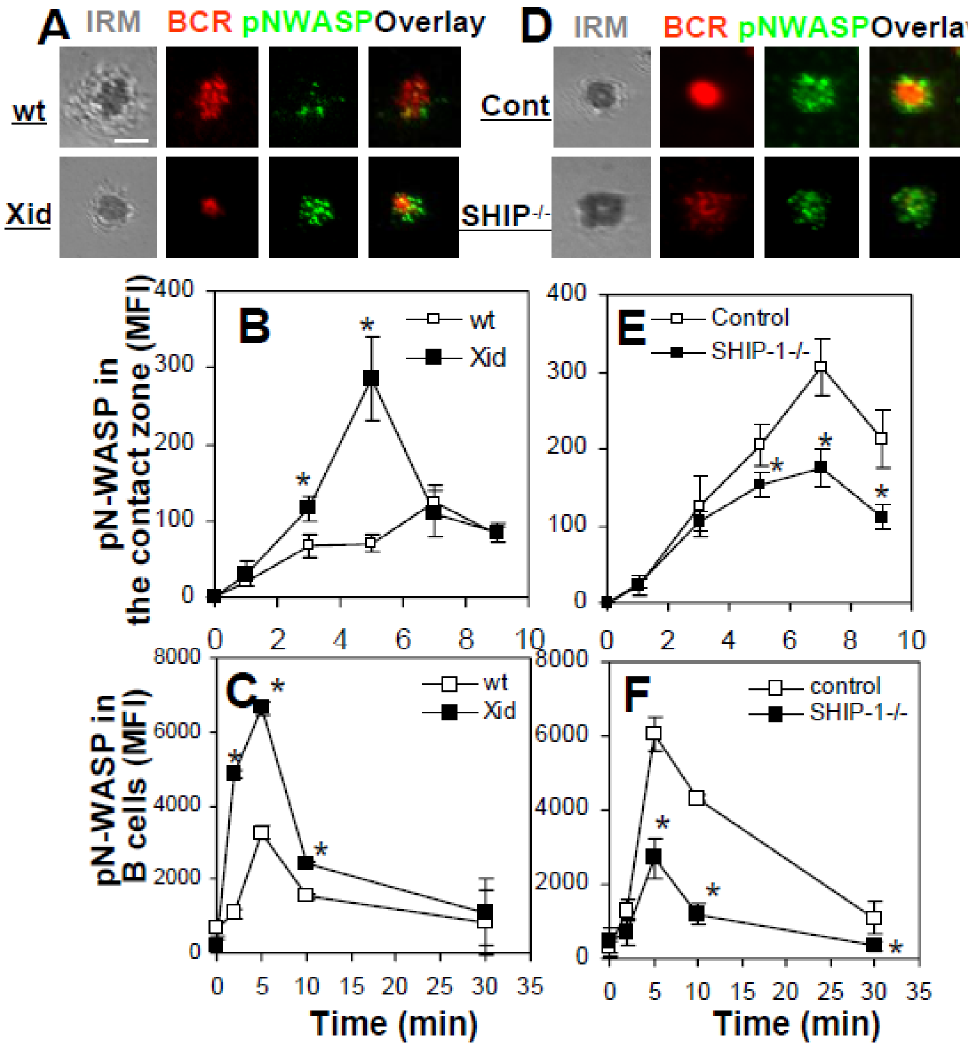
A
IRM
BCR
pNWASP
Overlay
wt
Xid
D
IRM
BCR
pNWASP
Overla
Cont
SHIP-/-
B
wt
Xid
pN-WASP in the contact zone (MFI)
0
100
200
300
400
0
2
4
6
8
10
*
*
E
Control
SHIP-1-/-
0
100
200
300
400
0
2
4
6
8
10
*
*
*
C
wt
Xid
pN-WASP in B cells (MFI)
0
2000
4000
6000
8000
0
5
10
15
20
25
30
35
Time (min)
*
*
*
F
control
SHIP-1-/-
0
2000
4000
6000
8000
0
5
10
15
20
25
30
35
Time (min)
*
*
*

4.5 Discussion

In this study, we demonstrate that in addition to the overlapping function with WASP in signaling activation, N-WASP plays a unique role in the down regulation of BCR signaling at the cell surface. This is showed by enhanced and/or prolonged tyrosine and Btk phosphorylation, increased calcium influx, and reduced SHIP-1 phosphorylation in cNKO B cells. Importantly, the enhanced signaling in response to in vitro antigen stimulation is associated with elevated levels of anti-nuclear and anti-dsDNA autoantibodies in the serum of cNKO mice. Since N-WASP is exclusively deleted from B cells, the increased autoantibody and BCR signaling is the result of B cell intrinsic defects. These results indicate that N-WASP-mediated signaling down regulation of surface BCRs is critical for the maintenance of B cell self tolerance.

Our studies find that there are more severe defects in BCR aggregation, B cell spreading and signal activation in cDKO B cells than in WKO B cells, indicating overlapping functions between N-WASP and WASP in these processes. This is consistent with their shared cellular function in promoting actin polymerization. However, WASP KO alone results in significant decreases in these processes, even though they are much less severe than those in cDKO B cells. These results suggest that N-WASP is unable to completely compensate for WASP in WKO B cells.

Our data show that the inhibition of the attenuation of BCR surface signaling is concurrent with increases in B cell spreading, delays in B cell contraction and the merger of BCR aggregates into the central cluster, and a blockage of BCR internalization in cNKO B cells. These results suggest that N-WASP promotes signaling attenuation via modulating BCR aggregation, B cell morphology, and BCR internalization. Similar to what we previously shown in SHIP-1$^{-/-}$ B cells [155], BCR aggregates in cNKO B cells remain smaller in size and exhibit much higher levels of tyrosine phosphorylation than those in control B cells while cNKO B cell contraction is delayed in comparison with control B cells. These data collectively demonstrate that B cell contraction, which can provide a force for the merger of small BCR aggregates into polarized central clusters, is an important mechanism for down regulating BCR signaling at the cell surface. The exact mechanism by which the size of BCR aggregates regulates receptor signaling is unknown. Our results show that the levels of pBtk and pSHIP-1 are increased and decreased respectively in the contact zone of cNKO B cells, suggesting an association of the activation of positive and negative signaling molecules with the size of BCR aggregates and N-WASP expression. N-WASP has been suggested to have a role in regulating the cellular location and activation of SHIP [243]. The dominant role of N-WASP in BCR internalization enables the removal of antigen-BCR complexes from the cell surface, which leads to both surface signaling attenuation and antigen presentation that provides another layer of control over B cell activation by T cells.

While N-WASP has both an overlapping role with WASP in signaling activation and a unique role in signaling down regulation in B cells, we demonstrate here that N-WASP exhibits the two opposing functions in different circumstances. N-WASP predominantly displays its function for signaling down regulation in B cells that have normal expression of WASP, since cNKO B cells have no defects in B cell spreading and signaling activation. However, it switches to signaling activation function in B cells lacking WASP expression, since cDKO B cells have more severe signaling defects than WKO B cells. The different functionalities of N-WASP in the presence or absence of WASP expression suggests that WASP is involved in the functional switch of N-WASP. Indeed, we found that in control B cells the pWASP level increases first, and the pN-WASP level does not peak until pWASP returns near to its basal level. In the absence of WASP, the pN-WASP level rises earlier and significantly higher in WKO B cells than that in control B cells. Conversely, in the absence of N-WASP, the pWASP level increases earlier and is sustained longer in cNKO B cells than that in control B cells. Moreover, we found similar results in human B cells from healthy subjects and WAS patients. These results indicate that WASP and N-WASP mutually suppress each other for activation in both human and mouse B cells. While the mechanism underlying the mutual suppression of WASP and N-WASP remains to be investigated, we speculate that competing for the limited docking sites and activation machinery at the plasma membrane may be a possible mechanism.

Previous studies have shown that WASP and N-WASP share the same activation mechanisms, including the interaction with the GTPase Cdc42 or Rac via the GBD domain and $PI(4,5)P_2$ via the PH domain, and tyrosine and serine phosphorylation [193,236,244]. We have previously shown that Btk is responsible for the activation of WASP in B cells by activating guanine nucleotide exchange factor Vav, increasing $PI(4,5)P_2$, and inducing WASP phosphorylation [118]. A surprising finding of this study is that N-WASP is not activated by the same pathway as WASP, since the level of pN-WASP is increased rather than decreased in Btk deficient B cells and is decreased rather than increased in SHIP-1$^{-/-}$ B cell as seen for pWASP. This suggests that SHIP-1 instead of Btk is involved in N-WASP activation. During BCR activation, Btk is activated before SHIP-1 [66,227,245], which provides an explanation for the activation of WASP before N-WASP. SHIP-1 inhibits Btk activation via dephosphorylating PI(3,4,5)P_3, the docking site of Btk at the plasma membrane [55], consequently suppressing WASP activation. Therefore, SHIP-1 induces N-WASP activation likely by inhibiting WASP activation, which releases N-WASP from the WASP suppression.

Studies accumulated from the last decade have clearly demonstrated that WASP and N-WASP share the same cellular function: stimulating actin polymerization by activating Arp2/3 [193,237,246]. This raises the question of how these two proteins possibly have opposing roles in B cell morphology and BCR clustering and activation. It should be noted that almost all of the studies so far examined the cellular function of WASP and N-WASP individually in the absence of their homolog. Consistent with these studies, we found that WASP and N-WASP appear to play a similar role in actin accumulation at the contact zone of WKO and cDKO B cells, shown by a smaller decrease in the level of F-actin in the contact zone of WKO B cells than that of cNKO B cells. Surprisingly, N-WASP KO alone causes a significant and sustained increase in the level of F-actin in the B cell contact zone, which is inconsistent with the current dogma that N-WASP functions as an actin nucleation promoting but not inhibitory factor. Our examination of the spatial relationship of activated WASP and N-WASP with Arp2/3 shows that pWASP has a significantly higher level of colocalization with Arp2 than pN-WASP, and that WASP KO increases the colocalization between pN-WASP and Arp2 but N-WASP KO does not lead to further increases in the colocalization of pWASP with Arp2. These results suggest a competition between WASP and N-WASP for binding to Arp2/3 complexes. Since WASP is activated and recruited to the B cell contact zone by Btk first, this allows WASP to win the competition for binding to Arp2/3, consequently competitively inhibiting the binding of N-WASP to Arp2/3.

How N-WASP reduces F-actin in the B cell contact zone is an interesting question. When Takenawa's group discovered N-WASP, N-WASP was identified as an actin depolymerizing protein since the VCA domain of N-WASP was capable of depolymerizing F-actin in vitro in the absence of Arp2/3 [235]. This raises the possibility that the VCA domain of active N-WASP, which is not bound to Arp2/3 due to losing competition to activated WASP, can depolymerize F-actin at the B cell contact zone. N-WASP also has unique functions in tethering F-actin to budding and moving vesicles [247,248], by which it may move F-actin away from the B cell contact zone to or activate actin polymerization at budding vesicles containing BCRs [249,250], facilitating BCR internalization.

WASP deficiency due to gene mutations causes an X-linked immune disorder, exhibiting immune deficiency, autoimmunity and lymphoma [164,166,232]. While defects in other immune cells contribute to the disease, recent studies have demonstrated that B cell intrinsic defects are critical for the development of autoimmunity in mouse models [167,168]. Here we show that WASP and N-WASP behave similarly in mouse and human B cells, including the sequential activation of N-WASP and WASP and the mutual regulation between the two. The B cell intrinsic roles of N-WASP in the down regulation of BCR signaling and B cell tolerance demonstrated here suggest a critical contribution of N-WASP to disease development. It is possible that without the competitive inhibition of WASP, the signaling promoting function of N-WASP is enhanced and its signaling attenuation function is reduced, leading to deregulation of BCR and B cell activation. This hypothesis will be pursued in our future studies.

Taking the results of this study and previous studies together enables us to propose a working model for the functional coordination of WASP and N-WASP during BCR activation (Figure 4.9). Antigen binding to the BCR induces an early activation of Btk (Figure 4.9A) that in turn activates and translocates WASP to the cell surface. Activated WASP stimulates actin polymerization by binding to Arp2/3, which modulates BCR lateral mobility and drives B cell spreading. Together, these facilitate BCR clustering and signaling (Figure 4.9B). The activation of SHIP-1 after the initial signaling inhibits Btk activation, which decreases the level of active WASP and releases N-WASP from the suppression of WASP. The activated N-WASP reduces the surface level of F-actin probably by depolymerizing and/or transferring F-actin to BCR containing budding vesicles. Reductions in F-actin at the B cell contact zone allow B cell contraction, which promotes the merger of BCR aggregates into a central cluster. Tethering F-actin to endocytosing vesicles by N-WASP is essential for the

Figure 4.9 A working model for the coordination of N-WASP with WASP in the regulation of BCR signaling. (A) Antigen binding to the BCR induces an early activation of Btk. (B) Activated Btk in turn activates and translocates WASP to the cell surface. Activated WASP (W) stimulates actin polymerization and reorganization by binding to Arp2/3 and suppresses N-WASP activation, which drives B cell spreading and facilitates BCR aggregation and signaling. (C) The activation of SHIP-1 induced by the BCR after initial signaling inhibits Btk and WASP activation, consequently releasing N-WASP from WASP suppression. Active N-WASP decreases actin accumulation at the B cell contact zone, which enables B cell contraction and promotes the merger of BCR aggregates into a central cluster and BCR internalization. The formation of BCR central clusters and BCR endocytosis lead to the down regulation of BCR signaling at the cell surface.

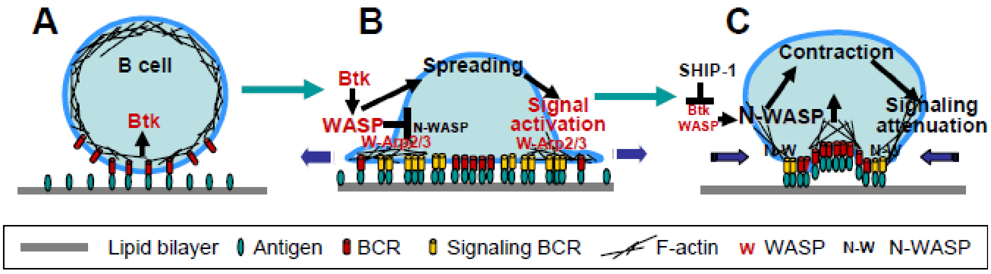
A
B cell
Btk
B
Btk
WASP
N-WASP
W-Arp2/3
Spreading
Signal activation
W-Arp2/3
C
SHIP-1
Btk
WASP
N-WASP
Contraction
Signaling attenuation
N-W
N-W
Lipid bilayer
Antigen
BCR
Signaling BCR
F-actin
W WASP
N-W N-WASP

endocytosis of antigen-BCR complexes. The formation of BCR central clusters and BCR endocytosis lead to the down regulation of BCR signaling at the cell surface (Figure 9C). While molecular details of this working model require further investigation, this study reveals a novel function of N-WASP in the down regulation of BCR signaling and a unique functional coordination between WASP with N-WASP during receptor signaling.

Chapter 5. General conclusions and future experiments

This thesis examined the functional relationship between the actin cytoskeleton and the BCR. The major finding of my research is that the actin cytoskeleton closely coordinates with the signal transduction and antigen processing functions of the BCR to provide regulatory feedbacks to the BCR. Using gene deficient mouse models, my results demonstrate that Btk, the key stimulatory kinase downstream of the BCR, promotes BCR clustering and B cell spreading by activating actin polymerization, while SHIP, a critical inhibitory phosphatase in B cells, promotes coalescence of BCR microclusters into a central cluster and B cell contraction by inhibiting actin polymerization. It is intriguing that B cell spreading is enhanced but the BCR clustering is reduced in SHIP deficient B cells. Further mechanistic investigation found that SHIP facilitates the formation of BCR central clusters by driving the centripetal movement of BCR microclusters. Similar to previous reports of B cells stimulated by soluble antigens [60,251], SHIP is responsible for inhibition of tyrosine phosphorylation and the phosphorylation of Btk and Akt at the B cell contact zone. The association of a reduction in BCR microcluster coalenscence with an increase in BCR signaling in SHIP knockout B cells suggests a relationship between the growth of BCR microclusters and the relative level of BCR signaling. The results from this thesis demonstrate that the initial formation and growth of BCR microclusters is associated with signaling activation, but the coalescence of BCR microclusters into the central cluster is associated with signaling attenuation. Therefore, SHIP can contribute signaling downregulation by promoting the coalescence of BCR microclusters and B cell contraction, in addition to its phosphatase activity. Previous published data from my lab have shown that Btk can stimulate actin reorganization via activating WASP in response to soluble antigens [118]. The results here show that SHIP negatively regulates the activation of WASP and actin polymerization via inhibiting the activation of Btk [55]. These results together indicate that BCR signaling can regulate BCR clustering and B cell spreading by modulating actin dynamics.

To address the question of how actin remodeling is controlled to provide optimal feedback to the BCR signaling, I examined the activation and function of WASP and N-WASP during BCR activation. My results show that both WASP and N-WASP are required for optimal activation of the BCR, but these two proteins are activated and recruited to the BCR in different times in response to antigenic stimulation and have distinct functions during BCR activation. While both WASP and N-WASP are indispensible for BCR clustering and B cell spreading, N-WASP is exclusively responsible for the B cell contraction. Consequently, both WASP and N-WASP are important for BCR signaling activation, but N-WASP has a unique role in the down regulation of BCR signaling. B cell spreading and BCR clustering promoted by WASP and N-WASP provide a positive feedback to BCR signaling, including Btk activation, and N-WASP-promoted B cell contraction and BCR microcluster coalescence offer a feedback to the inhibitory signaling, such as SHIP. My results demonstrate for the first time that N-WASP-mediated negative regulation of BCR signaling contributes the control of B cell mediated autoimmunity and the maintenance of B cell self tolerance. While the detail molecular mechanism is unknown, my results suggest that N-WASP mediates this negative regulation by promoting B cell contraction and the coalescence of BCR microclusters and by a its special relationship with SHIP-1. While this study has shown that N-WASP contribution to the regulation of B cell tolerance is B cell intrinsic, Rawling's group has shown that CD4 T cells and key mediators of Toll-receptors signaling pathways are involved in the generation of autoimmune antibodies in WASP germline knockout mice [168]. This suggests that WASP is involved in MyD88 involved TLR signaling pathways. It is possible that N-WASP positively reguates TLR-induced B cell activation, since my results have shown that N-WASP is hyperphosphorylated in B cells in WASP knockout mice and WASP-deficient WAS patients.

The results from this thesis discover differential roles of WASP and N-WASP in BCR-induced actin reorganization: WASP promotes and N-WASP inhibits F-actin accumulation at the activation surface. This implicates that N-WASP could have an actin depolymerization role during B cell contraction. Our studies further found that the differential actin regulatory functions are associated with the spatial relationship of WASP and N-WASP with Arp2/3. WASP preferencially colocalizes with Arp2/3, and N-WASP only exhibits significant colocalization with Arp2/3 in.WASP deficiency B cells. These data suggest that a competitive relationship between WASP and N-WASP for Arp2/3. However the molecular mechanism underlying the inhibitory role of N-WASP in F-actin accumulation remains elucive. There are two possible ways for N-WASP to reduce F-actin in the B cell contact zone: actin depolymerization and translocation. The inhibition effect of WASP on the interaction of N-WASP with Arp2/3 may induce the actin depolymerization activity of N-WASP, since previous studies have reported using an in vitro assay that the VCA domain of N-WASP has such an actin depolymerization activity in the absence of Arp2/3 [235]. In addition to WASP, that the binding of other proteins such as Abp1 or non-muscle myosin II may further inhibit the interaction of N-WASP with Arp2/3, particularly at later times post BCR activation when the level of WASP activation reduces. The interaction of N-WASP with Abp1 and/or non-muscle myosin II may be enable the recruitment of these actin regulators to the B cell surface, where they mediate actin depolymerization and/or contraction, facilitating B cell contraction and BCR microcluster coalescence.

These results from this study demonstrate that while both WASP and N-WASP are involved in BCR internalization, N-WASP plays a dominant role in this process. The involvement of N-WASP in endocytosis has been shown before, including the endocytosis of *Candida parapsilosis* in Human endothelial cells [252] and Fc receptor-mediated phagocytosis where N-WASP coordninates with NCK and Cdc42 [253]. We hypothesize N-WASP can promote BCR endocytosis by tether F-actin to clathrin coated pits.

Future experiment

From my results, we have learned that N-WASP is regulated by BCR signaling differently from WASP. SHIP rather than Btk promotes the activation of N-WASP.

However, the molecular mechanism by which SHIP regulates N-WASP activation is unknown. Since SHIP is a proximal signaling molecule in BCR signaling pathway, it is likely that multiple signaling intermediates downstream of SHIP can translate SHIP enzymetic activity into N-WASP activation. Based on literature, we hypothesize that the adaptor protein of SHIP, Dok1 [254], signaling adaptor proteins that interacting with WASP or N-WASP including Nck and Grb2 [113], and Tsk-5 that interacts with the enzymatic product of SHIP, PtdIn(3.4)P_2 are potential links between SHIP and N-WASP [255]. In addition, B cell contraction that requires the activation of both SHIP and WASP, probably relies on actin contraction motor, non-muscle myosin II [256]. In support of this hypothesis, my preliminary studies found that Nck, phosphorylated Dok-1, Tsk5, and non-muscle myosin IIA, phosphorylated myosin light chain (MLC), and ROCK that phosphorylates MLC were recruited to the B cell contact zone upon BCR activation. Further, the levels of most these proteins were reduced in the contact zone of B cells from B cell specific SHIP knockout mice, except for the level of Nck that was increased, in response to antigenic stimuli. The next step is to determine if N-WASP is in the signaling complex of SHIP and identify molecules in this complex that are involved in N-WASP activation. One approach is to pull the SHIP signaling complex using immunoprecipitation and identify protein components using western blots and mass spectrometry. The functions of identified proteins in N-WASP activation can be investigated using siRNA/shRNA knock down of individual proteins or gene deletion mouse models. For example, we can knock down the level of Rock-1, Dok-1 and myosin IIA or using B cell specific myosin IIA knockout mice that we have recently acquired to examine how gene knockdown and knockout affects the activation level, kinetics, and distribution of N-WASP as well as N-WASP-dependent B cell contraction and BCR central cluster formation. These experiments enable to identify missing links between SHIP and N-WASP and between N-WASP and actin-dependent signaling events.

My studies discovered a competitive relationship between WASP and N-WASP to interact with Arp2/3 with the domination of WASP over N-WASP. However, the underlying molecular mechanism is completely unknown. I postulate that WASP can compete Arp2/3 bettern than that of N-WASP. To test this hypothesis, we can analyze the spatial relationship between WASP and N-WASP, by simutaneoulsy staining these two proteins in primary B cells or A20 cells transfected with these two proteins as well as Arp2/3 fused with different fluorescence, the latter of which enable to analyze the dynamics relationship among these proteins in live cells and real time.

My results indicate that N-WASP-mediated signaling down regulation contributes to the maintainance of B cell self tolerance. BCR signaling is crutial for B cell negative selection in the bone marrow and positive selection in the germinal center, two important steps for B cell tolerance. A remaininig question is which selection step N-WASP is involved. Westerburg et al. [170] has shown that there is no significant changes in B cell maturation in the bone marrow, suggesting that B cell positive selection in the germinal center is potential target for N-WASP regulation. To test this hypothesis, I propose to analyze the impact of N-WASP deficiency on B cell development and differentiation of the germinal center and on B cell positive selection through affinity maturation in the germinal center in both non-immunized and immunized mice, using flow cytometry.

My thesis research has revealed new mechanisms that link the BCR signaling and actin reorganization during BCR activation, which contribute to the understanding of immune disorders caused by genetic mutations of actin regulators. The aberrance of BCR signaling can impact the normal function of actin cytoskeletion that controls the spatiotemporal organization of BCR. The dysregualtion of actin remodeling due to mutations of actin regulators interferes with BCR signaling.

References:

[1] H.A. Chapman, Endosomal proteolysis and MHC class II function, Curr Opin Immunol 10 (1998) 93-102.

[2] J. Ollila, M. Vihinen, B cells, Int J Biochem Cell Biol 37 (2005) 518-523.

[3] E.A. Clark, J.A. Ledbetter, How B and T cells talk to each other, Nature 367 (1994) 425-428.

[4] D.C. Parker, T cell-dependent B cell activation, Annu Rev Immunol 11 (1993) 331-360.

[5] A. Fischer, B. Malissen, Natural and engineered disorders of lymphocyte development, Science 280 (1998) 237-243.

[6] A.B. Kantor, L.A. Herzenberg, Origin of murine B cell lineages, Annu Rev Immunol 11 (1993) 501-538.

[7] A. Rolink, F. Melchers, B lymphopoiesis in the mouse, Adv Immunol 53 (1993) 123-156.

[8] S.A. Corfe, C.J. Paige, The many roles of IL-7 in B cell development; mediator of survival, proliferation and differentiation, Semin Immunol 24 (2012) 198-208.

[9] D.H. Ryan, B.L. Nuccie, C.N. Abboud, J.M. Winslow, Vascular cell adhesion molecule-1 and the integrin VLA-4 mediate adhesion of human B cell precursors to cultured bone marrow adherent cells, J Clin Invest 88 (1991) 995-1004.

[10] M. Gellert, Recent advances in understanding V(D)J recombination, Adv Immunol 64 (1997) 39-64.

[11] E.T. Luning Prak, M. Monestier, R.A. Eisenberg, B cell receptor editing in

tolerance and autoimmunity, Ann N Y Acad Sci 1217 (2011) 96-121.

[12] A.L. Foreman, J. Van de Water, M.L. Gougeon, M.E. Gershwin, B cells in autoimmune diseases: insights from analyses of immunoglobulin variable (Ig V) gene usage, Autoimmun Rev 6 (2007) 387-401.

[13] H. Azulay-Debby, D. Melamed, B cell receptor editing in tolerance and autoimmunity, Front Biosci 12 (2007) 2136-2147.

[14] F.W. Alt, G. Rathbun, E. Oltz, G. Taccioli, Y. Shinkai, Function and control of recombination-activating gene activity, Ann N Y Acad Sci 651 (1992) 277-294.

[15] C.B. Thompson, New insights into V(D)J recombination and its role in the evolution of the immune system, Immunity 3 (1995) 531-539.

[16] J.C. Cambier, S.B. Gauld, K.T. Merrell, B.J. Vilen, B-cell anergy: from transgenic models to naturally occurring anergic B cells?, Nat Rev Immunol 7 (2007) 633-643.

[17] E. Montecino-Rodriguez, K. Dorshkind, New perspectives in B-1 B cell development and function, Trends Immunol 27 (2006) 428-433.

[18] J.W. Tung, L.A. Herzenberg, Unraveling B-1 progenitors, Curr Opin Immunol 19 (2007) 150-155.

[19] D. Allman, B. Srivastava, R.C. Lindsley, Alternative routes to maturity: branch points and pathways for generating follicular and marginal zone B cells, Immunol Rev 197 (2004) 147-160.

[20] M. Balazs, F. Martin, T. Zhou, J. Kearney, Blood dendritic cells interact with splenic marginal zone B cells to initiate T-independent immune responses, Immunity 17 (2002) 341-352.

[21] T. Lopes-Carvalho, J. Foote, J.F. Kearney, Marginal zone B cells in lymphocyte activation and regulation, Curr Opin Immunol 17 (2005) 244-250.

[22] J. Stavnezer, Antibody class switching, Adv Immunol 61 (1996) 79-146.

[23] J.J. Mond, A. Lees, C.M. Snapper, T cell-independent antigens type 2, Annu Rev Immunol 13 (1995) 655-692.

[24] J.J. Mond, Q. Vos, A. Lees, C.M. Snapper, T cell independent antigens, Curr Opin Immunol 7 (1995) 349-354.

[25] M.R. Gold, A.L. DeFranco, Biochemistry of B lymphocyte activation, Adv Immunol 55 (1994) 221-295.

[26] M.C. Carroll, The complement system in B cell regulation, Mol Immunol 41 (2004) 141-146.

[27] M.C. Carroll, The role of complement in B cell activation and tolerance, Adv Immunol 74 (2000) 61-88.

[28] G.D. Victora, M.C. Nussenzweig, Germinal centers, Annu Rev Immunol 30 (2012) 429-457.

[29] U. Gowthaman, S.B. Chodisetti, J.N. Agrewala, T cell help to B cells in germinal centers: putting the jigsaw together, Int Rev Immunol 29 (2010) 403-420.

[30] C.D. Allen, T. Okada, J.G. Cyster, Germinal-center organization and cellular dynamics, Immunity 27 (2007) 190-202.

[31] M. Or-Guil, N. Wittenbrink, A.A. Weiser, J. Schuchhardt, Recirculation of germinal center B cells: a multilevel selection strategy for antibody maturation, Immunol Rev 216 (2007) 130-141.

[32] K.A. Vora, J.V. Ravetch, T. Manser, Insights into the mechanisms of antibody-affinity maturation and the generation of the memory B-cell compartment using genetically altered mice, Dev Immunol 6 (1998) 305-316.

[33] I.C. MacLennan, M. Casamayor-Palleja, K.M. Toellner, A. Gulbranson-Judge, J. Gordon, Memory B-cell clones and the diversity of their members, Semin Immunol 9 (1997) 229-234.

[34] A. Bortnick, D. Allman, What is and what should always have been: long-lived plasma cells induced by T cell-independent antigens, J Immunol 190 (2013) 5913-5918.

[35] D. Zotos, D.M. Tarlinton, Determining germinal centre B cell fate, Trends Immunol 33 (2012) 281-288.

[36] M.J. Shlomchik, F. Weisel, Germinal center selection and the development of memory B and plasma cells, Immunol Rev 247 (2012) 52-63.

[37] C.M. Pleiman, D. D'Ambrosio, J.C. Cambier, The B-cell antigen receptor complex: structure and signal transduction, Immunol Today 15 (1994) 393-399.

[38] A. Weiss, D.R. Littman, Signal transduction by lymphocyte antigen receptors, Cell 76 (1994) 263-274.

[39] M.L. Bireland, J.G. Monroe, Biochemistry of antigen receptor signaling in mature and developing B lymphocytes, Crit Rev Immunol 17 (1997) 353-385.

[40] M. Reth, J. Wienands, Initiation and processing of signals from the B cell antigen receptor, Annu Rev Immunol 15 (1997) 453-479.

[41] A.L. DeFranco, J.D. Richards, J.H. Blum, T.L. Stevens, D.A. Law, V.W. Chan, S.K.

Datta, S.P. Foy, S.L. Hourihane, M.R. Gold, et al., Signal transduction by the B-cell antigen receptor, Ann N Y Acad Sci 766 (1995) 195-201.

[42] R.R. Porter, The structure of immunoglobulins, Essays Biochem 3 (1967) 1-24.

[43] T. Webb, H.C. Goodman, The structure and function of immunoglobulins, Mod Trends Immunol 2 (1967) 151-187.

[44] R. Saada, M. Weinberger, G. Shahaf, R. Mehr, Models for antigen receptor gene rearrangement: CDR3 length, Immunol Cell Biol 85 (2007) 323-332.

[45] E.C. Franklin, B. Frangione, Immunoglobulins, Annu Rev Med 20 (1969) 155-174.

[46] N.M. Green, Electron microscopy of the immunoglobulins, Adv Immunol 11 (1969) 1-30.

[47] F.W. Putnam, Immunoglobulin structure: variability and homology, Science 163 (1969) 633-644.

[48] J.I. Healy, C.C. Goodnow, Positive versus negative signaling by lymphocyte antigen receptors, Annu Rev Immunol 16 (1998) 645-670.

[49] A.L. DeFranco, The complexity of signaling pathways activated by the BCR, Curr Opin Immunol 9 (1997) 296-308.

[50] T. Kurosaki, Molecular mechanisms in B cell antigen receptor signaling, Curr Opin Immunol 9 (1997) 309-318.

[51] T. Kurosaki, Molecular dissection of B cell antigen receptor signaling (review), Int J Mol Med 1 (1998) 515-527.

[52] D.T. Fearon, M.C. Carroll, Regulation of B lymphocyte responses to foreign and self-antigens by the CD19/CD21 complex, Annu Rev Immunol 18 (2000) 393-422.

[53] D. Depoil, S. Fleire, B.L. Treanor, M. Weber, N.E. Harwood, K.L. Marchbank, V.L. Tybulewicz, F.D. Batista, CD19 is essential for B cell activation by promoting B cell receptor-antigen microcluster formation in response to membrane-bound ligand, Nat Immunol 9 (2008) 63-72.

[54] T. Muta, T. Kurosaki, Z. Misulovin, M. Sanchez, M.C. Nussenzweig, J.V. Ravetch, A 13-amino-acid motif in the cytoplasmic domain of Fc gamma RIIB modulates B-cell receptor signalling, Nature 369 (1994) 340.

[55] S. Bolland, R.N. Pearse, T. Kurosaki, J.V. Ravetch, SHIP modulates immune receptor responses by regulating membrane association of Btk, Immunity 8 (1998) 509-516.

[56] A.M. Scharenberg, O. El-Hillal, D.A. Fruman, L.O. Beitz, Z. Li, S. Lin, I. Gout, L.C. Cantley, D.J. Rawlings, J.P. Kinet, Phosphatidylinositol-3,4,5-trisphosphate (PtdIns-3,4,5-P3)/Tec kinase-dependent calcium signaling pathway: a target for SHIP-mediated inhibitory signals, EMBO J 17 (1998) 1961-1972.

[57] Q. Liu, T. Sasaki, I. Kozieradzki, A. Wakeham, A. Itie, D.J. Dumont, J.M. Penninger, SHIP is a negative regulator of growth factor receptor-mediated PKB/Akt activation and myeloid cell survival, Genes Dev 13 (1999) 786-791.

[58] I. Tamir, J.C. Stolpa, C.D. Helgason, K. Nakamura, P. Bruhns, M. Daeron, J.C. Cambier, The RasGAP-binding protein p62dok is a mediator of inhibitory FcgammaRIIB signals in B cells, Immunity 12 (2000) 347-358.

[59] Y. Yamanashi, T. Tamura, T. Kanamori, H. Yamane, H. Nariuchi, T. Yamamoto, D. Baltimore, Role of the rasGAP-associated docking protein p62(dok) in negative

regulation of B cell receptor-mediated signaling, Genes Dev 14 (2000) 11-16.

[60] M.J. Aman, T.D. Lamkin, H. Okada, T. Kurosaki, K.S. Ravichandran, The inositol phosphatase SHIP inhibits Akt/PKB activation in B cells, J Biol Chem 273 (1998) 33922-33928.

[61] P. Tolar, H.W. Sohn, S.K. Pierce, The initiation of antigen-induced B cell antigen receptor signaling viewed in living cells by fluorescence resonance energy transfer, Nat Immunol 6 (2005) 1168-1176.

[62] P.K. Mongini, C.A. Blessinger, P.F. Highet, J.K. Inman, Membrane IgM-mediated signaling of human B cells. Effect of increased ligand binding site valency on the affinity and concentration requirements for inducing diverse stages of activation, J Immunol 148 (1992) 3892-3901.

[63] H.W. Sohn, S.K. Pierce, S.J. Tzeng, Live cell imaging reveals that the inhibitory FcgammaRIIB destabilizes B cell receptor membrane-lipid interactions and blocks immune synapse formation, J Immunol 180 (2008) 793-799.

[64] P.C. Cheng, M.L. Dykstra, R.N. Mitchell, S.K. Pierce, A role for lipid rafts in B cell antigen receptor signaling and antigen targeting, J Exp Med 190 (1999) 1549-1560.

[65] M. Dykstra, A. Cherukuri, H.W. Sohn, S.J. Tzeng, S.K. Pierce, Location is everything: lipid rafts and immune cell signaling, Annu Rev Immunol 21 (2003) 457-481.

[66] J.M. Dal Porto, S.B. Gauld, K.T. Merrell, D. Mills, A.E. Pugh-Bernard, J. Cambier, B cell antigen receptor signaling 101, Mol Immunol 41 (2004) 599-613.

[67] T. Kurosaki, Regulation of BCR signaling, Mol Immunol 48 (2011) 1287-1291.

[68] N.E. Harwood, F.D. Batista, Early events in B cell activation, Annu Rev Immunol 28 (2010) 185-210.

[69] S.A. Freeman, V. Lei, M. Dang-Lawson, K. Mizuno, C.D. Roskelley, M.R. Gold, Cofilin-Mediated F-Actin Severing Is Regulated by the Rap GTPase and Controls the Cytoskeletal Dynamics That Drive Lymphocyte Spreading and BCR Microcluster Formation, J Immunol 187 (2011) 5887-5900.

[70] B. Treanor, D. Depoil, A. Bruckbauer, F.D. Batista, Dynamic cortical actin remodeling by ERM proteins controls BCR microcluster organization and integrity, J Exp Med 208 (2011) 1055-1068.

[71] P. Tolar, J. Hanna, P.D. Krueger, S.K. Pierce, The constant region of the membrane immunoglobulin mediates B cell-receptor clustering and signaling in response to membrane antigens, Immunity 30 (2009) 44-55.

[72] H.W. Sohn, P. Tolar, S.K. Pierce, Membrane heterogeneities in the formation of B cell receptor-Lyn kinase microclusters and the immune synapse, J Cell Biol 182 (2008) 367-379.

[73] H.W. Sohn, P. Tolar, T. Jin, S.K. Pierce, Fluorescence resonance energy transfer in living cells reveals dynamic membrane changes in the initiation of B cell signaling, Proc Natl Acad Sci U S A 103 (2006) 8143-8148.

[74] M. Weber, B. Treanor, D. Depoil, H. Shinohara, N.E. Harwood, M. Hikida, T. Kurosaki, F.D. Batista, Phospholipase C-gamma2 and Vav cooperate within signaling microclusters to propagate B cell spreading in response to membrane-bound antigen, J Exp Med 205 (2008) 853-868.

[75] P. Tolar, H.W. Sohn, S.K. Pierce, Viewing the antigen-induced initiation of B-cell activation in living cells, Immunol Rev 221 (2008) 64-76.

[76] S.J. Fleire, J.P. Goldman, Y.R. Carrasco, M. Weber, D. Bray, F.D. Batista, B cell ligand discrimination through a spreading and contraction response, Science 312 (2006) 738-741.

[77] W. Liu, H. Won Sohn, P. Tolar, T. Meckel, S.K. Pierce, Antigen-induced oligomerization of the B cell receptor is an early target of Fc gamma RIIB inhibition, J Immunol 184 (2010) 1977-1989.

[78] P.K. Mattila, C. Feest, D. Depoil, B. Treanor, B. Montaner, K.L. Otipoby, R. Carter, L.B. Justement, A. Bruckbauer, F.D. Batista, The actin and tetraspanin networks organize receptor nanoclusters to regulate B cell receptor-mediated signaling, Immunity 38 (2013) 461-474.

[79] J. Yang, M. Reth, Oligomeric organization of the B-cell antigen receptor on resting cells, Nature 467 (2010) 465-469.

[80] J. Yang, M. Reth, The dissociation activation model of B cell antigen receptor triggering, FEBS Lett 584 (2010) 4872-4877.

[81] P. Tolar, H.W. Sohn, W. Liu, S.K. Pierce, The molecular assembly and organization of signaling active B-cell receptor oligomers, Immunol Rev 232 (2009) 34-41.

[82] M. Fujimoto, J.C. Poe, A.B. Satterthwaite, M.I. Wahl, O.N. Witte, T.F. Tedder, Complementary roles for CD19 and Bruton's tyrosine kinase in B lymphocyte signal transduction, J Immunol 168 (2002) 5465-5476.

[83] W.N. Khan, F.W. Alt, R.M. Gerstein, B.A. Malynn, I. Larsson, G. Rathbun, L. Davidson, S. Muller, A.B. Kantor, L.A. Herzenberg, et al., Defective B cell development and function in Btk-deficient mice, Immunity 3 (1995) 283-299.

[84] B.J. Mayer, R. Ren, K.L. Clark, D. Baltimore, A putative modular domain present in diverse signaling proteins, Cell 73 (1993) 629-630.

[85] R.J. Haslam, H.B. Koide, B.A. Hemmings, Pleckstrin domain homology, Nature 363 (1993) 309-310.

[86] A. Musacchio, T. Gibson, P. Rice, J. Thompson, M. Saraste, The PH domain: a common piece in the structural patchwork of signalling proteins, Trends Biochem Sci 18 (1993) 343-348.

[87] G. Shaw, Identification of novel pleckstrin homology (PH) domains provides a hypothesis for PH domain function, Biochem Biophys Res Commun 195 (1993) 1145-1151.

[88] M. de Weers, M.C. Verschuren, M.E. Kraakman, R.G. Mensink, R.K. Schuurman, J.J. van Dongen, R.W. Hendriks, The Bruton's tyrosine kinase gene is expressed throughout B cell differentiation, from early precursor B cell stages preceding immunoglobulin gene rearrangement up to mature B cell stages, Eur J Immunol 23 (1993) 3109-3114.

[89] C.I. Smith, B. Baskin, P. Humire-Greiff, J.N. Zhou, P.G. Olsson, H.S. Maniar, P. Kjellen, J.D. Lambris, B. Christensson, L. Hammarstrom, et al., Expression of Bruton's agammaglobulinemia tyrosine kinase gene, BTK, is selectively down-regulated in T lymphocytes and plasma cells, J Immunol 152 (1994) 557-565.

[90] W.N. Khan, P. Sideras, F.S. Rosen, F.W. Alt, The role of Bruton's tyrosine kinase in B-cell development and function in mice and man, Ann N Y Acad Sci 764 (1995) 27-38.

[91] S.J. Saouaf, S. Mahajan, R.B. Rowley, S.A. Kut, J. Fargnoli, A.L. Burkhardt, S. Tsukada, O.N. Witte, J.B. Bolen, Temporal differences in the activation of three classes of non-transmembrane protein tyrosine kinases following B-cell antigen receptor surface engagement, Proc Natl Acad Sci U S A 91 (1994) 9524-9528.

[92] Y. Aoki, K.J. Isselbacher, B.J. Cherayil, S. Pillai, Tyrosine phosphorylation of Blk and Fyn Src homology 2 domain-binding proteins occurs in response to antigen-receptor ligation in B cells and constitutively in pre-B cells, Proc Natl Acad Sci U S A 91 (1994) 4204-4208.

[93] J. Hasbold, G.G. Klaus, B cells from CBA/N mice do not proliferate following ligation of CD40, Eur J Immunol 24 (1994) 152-157.

[94] N.F. Go, B.E. Castle, R. Barrett, R. Kastelein, W. Dang, T.R. Mosmann, K.W. Moore, M. Howard, Interleukin 10, a novel B cell stimulatory factor: unresponsiveness of X chromosome-linked immunodeficiency B cells, J Exp Med 172 (1990) 1625-1631.

[95] S. Sato, T. Katagiri, S. Takaki, Y. Kikuchi, Y. Hitoshi, S. Yonehara, S. Tsukada, D. Kitamura, T. Watanabe, O. Witte, K. Takatsu, IL-5 receptor-mediated tyrosine phosphorylation of SH2/SH3-containing proteins and activation of Bruton's tyrosine and Janus 2 kinases, J Exp Med 180 (1994) 2101-2111.

[96] L. Santos-Argumedo, F.E. Lund, A.W. Heath, N. Solvason, W.W. Wu, J.C. Grimaldi, R.M. Parkhouse, M. Howard, CD38 unresponsiveness of xid B cells

implicates Bruton's tyrosine kinase (btk) as a regular of CD38 induced signal transduction, Int Immunol 7 (1995) 163-170.

[97] J.D. Thomas, P. Sideras, C.I. Smith, I. Vorechovsky, V. Chapman, W.E. Paul, Colocalization of X-linked agammaglobulinemia and X-linked immunodeficiency genes, Science 261 (1993) 355-358.

[98] D.J. Rawlings, D.C. Saffran, S. Tsukada, D.A. Largaespada, J.C. Grimaldi, L. Cohen, R.N. Mohr, J.F. Bazan, M. Howard, N.G. Copeland, et al., Mutation of unique region of Bruton's tyrosine kinase in immunodeficient XID mice, Science 261 (1993) 358-361.

[99] A.B. Satterthwaite, Z. Li, O.N. Witte, Btk function in B cell development and response, Semin Immunol 10 (1998) 309-316.

[100] L. Yao, Y. Kawakami, T. Kawakami, The pleckstrin homology domain of Bruton tyrosine kinase interacts with protein kinase C, Proc Natl Acad Sci U S A 91 (1994) 9175-9179.

[101] M. Leitges, C. Schmedt, R. Guinamard, J. Davoust, S. Schaal, S. Stabel, A. Tarakhovsky, Immunodeficiency in protein kinase cbeta-deficient mice, Science 273 (1996) 788-791.

[102] K. Salim, M.J. Bottomley, E. Querfurth, M.J. Zvelebil, I. Gout, R. Scaife, R.L. Margolis, R. Gigg, C.I. Smith, P.C. Driscoll, M.D. Waterfield, G. Panayotou, Distinct specificity in the recognition of phosphoinositides by the pleckstrin homology domains of dynamin and Bruton's tyrosine kinase, EMBO J 15 (1996) 6241-6250.

[103] L.E. Rameh, A. Arvidsson, K.L. Carraway, 3rd, A.D. Couvillon, G. Rathbun, A.

Crompton, B. VanRenterghem, M.P. Czech, K.S. Ravichandran, S.J. Burakoff, D.S. Wang, C.S. Chen, L.C. Cantley, A comparative analysis of the phosphoinositide binding specificity of pleckstrin homology domains, J Biol Chem 272 (1997) 22059-22066.

[104] J.T. Ransom, L.K. Harris, J.C. Cambier, Anti-Ig induces release of inositol 1,4,5-trisphosphate, which mediates mobilization of intracellular Ca++ stores in B lymphocytes, J Immunol 137 (1986) 708-714.

[105] Y. Wan, K. Bence, A. Hata, T. Kurosaki, A. Veillette, X.Y. Huang, Genetic evidence for a tyrosine kinase cascade preceding the mitogen-activated protein kinase cascade in vertebrate G protein signaling, J Biol Chem 272 (1997) 17209-17215.

[106] K. Brorson, M. Brunswick, S. Ezhevsky, D.G. Wei, R. Berg, D. Scott, K.E. Stein, xid affects events leading to B cell cycle entry, J Immunol 159 (1997) 135-143.

[107] L.R. Rohrschneider, J.F. Fuller, I. Wolf, Y. Liu, D.M. Lucas, Structure, function, and biology of SHIP proteins, Genes Dev 14 (2000) 505-520.

[108] S. Tridandapani, T. Kelley, M. Pradhan, D. Cooney, L.B. Justement, K.M. Coggeshall, Recruitment and phosphorylation of SH2-containing inositol phosphatase and Shc to the B-cell Fc gamma immunoreceptor tyrosine-based inhibition motif peptide motif, Mol Cell Biol 17 (1997) 4305-4311.

[109] M.A. Osborne, G. Zenner, M. Lubinus, X. Zhang, Z. Songyang, L.C. Cantley, P. Majerus, P. Burn, J.P. Kochan, The inositol 5'-phosphatase SHIP binds to immunoreceptor signaling motifs and responds to high affinity IgE receptor

aggregation, J Biol Chem 271 (1996) 29271-29278.

[110] M. Huber, C.D. Helgason, J.E. Damen, M. Scheid, V. Duronio, L. Liu, M.D. Ware, R.K. Humphries, G. Krystal, The role of SHIP in growth factor induced signalling, Prog Biophys Mol Biol 71 (1999) 423-434.

[111] M. Ono, S. Bolland, P. Tempst, J.V. Ravetch, Role of the inositol phosphatase SHIP in negative regulation of the immune system by the receptor Fc(gamma)RIIB, Nature 383 (1996) 263-266.

[112] H. Okada, S. Bolland, A. Hashimoto, M. Kurosaki, Y. Kabuyama, M. Iino, J.V. Ravetch, T. Kurosaki, Role of the inositol phosphatase SHIP in B cell receptor-induced Ca2+ oscillatory response, J Immunol 161 (1998) 5129-5132.

[113] S.K. O'Neill, A. Getahun, S.B. Gauld, K.T. Merrell, I. Tamir, M.J. Smith, J.M. Dal Porto, Q.Z. Li, J.C. Cambier, Monophosphorylation of CD79a and CD79b ITAM motifs initiates a SHIP-1 phosphatase-mediated inhibitory signaling cascade required for B cell anergy, Immunity 35 (2011) 746-756.

[114] M. Huber, C.D. Helgason, J.E. Damen, M.P. Scheid, V. Duronio, V. Lam, R.K. Humphries, G. Krystal, The role of the SRC homology 2-containing inositol 5'-phosphatase in Fc epsilon R1-induced signaling, Curr Top Microbiol Immunol 244 (1999) 29-41.

[115] A. Brauweiler, I. Tamir, J. Dal Porto, R.J. Benschop, C.D. Helgason, R.K. Humphries, J.H. Freed, J.C. Cambier, Differential regulation of B cell development, activation, and death by the src homology 2 domain-containing 5' inositol phosphatase (SHIP), J Exp Med 191 (2000) 1545-1554.

[116] W.H. Leung, T. Tarasenko, S. Bolland, Differential roles for the inositol phosphatase SHIP in the regulation of macrophages and lymphocytes, Immunol Res 43 (2009) 243-251.

[117] T. Tarasenko, H.K. Kole, A.W. Chi, M.M. Mentink-Kane, T.A. Wynn, S. Bolland, T cell-specific deletion of the inositol phosphatase SHIP reveals its role in regulating Th1/Th2 and cytotoxic responses, Proc Natl Acad Sci U S A 104 (2007) 11382-11387.

[118] S. Sharma, G. Orlowski, W. Song, Btk regulates B cell receptor-mediated antigen processing and presentation by controlling actin cytoskeleton dynamics in B cells, J Immunol 182 (2009) 329-339.

[119] A. Stoddart, M.L. Dykstra, B.K. Brown, W. Song, S.K. Pierce, F.M. Brodsky, Lipid Rafts Unite Signaling Cascades with Clathrin to Regulate BCR Internalization, Immunity 17 (2002) 451-462.

[120] V.R. Aluvihare, A.A. Khamlichi, G.T. Williams, L. Adorini, M.S. Neuberger, Acceleration of intracellular targeting of antigen by the B-cell antigen receptor: importance depends on the nature of the antigen-antibody interaction, Embo J 16 (1997) 3553-3562.

[121] W. Song, H. Cho, P. Cheng, S.K. Pierce, Entry of B cell antigen receptor and antigen into class II peptide- loading compartment is independent of receptor cross-linking, J Immunol 155 (1995) 4255-4263.

[122] F. Vascotto, D. Le Roux, D. Lankar, G. Faure-Andre, P. Vargas, P. Guermonprez, A.M. Lennon-Dumenil, Antigen presentation by B lymphocytes: how receptor signaling directs membrane trafficking, Curr Opin Immunol 19 (2007) 93-98.

[123] K. Siemasko, M.R. Clark, The control and facilitation of MHC class II antigen processing by the BCR, Curr Opin Immunol 13 (2001) 32-36.

[124] D.R. Fooksman, S. Vardhana, G. Vasiliver-Shamis, J. Liese, D. Blair, J. Waite, C. Sacristan, G. Victora, A. Zanin-Zhorov, M.L. Dustin, Functional Anatomy of T Cell Activation and Synapse Formation, Annu Rev Immunol 28 (2010) 79-105.

[125] N.A. Mitchison, T-cell-B-cell cooperation, Nat Rev Immunol 4 (2004) 308-312.

[126] T. Yokosuka, T. Saito, The immunological synapse, TCR microclusters, and T cell activation, Curr Top Microbiol Immunol 340 (2010) 81-107.

[127] M.L. Dustin, T-cell activation through immunological synapses and kinapses, Immunol Rev 221 (2008) 77-89.

[128] L.M. Carlin, K. Yanagi, A. Verhoef, E.N. Nolte-'t Hoen, J. Yates, L. Gardner, J. Lamb, G. Lombardi, M.J. Dallman, D.M. Davis, Secretion of IFN-gamma and not IL-2 by anergic human T cells correlates with assembly of an immature immune synapse, Blood 106 (2005) 3874-3879.

[129] T. Saito, T. Yokosuka, Immunological synapse and microclusters: the site for recognition and activation of T cells, Curr Opin Immunol 18 (2006) 305-313.

[130] A. Stoddart, A.P. Jackson, F.M. Brodsky, Plasticity of B cell receptor internalization upon conditional depletion of clathrin, Mol Biol Cell 16 (2005) 2339-2348.

[131] L.E. Guagliardi, B. Koppelman, J.S. Blum, M.S. Marks, P. Cresswell, F.M. Brodsky, Co-localization of molecules involved in antigen processing and presentation in an early endocytic compartment, Nature 343 (1990) 133-139.

[132] S. Malhotra, S. Kovats, W. Zhang, K.M. Coggeshall, B cell antigen receptor endocytosis and antigen presentation to T cells require Vav and dynamin, J Biol Chem 284 (2009) 24088-24097.

[133] A. Chaturvedi, R. Martz, D. Dorward, M. Waisberg, S.K. Pierce, Endocytosed BCRs sequentially regulate MAPK and Akt signaling pathways from intracellular compartments, Nat Immunol 12 (2011) 1119-1126.

[134] B.K. Brown, W. Song, The actin cytoskeleton is required for the trafficking of the B cell antigen receptor to the late endosomes, Traffic 2 (2001) 414-427.

[135] O.O. Onabajo, M.K. Seeley, A. Kale, B. Qualmann, M. Kessels, J. Han, T.H. Tan, W. Song, Actin-binding protein 1 regulates B cell receptor-mediated antigen processing and presentation in response to B cell receptor activation, J Immunol 180 (2008) 6685-6695.

[136] B. Qualmann, D. Koch, M.M. Kessels, Let's go bananas: revisiting the endocytic BAR code, Embo J 30 (2011) 3501-3515.

[137] J. Saarikangas, H. Zhao, P. Lappalainen, Regulation of the actin cytoskeleton-plasma membrane interplay by phosphoinositides, Physiol Rev 90 (2010) 259-289.

[138] B.J. Galletta, O.L. Mooren, J.A. Cooper, Actin dynamics and endocytosis in yeast and mammals, Curr Opin Biotechnol 21 (2010) 604-610.

[139] G. Ren, P. Vajjhala, J.S. Lee, B. Winsor, A.L. Munn, The BAR domain proteins: molding membranes in fission, fusion, and phagy, Microbiol Mol Biol Rev 70 (2006) 37-120.

[140] J.C. Dawson, J.A. Legg, L.M. Machesky, Bar domain proteins: a role in tubulation, scission and actin assembly in clathrin-mediated endocytosis, Trends Cell Biol 16 (2006) 493-498.

[141] P. Gonnord, C.M. Blouin, C. Lamaze, Membrane trafficking and signaling: two sides of the same coin, Semin Cell Dev Biol 23 (2012) 154-164.

[142] G.F. Schreiner, E.R. Unanue, Membrane and cytoplasmic changes in B lymphocytes induced by ligand-surface immunoglobulin interaction, Adv Immunol 24 (1976) 37-165.

[143] G.F. Schreiner, K. Fujiwara, T.D. Pollard, E.R. Unanue, Redistribution of myosin accompanying capping of surface Ig, J Exp Med 145 (1977) 1393-1398.

[144] T.D. Pollard, J.A. Cooper, Actin, a central player in cell shape and movement, Science 326 (2009) 1208-1212.

[145] R.G. Fehon, A.I. McClatchey, A. Bretscher, Organizing the cell cortex: the role of ERM proteins, Nat Rev Mol Cell Biol 11 (2010) 276-287.

[146] S. Tsukita, S. Yonemura, S. Tsukita, ERM proteins: head-to-tail regulation of actin-plasma membrane interaction, Trends Biochem Sci 22 (1997) 53-58.

[147] A. Kusumi, T.K. Fujiwara, N. Morone, K.J. Yoshida, R. Chadda, M. Xie, R.S. Kasai, K.G. Suzuki, Membrane mechanisms for signal transduction: the coupling of the meso-scale raft domains to membrane-skeleton-induced compartments and dynamic protein complexes, Semin Cell Dev Biol 23 (2012) 126-144.

[148] A. Kusumi, T.K. Fujiwara, R. Chadda, M. Xie, T.A. Tsunoyama, Z. Kalay, R.S. Kasai, K.G. Suzuki, Dynamic organizing principles of the plasma membrane that

regulate signal transduction: commemorating the fortieth anniversary of Singer and Nicolson's fluid-mosaic model, Annu Rev Cell Dev Biol 28 (2012) 215-250.

[149] B. Treanor, D. Depoil, A. Gonzalez-Granja, P. Barral, M. Weber, O. Dushek, A. Bruckbauer, F.D. Batista, The membrane skeleton controls diffusion dynamics and signaling through the B cell receptor, Immunity 32 (2010) 187-199.

[150] N. Gupta, B. Wollscheid, J.D. Watts, B. Scheer, R. Aebersold, A.L. DeFranco, Quantitative proteomic analysis of B cell lipid rafts reveals that ezrin regulates antigen receptor-mediated lipid raft dynamics, Nat Immunol 7 (2006) 625-633.

[151] J. Braun, P.S. Hochman, E.R. Unanue, Ligand-induced association of surface immunoglobulin with the detergent-insoluble cytoskeletal matrix of the B lymphocyte, J Immunol 128 (1982) 1198-1204.

[152] J.H. Hartwig, L.S. Jugloff, N.J. De Groot, S.A. Grupp, J. Jongstra-Bilen, The ligand-induced membrane IgM association with the cytoskeletal matrix of B cells is not mediated through the Ig alpha beta heterodimer, J Immunol 155 (1995) 3769-3779.

[153] L.S. Jugloff, J. Jongstra-Bilen, Cross-linking of the IgM receptor induces rapid translocation of IgM-associated Ig alpha, Lyn, and Syk tyrosine kinases to the membrane skeleton, J Immunol 159 (1997) 1096-1106.

[154] J.Y. Park, J. Jongstra-Bilen, Interactions between membrane IgM and the cytoskeleton involve the cytoplasmic domain of the immunoglobulin receptor, Eur J Immunol 27 (1997) 3001-3009.

[155] C. Liu, H. Miller, K.L. Hui, B. Grooman, S. Bolland, A. Upadhyaya, W. Song, A balance of Bruton's tyrosine kinase and SHIP activation regulates B cell receptor

cluster formation by controlling actin remodeling, J Immunol 187 (2011) 230-239.

[156] C. Liu, H. Miller, G. Orlowski, H. Hang, A. Upadhyaya, W. Song, Actin reorganization is required for the formation of polarized B cell receptor signalosomes in response to both soluble and membrane-associated antigens, J Immunol 188 (2012) 3237-3246.

[157] K.E. Prehoda, J.A. Scott, R.D. Mullins, W.A. Lim, Integration of multiple signals through cooperative regulation of the N-WASP-Arp2/3 complex, Science 290 (2000) 801-806.

[158] R. Rohatgi, L. Ma, H. Miki, M. Lopez, T. Kirchhausen, T. Takenawa, M.W. Kirschner, The interaction between N-WASP and the Arp2/3 complex links Cdc42-dependent signals to actin assembly, Cell 97 (1999) 221-231.

[159] S.B. Snapper, F.S. Rosen, The Wiskott-Aldrich syndrome protein (WASP): roles in signaling and cytoskeletal organization, Annu Rev Immunol 17 (1999) 905-929.

[160] T.H. Millard, S.J. Sharp, L.M. Machesky, Signalling to actin assembly via the WASP (Wiskott-Aldrich syndrome protein)-family proteins and the Arp2/3 complex, Biochem J 380 (2004) 1-17.

[161] H.N. Higgs, T.D. Pollard, Activation by Cdc42 and PIP(2) of Wiskott-Aldrich syndrome protein (WASp) stimulates actin nucleation by Arp2/3 complex, J Cell Biol 150 (2000) 1311-1320.

[162] M.P. Blundell, G. Bouma, J. Metelo, A. Worth, Y. Calle, L.A. Cowell, L.S. Westerberg, D.A. Moulding, S. Mirando, C. Kinnon, G.O. Cory, G.E. Jones, S.B. Snapper, S.O. Burns, A.J. Thrasher, Phosphorylation of WASp is a key regulator of

activity and stability in vivo, Proc Natl Acad Sci U S A 106 (2009) 15738-15743.

[163] G.O. Cory, R. Garg, R. Cramer, A.J. Ridley, Phosphorylation of tyrosine 291 enhances the ability of WASp to stimulate actin polymerization and filopodium formation, J Biol Chem (2002).

[164] S.Y. Cleland, R.M. Siegel, Wiskott-Aldrich Syndrome at the nexus of autoimmune and primary immunodeficiency diseases, FEBS Lett 585 (2011) 3710-3714.

[165] L.D. Notarangelo, C.H. Miao, H.D. Ochs, Wiskott-Aldrich syndrome, Curr Opin Hematol 15 (2008) 30-36.

[166] H.D. Ochs, A.J. Thrasher, The Wiskott-Aldrich syndrome, J Allergy Clin Immunol 117 (2006) 725-738; quiz 739.

[167] M. Recher, S.O. Burns, M.A. de la Fuente, S. Volpi, C. Dahlberg, J.E. Walter, K. Moffitt, D. Mathew, N. Honke, P.A. Lang, L. Patrizi, H. Falet, M. Keszei, M. Mizui, E. Csizmadia, F. Candotti, K. Nadeau, G. Bouma, O.M. Delmonte, F. Frugoni, A.B. Fomin, D. Buchbinder, E.M. Lundequist, M.J. Massaad, G.C. Tsokos, J. Hartwig, J. Manis, C. Terhorst, R.S. Geha, S. Snapper, K.S. Lang, R. Malley, L. Westerberg, A.J. Thrasher, L.D. Notarangelo, B cell-intrinsic deficiency of the Wiskott-Aldrich syndrome protein (WASp) causes severe abnormalities of the peripheral B-cell compartment in mice, Blood 119 (2012) 2819-2828.

[168] S. Becker-Herman, A. Meyer-Bahlburg, M.A. Schwartz, S.W. Jackson, K.L. Hudkins, C. Liu, B.D. Sather, S. Khim, D. Liggitt, W. Song, G.J. Silverman, C.E. Alpers, D.J. Rawlings, WASp-deficient B cells play a critical, cell-intrinsic role in triggering

autoimmunity, J Exp Med 208 (2011) 2033-2042.

[169] S.H. Zigmond, How WASP regulates actin polymerization, J Cell Biol 150 (2000) F117-120.

[170] L.S. Westerberg, C. Dahlberg, M. Baptista, C.J. Moran, C. Detre, M. Keszei, M.A. Eston, F.W. Alt, C. Terhorst, L.D. Notarangelo, S.B. Snapper, Wiskott-Aldrich syndrome protein (WASP) and N-WASP are critical for peripheral B-cell development and function, Blood 119 (2012) 3966-3974.

[171] T. Kurosaki, Genetic analysis of B cell antigen receptor signaling, Annu Rev Immunol 17 (1999) 555-592.

[172] T. Kurosaki, H. Shinohara, Y. Baba, B cell signaling and fate decision, Annu Rev Immunol 28 (2010) 21-55.

[173] M.T. Crowley, S.L. Harmer, A.L. DeFranco, Activation-induced association of a 145-kDa tyrosine-phosphorylated protein with Shc and Syk in B lymphocytes and macrophages, J Biol Chem 271 (1996) 1145-1152.

[174] N.E. Harwood, F.D. Batista, Visualizing the molecular and cellular events underlying the initiation of B-cell activation, Curr Top Microbiol Immunol 334 (2009) 153-177.

[175] Y.R. Carrasco, S.J. Fleire, T. Cameron, M.L. Dustin, F.D. Batista, LFA-1/ICAM-1 interaction lowers the threshold of B cell activation by facilitating B cell adhesion and synapse formation, Immunity 20 (2004) 589-599.

[176] A. Kusumi, C. Nakada, K. Ritchie, K. Murase, K. Suzuki, H. Murakoshi, R.S. Kasai, J. Kondo, T. Fujiwara, Paradigm shift of the plasma membrane concept from

the two-dimensional continuum fluid to the partitioned fluid: high-speed single-molecule tracking of membrane molecules, Annu Rev Biophys Biomol Struct 34 (2005) 351-378.

[177] E. Arana, A. Vehlow, N.E. Harwood, E. Vigorito, R. Henderson, M. Turner, V.L. Tybulewicz, F.D. Batista, Activation of the small GTPase Rac2 via the B cell receptor regulates B cell adhesion and immunological-synapse formation, Immunity 28 (2008) 88-99.

[178] M.C. Karlsson, R. Guinamard, S. Bolland, M. Sankala, R.M. Steinman, J.V. Ravetch, Macrophages control the retention and trafficking of B lymphocytes in the splenic marginal zone, J Exp Med 198 (2003) 333-340.

[179] S.B. Snapper, F.S. Rosen, E. Mizoguchi, P. Cohen, W. Khan, C.H. Liu, T.L. Hagemann, S.P. Kwan, R. Ferrini, L. Davidson, A.K. Bhan, F.W. Alt, Wiskott-Aldrich syndrome protein-deficient mice reveal a role for WASP in T but not B cell activation, Immunity 9 (1998) 81-91.

[180] P. Peluso, D.S. Wilson, D. Do, H. Tran, M. Venkatasubbaiah, D. Quincy, B. Heidecker, K. Poindexter, N. Tolani, M. Phelan, K. Witte, L.S. Jung, P. Wagner, S. Nock, Optimizing antibody immobilization strategies for the construction of protein microarrays, Anal Biochem 312 (2003) 113-124.

[181] A. Grakoui, S.K. Bromley, C. Sumen, M.M. Davis, A.S. Shaw, P.M. Allen, M.L. Dustin, The immunological synapse: a molecular machine controlling T cell activation, Science 285 (1999) 221-227.

[182] J.A. Berger, S. Hautaniemi, A.K. Jarvinen, H. Edgren, S.K. Mitra, J. Astola,

Optimized LOWESS normalization parameter selection for DNA microarray data, BMC Bioinformatics 5 (2004) 194.

[183] W.S. Cleveland, S.J. Devlin, Locally weighted regression: an approach to regression analysis by local fitting., Journal of the American Statistical Association 83 (1988) 596-610.

[184] A.Y. Chan, S. Raft, M. Bailly, J.B. Wyckoff, J.E. Segall, J.S. Condeelis, EGF stimulates an increase in actin nucleation and filament number at the leading edge of the lamellipod in mammary adenocarcinoma cells, J Cell Sci 111 (Pt 2) (1998) 199-211.

[185] A.B. Satterthwaite, H. Cheroutre, W.N. Khan, P. Sideras, O.N. Witte, Btk dosage determines sensitivity to B cell antigen receptor cross-linking, Proc Natl Acad Sci U S A 94 (1997) 13152-13157.

[186] M. de Weers, R.G. Mensink, M.E. Kraakman, R.K. Schuurman, R.W. Hendriks, Mutation analysis of the Bruton's tyrosine kinase gene in X-linked agammaglobulinemia: identification of a mutation which affects the same codon as is altered in immunodeficient xid mice, Hum Mol Genet 3 (1994) 161-166.

[187] W.H. Leung, T. Tarasenko, Z. Biesova, H. Kole, E.R. Walsh, S. Bolland, Aberrant antibody affinity selection in SHIP-deficient B cells, Eur J Immunol 43 (2013) 371-381.

[188] W. Liu, T. Meckel, P. Tolar, H.W. Sohn, S.K. Pierce, Intrinsic properties of immunoglobulin IgG1 isotype-switched B cell receptors promote microclustering and the initiation of signaling, Immunity 32 (2010) 778-789.

[189] R. Varma, G. Campi, T. Yokosuka, T. Saito, M.L. Dustin, T cell receptor-proximal

signals are sustained in peripheral microclusters and terminated in the central supramolecular activation cluster, Immunity 25 (2006) 117-127.

[190] A. Meyer-Bahlburg, S. Becker-Herman, S. Humblet-Baron, S. Khim, M. Weber, G. Bouma, A.J. Thrasher, F.D. Batista, D.J. Rawlings, Wiskott-Aldrich syndrome protein deficiency in B cells results in impaired peripheral homeostasis, Blood 112 (2008) 4158-4169.

[191] L.D. Notarangelo, H.D. Ochs, Wiskott-Aldrich Syndrome: a model for defective actin reorganization, cell trafficking and synapse formation, Curr Opin Immunol 15 (2003) 585-591.

[192] L. Dupre, A. Aiuti, S. Trifari, S. Martino, P. Saracco, C. Bordignon, M.G. Roncarolo, Wiskott-Aldrich syndrome protein regulates lipid raft dynamics during immunological synapse formation, Immunity 17 (2002) 157-166.

[193] H. Miki, T. Takenawa, Regulation of actin dynamics by WASP family proteins, J Biochem 134 (2003) 309-313.

[194] J.G. Cyster, K.M. Ansel, K. Reif, E.H. Ekland, P.L. Hyman, H.L. Tang, S.A. Luther, V.N. Ngo, Follicular stromal cells and lymphocyte homing to follicles, Immunol Rev 176 (2000) 181-193.

[195] M.D. Gunn, V.N. Ngo, K.M. Ansel, E.H. Ekland, J.G. Cyster, L.T. Williams, A B-cell-homing chemokine made in lymphoid follicles activates Burkitt's lymphoma receptor-1, Nature 391 (1998) 799-803.

[196] S.F. Gonzalez, S.E. Degn, L.A. Pitcher, M. Woodruff, B.A. Heesters, M.C. Carroll, Trafficking of B cell antigen in lymph nodes, Annu Rev Immunol 29 (2011)

215-233.

[197] K.A. Pape, D.M. Catron, A.A. Itano, M.K. Jenkins, The humoral immune response is initiated in lymph nodes by B cells that acquire soluble antigen directly in the follicles, Immunity 26 (2007) 491-502.

[198] M. Bajenoff, R.N. Germain, B-cell follicle development remodels the conduit system and allows soluble antigen delivery to follicular dendritic cells, Blood 114 (2009) 4989-4997.

[199] R. Roozendaal, T.R. Mempel, L.A. Pitcher, S.F. Gonzalez, A. Verschoor, R.E. Mebius, U.H. von Andrian, M.C. Carroll, Conduits mediate transport of low-molecular-weight antigen to lymph node follicles, Immunity 30 (2009) 264-276.

[200] T. Junt, E.A. Moseman, M. Iannacone, S. Massberg, P.A. Lang, M. Boes, K. Fink, S.E. Henrickson, D.M. Shayakhmetov, N.C. Di Paolo, N. van Rooijen, T.R. Mempel, S.P. Whelan, U.H. von Andrian, Subcapsular sinus macrophages in lymph nodes clear lymph-borne viruses and present them to antiviral B cells, Nature 450 (2007) 110-114.

[201] T.G. Phan, J.A. Green, E.E. Gray, Y. Xu, J.G. Cyster, Immune complex relay by subcapsular sinus macrophages and noncognate B cells drives antibody affinity maturation, Nat Immunol 10 (2009) 786-793.

[202] T.G. Phan, E.E. Gray, J.G. Cyster, The microanatomy of B cell activation, Curr Opin Immunol 21 (2009) 258-265.

[203] K. Suzuki, I. Grigorova, T.G. Phan, L.M. Kelly, J.G. Cyster, Visualizing B cell capture of cognate antigen from follicular dendritic cells, J Exp Med 206 (2009)

1485-1493.

[204] A.K. Szakal, M.H. Kosco, J.G. Tew, A novel in vivo follicular dendritic cell-dependent iccosome-mediated mechanism for delivery of antigen to antigen-processing cells, J Immunol 140 (1988) 341-353.

[205] G.F. Schreiner, E.R. Unanue, Capping and the lymphocyte: models for membrane reorganization, J Immunol 119 (1977) 1549-1551.

[206] E.R. Unanue, W.D. Perkins, M.J. Karnovsky, Ligand-induced movement of lymphocyte membrane macromolecules. I. Analysis by immunofluorescence and ultrastructural radioautography, J Exp Med 136 (1972) 885-906.

[207] T. Kurosaki, Functional dissection of BCR signaling pathways, Curr Opin Immunol 12 (2000) 276-281.

[208] R. Thyagarajan, N. Arunkumar, W. Song, Polyvalent antigens stabilize B cell antigen receptor surface signaling microdomains, J Immunol 170 (2003) 6099-6106.

[209] N.E. Harwood, F.D. Batista, The cytoskeleton coordinates the early events of B-cell activation, Cold Spring Harb Perspect Biol 3 (2011).

[210] G. Gabbiani, C. Chaponnier, A. Zumbe, P. Vassalli, Actin and tubulin co-cap with surface immunoglobulins in mouse B lymphocytes, Nature 269 (1977) 697-698.

[211] J. Braun, K. Fujiwara, T.D. Pollard, E.R. Unanue, Two distinct mechanisms for redistribution of lymphocyte surface macromolecules. I. Relationship to cytoplasmic myosin, J Cell Biol 79 (1978) 409-418.

[212] T.R. Baeker, E.R. Simons, T.L. Rothstein, Cytochalasin induces an increase in cytosolic free calcium in murine B lymphocytes, J Immunol 138 (1987) 2691-2697.

[213] S. Hao, A. August, Actin depolymerization transduces the strength of B-cell receptor stimulation, Mol Biol Cell 16 (2005) 2275-2284.

[214] B. Treanor, F.D. Batista, Organisation and dynamics of antigen receptors: implications for lymphocyte signalling, Curr Opin Immunol 22 (2010) 299-307.

[215] E.M.M. Manders, F.J. Verbeek, J.A. Aten, Measurement of co-localization of object in dual-colour confocal images., J. Microscopy 169 (1993) 375-382.

[216] M. Van Troys, L. Huyck, S. Leyman, S. Dhaese, J. Vandekerkhove, C. Ampe, Ins and outs of ADF/cofilin activity and regulation, Eur J Cell Biol 87 (2008) 649-667.

[217] A.M. McGough, C.J. Staiger, J.K. Min, K.D. Simonetti, The gelsolin family of actin regulatory proteins: modular structures, versatile functions, FEBS Lett 552 (2003) 75-81.

[218] T.Y. Huang, C. DerMardirossian, G.M. Bokoch, Cofilin phosphatases and regulation of actin dynamics, Curr Opin Cell Biol 18 (2006) 26-31.

[219] I. Spector, N.R. Shochet, Y. Kashman, A. Groweiss, Latrunculins: novel marine toxins that disrupt microfilament organization in cultured cells, Science 219 (1983) 493-495.

[220] M.R. Bubb, A.M. Senderowicz, E.A. Sausville, K.L. Duncan, E.D. Korn, Jasplakinolide, a cytotoxic natural product, induces actin polymerization and competitively inhibits the binding of phalloidin to F-actin, J Biol Chem 269 (1994) 14869-14871.

[221] P. Silacci, L. Mazzolai, C. Gauci, N. Stergiopulos, H.L. Yin, D. Hayoz, Gelsolin superfamily proteins: key regulators of cellular functions, Cell Mol Life Sci 61 (2004)

2614-2623.

[222] B.W. Bernstein, J.R. Bamburg, ADF/cofilin: a functional node in cell biology, Trends Cell Biol 20 187-195.

[223] D. Depoil, M. Weber, B. Treanor, S.J. Fleire, Y.R. Carrasco, N.E. Harwood, F.D. Batista, Early events of B cell activation by antigen, Sci Signal 2 (2009) pt1.

[224] I. Rhee, A. Veillette, Protein tyrosine phosphatases in lymphocyte activation and autoimmunity, Nat Immunol 13 (2012) 439-447.

[225] G.V. Baracho, A.V. Miletic, S.A. Omori, M.H. Cato, R.C. Rickert, Emergence of the PI3-kinase pathway as a central modulator of normal and aberrant B cell differentiation, Curr Opin Immunol 23 (2011) 178-183.

[226] S.D. Pauls, S.T. Lafarge, I. Landego, T. Zhang, A.J. Marshall, The phosphoinositide 3-kinase signaling pathway in normal and malignant B cells: activation mechanisms, regulation and impact on cellular functions, Front Immunol 3 (2012) 224.

[227] A.M. Brauweiler, I. Tamir, J.C. Cambier, Bilevel control of B-cell activation by the inositol 5-phosphatase SHIP, Immunol Rev, 2000, pp. 69-74.

[228] P. Youinou, S. Hillion, C. Jamin, J.O. Pers, A. Saraux, Y. Renaudineau, B lymphocytes on the front line of autoimmunity, Autoimmun Rev 5 (2006) 215-221.

[229] W. Liu, T. Meckel, P. Tolar, H.W. Sohn, S.K. Pierce, Antigen affinity discrimination is an intrinsic function of the B cell receptor, J Exp Med 207 (2010) 1095-1111.

[230] J.M. Derry, H.D. Ochs, U. Francke, Isolation of a novel gene mutated in

Wiskott-Aldrich syndrome, Cell 78 (1994) 635-644.

[231] K. Imai, T. Morio, Y. Zhu, Y. Jin, S. Itoh, M. Kajiwara, J. Yata, S. Mizutani, H.D. Ochs, S. Nonoyama, Clinical course of patients with WASP gene mutations, Blood 103 (2004) 456-464.

[232] M. Bosticardo, F. Marangoni, A. Aiuti, A. Villa, M. Grazia Roncarolo, Recent advances in understanding the pathophysiology of Wiskott-Aldrich syndrome, Blood 113 (2009) 6288-6295.

[233] L. Westerberg, M. Larsson, S.J. Hardy, C. Fernandez, A.J. Thrasher, E. Severinson, Wiskott-Aldrich syndrome protein deficiency leads to reduced B-cell adhesion, migration, and homing, and a delayed humoral immune response, Blood 105 (2005) 1144-1152.

[234] S. Dupuis-Girod, J. Medioni, E. Haddad, P. Quartier, M. Cavazzana-Calvo, F. Le Deist, G. de Saint Basile, J. Delaunay, K. Schwarz, J.L. Casanova, S. Blanche, A. Fischer, Autoimmunity in Wiskott-Aldrich syndrome: risk factors, clinical features, and outcome in a single-center cohort of 55 patients, Pediatrics 111 (2003) e622-627.

[235] H. Miki, K. Miura, T. Takenawa, N-WASP, a novel actin-depolymerizing protein, regulates the cortical cytoskeletal rearrangement in a PIP2-dependent manner downstream of tyrosine kinases, EMBO J 15 (1996) 5326-5335.

[236] S.B. Padrick, M.K. Rosen, Physical mechanisms of signal integration by WASP family proteins, Annu Rev Biochem 79 (2010) 707-735.

[237] T.E. Stradal, G. Scita, Protein complexes regulating Arp2/3-mediated actin assembly, Curr Opin Cell Biol 18 (2006) 4-10.

[238] A.J. Thrasher, S.O. Burns, WASP: a key immunological multitasker, Nat Rev Immunol 10 (2010) 182-192.

[239] G.O. Cory, R. Cramer, L. Blanchoin, A.J. Ridley, Phosphorylation of the WASP-VCA domain increases its affinity for the Arp2/3 complex and enhances actin polymerization by WASP, Mol Cell 11 (2003) 1229-1239.

[240] W.H. Leung, T. Tarasenko, Z. Biesova, H. Kole, E.R. Walsh, S. Bolland, Aberrant antibody affinity selection in SHIP-deficient B cells, Eur J Immunol (2012).

[241] J.R. Peterson, L.C. Bickford, D. Morgan, A.S. Kim, O. Ouerfelli, M.W. Kirschner, M.K. Rosen, Chemical inhibition of N-WASP by stabilization of a native autoinhibited conformation, Nat Struct Mol Biol 11 (2004) 747-755.

[242] K. Siemasko, B.J. Eisfelder, E. Williamson, S. Kabak, M.R. Clark, Cutting edge: signals from the B lymphocyte antigen receptor regulate MHC class II containing late endosomes, J Immunol 160 (1998) 5203-5208.

[243] S. McNulty, K. Powell, C. Erneux, D. Kalman, The host phosphoinositide 5-phosphatase SHIP2 regulates dissemination of vaccinia virus, J Virol 85 (2011) 7402-7410.

[244] T. Takenawa, H. Miki, WASP and WAVE family proteins: key molecules for rapid rearrangement of cortical actin filaments and cell movement, J Cell Sci 114 (2001) 1801-1809.

[245] G.W. Chacko, S. Tridandapani, J.E. Damen, L. Liu, G. Krystal, K.M. Coggeshall, Negative signaling in B lymphocytes induces tyrosine phosphorylation of the 145-kDa inositol polyphosphate 5-phosphatase, SHIP, J Immunol 157 (1996) 2234-2238.

[246] V.O. Paavilainen, E. Bertling, S. Falck, P. Lappalainen, Regulation of cytoskeletal dynamics by actin-monomer-binding proteins, Trends Cell Biol 14 (2004) 386-394.

[247] W. Bu, A.M. Chou, K.B. Lim, T. Sudhaharan, S. Ahmed, The Toca-1-N-WASP complex links filopodial formation to endocytosis, J Biol Chem 284 (2009) 11622-11636.

[248] K. Takano, K. Toyooka, S. Suetsugu, EFC/F-BAR proteins and the N-WASP-WIP complex induce membrane curvature-dependent actin polymerization, Embo J 27 (2008) 2817-2828.

[249] S. Benesch, S. Polo, F.P. Lai, K.I. Anderson, T.E. Stradal, J. Wehland, K. Rottner, N-WASP deficiency impairs EGF internalization and actin assembly at clathrin-coated pits, J Cell Sci 118 (2005) 3103-3115.

[250] C.J. Merrifield, B. Qualmann, M.M. Kessels, W. Almers, Neural Wiskott Aldrich Syndrome Protein (N-WASP) and the Arp2/3 complex are recruited to sites of clathrin-mediated endocytosis in cultured fibroblasts, Eur J Cell Biol 83 (2004) 13-18.

[251] D.J. Carver, M.J. Aman, K.S. Ravichandran, SHIP inhibits Akt activation in B cells through regulation of Akt membrane localization, Blood 96 (2000) 1449-1456.

[252] T. Shintaku, K.A. Glass, M.P. Hirakawa, S.J. Longley, R. Bennett, J.M. Bliss, S.K. Shaw, Human endothelial cells internalize Candida parapsilosis via N-WASP mediated endocytosis, Infect Immun (2013).

[253] A.E. Dart, S.K. Donnelly, D.W. Holden, M. Way, E. Caron, Nck and Cdc42 co-operate to recruit N-WASP to promote FcgammaR-mediated phagocytosis, J Cell

Sci 125 (2012) 2825-2830.

[254] R. Mashima, Y. Hishida, T. Tezuka, Y. Yamanashi, The roles of Dok family adapters in immunoreceptor signaling, Immunol Rev 232 (2009) 273-285.

[255] T. Oikawa, T. Takenawa, PtdIns(3,4)P2 instigates focal adhesions to generate podosomes, Cell Adh Migr 3 (2009) 195-197.

[256] M. Mishra, J. Kashiwazaki, T. Takagi, R. Srinivasan, Y. Huang, M.K. Balasubramanian, I. Mabuchi, In vitro contraction of cytokinetic ring depends on myosin II but not on actin dynamics, Nat Cell Biol (2013).